Forschungszentrum Jülich

Programmgruppe Technologiefolgenforschung

Possible Applications of Commercial Satellite Imagery for International Safeguards: Some case studies using optical and radar data

B. Jasani *M.J. Canty* *I. Niemeyer*
B. Richter *G. Stein* *D. Klaus*

Jül-3650

Possible Applications of Commercial Satellite Imagery for International Safeguards: Some case studies using optical and radar data

Bhupendra Jasani[1] *Morton J. Canty*[2] *Irmgard Niemeyer*[2]
Bernd Richter[2] *Gotthard Stein*[2] *Dieter Klaus*[3]

This report was prepared as an account of work sponsored by the Government of the Federal Republic of Germany: Federal Ministry of Education, Science, Research, and Technology under contract no. 02W61840. The authors are responsible for the content of this report.

[1] Department of War Studies, King's College London, United Kingdom
[2] Forschungszentrum Jülich GmbH, Germany
[3] Geographische Institute der Universität Bonn, Germany

Berichte des Forschungszentrums Jülich ; 3650
ISSN 0944-2952
Programmgruppe Technologiefolgenforschung Jül-3650

Zu beziehen durch: Forschungszentrum Jülich GmbH · Zentralbibliothek
D-52425 Jülich · Bundesrepublik Deutschland
☎ 02461/61-6102 · Telefax: 02461/61-6103 · e-mail: zb-publikation@fz-juelich.de

CONTENTS

FOREWORD

1 INTRODUCTION 3

1.1 Background 3

1.2 Why commercial satellites? 4

1.3 The IAEA and observation satellites 6

2 IMAGE SPECIFICATION AND ANALYSIS 8

2.1 Types of data available 8

2.2 Some image processing techniques 11

2.3 Methods of data recording and retrieval 12

3 OBSERVATIONS OF SOME NUCLEAR FACILITIES FROM SPACE: CASE STUDIES 13

3.1 Iraqi Tuwaitha nuclear facilities 14

3.2 Israel's Dimona reactor complex 24

3.3 Pakistani nuclear facilities 29

3.4 The DPRK's nuclear facilities 33

3.5 Russian Kyshtym plutonium production complex 42

3.6 Sellafield complex in the UK 49

3.7 Enrichment plant at Almelo in the Netherlands 58

3.8 Enrichment plant at Gronau in Germany 64

3.9 Fuel fabrication plant at Hanau in Germany 68

3.10 Two nuclear facilities observed by optical and radar sensors 71

3.11 A Russian facility observed by optical and radar sensors 78

3.12 Gorleben, the German back end of the fuel cycle facilities 85

4 CONCLUSIONS 92

APPENDICES

I AVAILABILITY AND CAPABILITIES OF CIVIL/COMMERCIAL REMOTE SENSING SATELLITES 97

II INTERPRETATION OF SATELLITE INFORMATION 103

III CHANGE DETECTION PRE-PROCESSING 110

IV MATHEMATICAL DESCRIPTION OF PRINCIPAL COMPONENT ANALYSIS AND MULTIVARIATE ALTERATION DETECTION 111

V EQUIPMENT AND TRAINING REQUIREMENTS 113

VI ACRONYMS 121

FOREWORD

Remote sensing from space has a long standing tradition in earth observation and environmental monitoring. However, the use of commercial satellite imagery for monitoring arms control is a new field.

This study deals with the application of commercial satellite imagery for international safeguards by the International Atomic Energy Agency (IAEA).

The report summarises research activities which started in 1994 and have been carried out in co-operation between King's College London, the University of London, the Research Centre Jülich, Program Group Technology Assessment and the Department of Geography of the University of Bonn. Part of the work has been performed under the British and German support programmes for the IAEA and have been funded by the British Department of Trade and Industry UK (DTI) and the German Federal Ministry of Education, Science, Research and Technology (BMBF).

1 INTRODUCTION

1.1 Background

During the 1960s, there was a general agreement that the further proliferation of nuclear weapons, both horizontal as well as vertical, would jeopardise world security. Therefore, non-proliferation was seen to be to the advantage of all states. This was to be achieved through a series of bilateral, regional and multilateral arms control measures. The 1970 Treaty on Non-Proliferation of Nuclear Weapons (NPT) was the first international agreement to control the spread of nuclear weapons. By the end of June 1997, 185 states were parties to the NPT including all five nuclear-weapon states (NWS). The five NWS have voluntary Safeguards Agreements with the International Atomic Energy Agency (IAEA).[1]

One of the most important tasks for the IAEA was "to establish and administer safeguards designed to ensure that special fissionable and other materials, services, equipment, facilities, and information made available by the Agency or at its request or under its supervision or control are not used in such a way as to further any military purposes; and to apply safeguards, at the request of the parties, to any bilateral or multilateral arrangement, or at the request of a State, to any of that State's activities in the field of atomic energy" (article III.5, IAEA Statute). Thus, the Agency provides a legal institutional framework for managing international co-operation as well as control in the use of nuclear energy.

The IAEA verifies compliance with the NPT related safeguards and three regional nuclear agreements, the 1967 Treaty on the Prohibition of Nuclear Weapons in Latin America (Tlatelolco Treaty), the 1986 South Pacific Nuclear Free Zone Treaty (Rarotonga Treaty) and the 1996 African Nuclear-Free Zone Treaty (Pelindaba Treaty). Thus, the importance of the Agency's safeguards cannot be over emphasised. For the EUROPEAN COMMISSION Safeguards are carried out under the EURATOM treaty by the EUROPEAN Safeguards Directorate. The interface and the relation to the NPT Safeguards are regulated through the verification agreement.

As required by the NPT (article X.2), the Review and Extension Conference was convened between 17 April and 12 May 1995 in New York. At the time of the Review Conference there were 178 parties of which 175 participated in the conference. The Parties, without a vote, adopted, as part of three Presidential proposals, indefinite extension of the Treaty. The parties also stated that "Decisions adopted by its Board of Governors aimed at further strengthening the effectiveness of Agency safeguards should be supported and implemented and the Agency's capability to detect undeclared nuclear activities should be increased."[2]

The Agency's efforts to detect undeclared nuclear activities resulted from the discovery, in the early 1990, of Iraq's clandestine nuclear programme. In 1993 and 1994, the Director General's Standing Advisory Group on Safeguards Implementation (SAGSI) formulated specific recommendations regarding the detection of undeclared activities. One of the recommendations advised "assessment of the usefulness, technical feasibility associated costs and acceptability of the Agency obtaining satellite

[1] **IAEA Yearbook**, 1991, (IAEA, Vienna), p. E3.
[2] The document NPT/Conf.1995/L5, the second principle.

photographs from commercial sources".[3] In June 1993, after discussions in the Board of Governors, these recommendations were translated into the Secretariat's development programme to strengthen safeguards, known as "Programme 93+2", for cost-effectively strengthening the safeguards procedures.[4] (INFCIRC 540)

1.2 Why commercial satellites?

The attitude of the Democratic People's Republic of Korea (DPRK) was important in 1995 because it may have influenced the thinking of other states in the region on their approach to the 1995 NPT Review Conference. North Korea joined the NPT on 12 December 1985, but it was not until 30 January 1992 that it signed the safeguards agreement with the IAEA. On 9 April 1992 the North Korean parliament ratified it[5] and the safeguards agreement came into force on the following day committing the country to open its nuclear facilities to IAEA inspections within 90 days. The DPRK, on 4 May 1992, provided the IAEA a list of its nuclear facilities. This included uranium mining, refining facilities, a fuel fabrication plant, and three operating reactors (two of which are believed to be plutonium production reactors).[6]

It is worth considering the events in the DPRK over a period between 1989 and 1993. As part of the safeguards agreement, in order to establish the correctness of the information provided, the IAEA began its first inspection of North Korea's nuclear facilities between 25 May and 6 June 1992.[7] The second inspection began on 6 July 1992 during which the focus was, among other things, on the reprocessing facilities. Prior to these inspections, the IAEA Director General Hans Blix visited some of these facilities and reported that North Korea was building a reprocessing plant which had been claimed by them to be a "radiochemical laboratory".[8] At this facility small amounts of plutonium have been separated. When operational, it may be capable of 200 kg/a throughput.[9] The extraction of plutonium for use in North Korea's breeder programme had been given as the justification for such a plant. The third inspection was carried out between 31 August and 15 September 1992. Since this time there have been more inspections.

Perhaps the most important activity under the IAEA inspections of the DPRK was the sampling of material presented for verification at the reprocessing (radiochemical laboratory) plant. The material was declared by the DPRK as the plutonium product and associated waste solutions resulting from a single reprocessing campaign carried out in 1990 of spent fuel from its 5 MWe reactor.[10] By July 1992, differences began to appear between the isotopic analyses made by the IAEA on the spent fuel and the information given by the DPRK on the reprocessing of the fuel. Three different amounts of americium-241 (^{241}Am) were measured by the IAEA in a plutonium sample provided by the DPRK in 1992. This suggested that it had reprocessed the spent fuel on three occasions in 1989, 1990 and 1991 and not once as declared by the DPRK. The ^{241}Am, a decay product from plutonium-241, begins to build up after removal of ^{241}Pu from reprocessing effectively providing the date when the fuel had been

---

[3] SAR-17, Report to the Director General on the 38th Series of SAGSI meeting, 21-24 March 1994.
[4] Pellaud, B., "Safeguards in transition: Status, challenges, and opportunities", **IAEA Bulletin,** vol. 36, no. 3, September 1994, pp.2-7.
[5] **IAEA Press Release**, PR 92/20, 10 April 1992.
[6] **IAEA Press Release**, PR 92/24, 5 May 1992.
[7] **Nuclear Fuel**, 22 June 1992, pp.15-16.
[8] **IAEA Press Release**, PR 92/25, 15 May 1992.
[9] *Ibid*, **Nuclear Fuel**.
[10] **IAEA, INFCIRC/419**, 8 April 1993.

reprocessed. Moreover, the ratio of uranium to plutonium and ^{239}Pu, ^{240}Pu and ^{241}Pu in separated plutonium could provide additional information on the date when separation occurred. It appeared that reprocessing had occurred several times and not only once.

As a result of this and the information acquired by the IAEA from other sources, the Agency requested several more samples and permission to visit two sites located in the Yongbyon Nuclear Research Centre. The Agency believed these facilities to be related to nuclear waste. Initially the permission to inspect these sites was granted. It was found that one site was not related to any nuclear activities. Inspection of the second site, which was under military control, was limited to observations of the one floor only while the building had another floor below ground. It is also under military control. Even with additional information provided by the North Korean authorities, the discrepancy between the IAEA measurements and the information provided remained, forcing the Agency to conclude that undeclared reprocessed fuel may be stored at the site.[11] If true then the implication was that there was more plutonium in the country than declared to the Agency.

In February 1993, the IAEA requested "special inspections" of the two undeclared sites that were suspected to be linked to North Korea's weapons programme.[12] Essentially this triggered, on 12 March 1993, the DPRK to announce, under the provision of article X.I of the NPT, its intention to withdraw from the NPT. The reasons for this were given in a statement to the 154 NPT parties and the three depository States, Russia, the UK and the USA. In defence of this action, the DPRK stated that "It is on the basis of the "intelligence information" fabricated by the United States...that some officials of the IAEA secretariat are trying to enforce the inspection of our major military installations which are unrelated to nuclear activities".[13] It was also stated that the IAEA's insistence on the inspections of the two sites was "an encroachment on the sovereignty of (North Korea), an interference in its internal affairs, and a hostile act aimed at stifling our socialism."[14]

In spite of several efforts by the Agency to resolve the dispute, the DPRK conveyed to the Director General that its decision to withdraw from the NPT would remain unchanged "until... IAEA Secretariat returns to its principle of independence and impartiality."[15] In view of all of this, the IAEA's Director General Hans Blix informed the Board on 21 March 1993 that "as of now, the DPRK continues to be in non-compliance with its general obligation to co-operate in the implementation of the Safeguards Agreement provided for in Article 3 of that Agreement."[16] After intense negotiations, at the end of 1993, the DPRK agreed to IAEA's access to the seven declared nuclear facilities for one-time inspection with no question of granting entry to the two suspected nuclear waste sites.

This whole saga illustrated the need for the Agency to acquire independently information relevant to its safeguards activities. In order to have confidence in the indefinitely extended NPT, it is essential to consider ways of strengthening of the IAEA's safeguards procedures. To this end an examination of contribution from observations from space becomes vital. For example, in the case of the DPRK, the Agency could have used both SPOT and some Russian data to support its need to carry out "special inspections".

---

[11] *Ibid*, p.4.
[12] **Nucleonics Week**, vol. 34, no. 11, 18 March 1993, pp.1 and 9-10.
[13] **Statement of the Government of the Democratic People's Republic of Korea,** 12 March 1993, IAEA INFCIRC/419, 8 April 1993, Annex 7.
[14] *Ibid*, p.10.
[15] *Ibid*, p.6.
[16] *Ibid*, p.7.

Had the DPRK carried out its threat to leave the NPT, it would have had a serious impact on the 1995 NPT Review Conference and on the treaty itself. For example, with the development and testing (on 29 May 1993) by the DPRK of its Rodong 1 missile with a range of about 1,000 km, some countries in the region may have become concerned about their securities.[17] A renunciation of the NPT by the DPRK might have triggered others in the region to re-consider their attitude to the NPT. Thus, unless better safeguards procedures are developed soon for the IAEA, the success of the NPT may be jeopardised.

Information gathered from space played an important role in uncovering the nuclear activities of, for example, Iraq and the DPRK. The non-intrusive nature of observations from space adds to its attractiveness. However, the nature of the source of information about Iraq and the DPRK was such that detailed analysis by the IAEA on them would not have been possible. On the other hand commercial satellite data are generally available without restrictions. Therefore, it is important now to examine how feasible, practical and cost-effective such a technique is for the enhancement of the IAEA's safeguards system. It is important, however, to realise that satellite observation by itself is not enough. Collateral information from many sources needs to be collected and examined.

At present the PRC, France, India, Japan, Russia and the United States launch and operate civil remote sensing satellites (see appendix I). The European Space Agency (ESA, a 15-nation consortium) joined these when the ERS-1 satellite was launched on 16 July 1991. Of these, only France and the USA have been actively distributing their satellite data on a commercial basis. These have now been joined by India, Japan and the Russian Federation.

Since the launch of the first civil remote sensing satellite by the USA in 1972 (Landsat 1), the quality of images, measured in terms of the resolution of a sensor (see appendix I), from subsequent civil satellites has improved some 70 to 80 fold. For example, Russia is marketing images with about 2m resolution and the USA has been declassifying images with similar resolutions acquired from its early (until about 1972) classified satellites. It should be mentioned here that recently the USA has also been considering the sale of data with resolution of about one metre obtained from its planned commercial satellites.[18] Thus, verification, using such satellites, becomes possible.

1.3 The IAEA and observation satellites

During the past few years some criticism has been levelled against the verification procedures carried out by the IAEA. The main criticism, for example, has been its failure to detect until quite late much of the Iraqi nuclear weapon programmes. By and large this has been because of the lack of adequate information available to the IAEA on the undeclared nuclear activities in such regions. This has been recognised by the Director General of the Agency who has stated that "...satellite imagery can be very helpful to inform inspectors where there is reason to look for evidence. ...it does not seem reasonable that the Agency should refrain from utilising a type of information that is available to the whole world even commercially - and that has long been used for confidence building in the field of arms control. ...it would be preferable for an international organisation to obtain such imagery from several sources or from an international satellite agency."[19]

---

[17]Imai, R., "Asian ambitions, rising tensions", **The Bulletin of Atomic Scientist**, vol. 49, no. 5, June 1993, pp. 33-36.
[18]"Ever have the feeling someone's watching you?", **Time International**, vol. 142, no. 23, 29 November 1993, p. 21.
[19]Hans Blix, "Statement to the Review and Extension Conference of the Parties to the Treaty on the Non-Proliferation of Nuclear Weapons, New York, 17 April 1995", **IAEA, C22**.

Also it should be noted here that IAEA's safeguards would be triggered when sales of nuclear materials or facilities occur and are reported to the Agency by the exporters and or by the recipients (article III.1 and 2 of the NPT, Paragraph 34, INFCIRC/153, and Paragraph 15, INFCIRC/66/Rev.2). If a facility is built or nuclear material is acquired indigenously, then it is the responsibility of the non-nuclear-weapon-state (NNWS) party to the safeguards agreement to inform the IAEA so that it can apply safeguards. If this does not occur, as seems to have been the case with Iraq, the Agency, at present, has no possibility to know when and where to carry out its inspections unless a member state with better sources of information informs the Agency of any undeclared facilities of another State party to the Treaty. Such a source could be observations from satellites.

Here is the importance of observation satellites for monitoring nuclear activities of parties to the NPT as well as of those to the other two regional non-proliferation treaties. The use of satellites for this was first recognised publicly when US spacecraft detected the undeclared nuclear facilities of, for example, Iraq. The USA gave the IAEA the relevant information for it to conduct inspections. This method worked for Iraq because it followed the 1991 Gulf War. On the other hand, the use of such a technique could cause considerable political difficulties, highlighting the general problems that the IAEA faces, and illustrating the need for the IAEA to acquire its own information. At present one possible source is information gathered by civil commercial satellites.

The intrusive nature of any verification procedure complicates the control of the spread of weapons and the IAEA's safeguards procedure is no exception. It is important to devise a non-intrusive monitoring method for the Agency in order to enhance its safeguards without creating political difficulties. Observations from space could help. This is particularly true for the detection of possible undeclared nuclear sites. It is, therefore, useful to investigate the possibilities of using information acquired from civil remote sensing satellites.

2 IMAGE SPECIFICATION AND ANALYSIS

2.1 Types of data available

Generally optical and radar sensors are carried on separate observation satellites. For example, the French SPOT, the Indian IRS-1C and the US Landsat have optical sensors only while the European ERS and the Japanese JERS series of satellites and the Canadian Radarsat carry only a radar sensor. While the SPOT satellites carry both panchromatic (with a spatial resolution of 10m) and multispectral sensors (20m), the range and the spectral resolutions are not as good as those of the US Landsat satellites (30m). However, the latter does not have a panchromatic sensor on board. On the other hand the Indian IRS-1C carries both panchromatic (5,8m) and multispectral sensors (23m), the latter being as good as the Landsat TM sensor with the exception of the thermal IR sensor. The IRS-1C has no thermal sensor. Consider first optical multispectral images only.

A multispectral image over a specific area is one in which simultaneous data collection is carried out in three or more spectral regions of the electromagnetic (EM) spectrum. The sensor may measure reflections or emissions of radiation from the earth's surface or objects on the earth's surface. The oldest and the best known multispectral sensor is the human eye but this is sensitive only in the visible part of the EM spectrum (see Figure 2.1).

Optical images could be divided into multispectral, hyper-spectral or ultra-spectral data. These are distinguished by bandwidth and the number of the spectral bands. For example, a multispectral sensor has a broad bandwidth and less than ten spectral bands. Examples of this are the US Landsat TM with seven bands, the Indian IRS-1C with four and the French SPOT satellite with three bands. Such satellites have been in orbit since 1972. On the other hand a hyper-spectral sensor has a narrow bandwidth and several hundreds of spectral bands. An example of this is the US satellite called Lewis which was put in orbit on August 1997, but the contact with the satellite was lost permanently. This satellite has been developed under the US Small Spacecraft Technology Initiative. It had a Hyper Spectral Imager (HSI) consisting of 384 spectral bands in the range of 0.4 to 2.5μm with a spectral resolution of 5 to 6.25 nm and a spatial resolution of 30m. The satellite also had onboard a panchromatic camera with a spatial resolution of 5m. Another type of sensor under development is an ultra-spectral sensor, with a very narrow bandwidth and thousands of spectral bands.

Figure 2.1: Sensitivity of various satellite sensors and spectral responses of some materials to different wavelengths of the electromagnetic radiation.

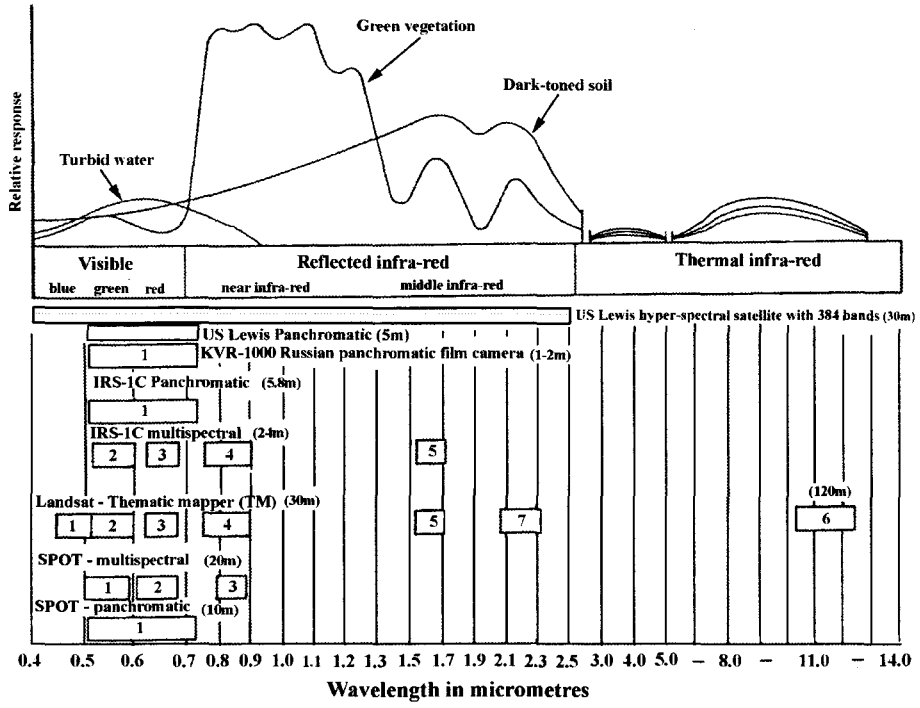

In the studies carried out so far, only panchromatic and some multispectral data in the visible range have been explored. In the case of the latter, the near infrared (NIR), short-wave IR (SWIR), mid-wave IR (MWIR) and long-wave IR (LWIR) could be used to identify features such as disturbed soils and vegetation which may not be visible to the human eyes. A sensor sensitive to LWIR can detect emitted radiance from, for example, heated buildings and warm water used for cooling nuclear facilities and discharged into rivers, water reservoirs or lakes.

Ultra-spectral sensors are still at a research and development stage. These sensors could be used to detect subtle spectral differences in signatures that are too narrow to be detected using simple three-band multispectral data. Hyper- and ultra-spectral imaging is an emerging technology. Using this, identification of specific materials, components of aerosols, gas plumes and effluents could be possible.

Each object or material has a unique signature based on its reflectance properties. A multispectral sensor records these reflectance characteristics. Using sophisticated image processing techniques, the spectral differences of materials could be exploited in identifying them. For example, when different types camouflage are used, it would be possible to detect this using multispectral images. Also if underground facilities are constructed, stressed vegetation, which grows on the earth-covered bunkers, could be distinguished from normal vegetation because of the root growth, drainage, and soil conditions are different.

Information derived from imaging radar, such as a synthetic aperture radar (SAR), is very different from that obtained from optical sensors. This is because a SAR is particularly sensitive to the geometrical characteristics of the surface and the object being monitored as well as to their dielectric properties. While the interaction between the optical radiation and an object is determined by structures on micron scales and by processes that involve chemical absorption, microwave radiation can

penetrate significant distances into an object, the depth of which could be comparable to the wavelengths of the radiation. This could be a few centimetres to a few tens of metres. Generally the longer the wavelength the greater the penetration. For example, there is very limited penetration through the surface layers by radiation with C-band wavelength and the radar backscatter is determined by the surface structure of the objects. On the other hand at L-band, SIR-C radar beam is known to have penetrated several metres of dry sand.

Interaction of microwave energy with materials does not only depend on the wavelength but also on the polarisation of the radar beam. For example, a vertically polarised electric field of the ERS SAR interacts more strongly with objects with steep surfaces than would a horizontally-polarised beam. Such interactions lead to differences both in the power scattered back in those different polarisation modes and in the degree of penetration through the surface of the object.

A number of SAR sensors are now in orbit operated by various countries. A multi-channel radar exploits the fact that the interaction of microwave beam with matter is influenced by frequency and polarisation of a radar beam. The response of the latter to different shapes or scattering elements of an object will depend on the selection of horizontal or vertical polarisation. The US SIR-C/X-SAR experiments during April and October 1994 generated such multi-parameter SAR data from space. Clearly in addition to the optical data, such radar information should now be tried when monitoring nuclear fuel cycle. For example, if the scattered radar signals from an object reflect the dielectric properties of the object, then a change in temperature of, for instance, water in a lake or a river due to the discharge of cooling water, should be reflected in the returned radar beam. In a single test such a change has been detected but more rigorous work needs to be carried out. The greatest advantage of a SAR sensor is its ability to provide all-weather day and night information. Combining this with optical data, the technique could become a very powerful tool for the IAEA.

2.2 Some image processing techniques

Basic interpretation of images using such simple image enhancement techniques as contrast stretching and edge enhancement is possible particularly when panchromatic images are used and geometrical shapes, such as buildings and roads, are involved. However, more sophisticated interpretation requires not only the use of multispectral data but complex image processing techniques. For example, in a multi-band image, the subtraction of one band from another creates a new image which may provide a black and white image with better contrast to aid analysis. Using a ratio of two bands, for example TM band 4 and band 3, would highlight information differently. Such enhancement may be used to differentiate camouflaged targets from background terrain. Thus, in general, image processing can be summarised as image restoration, rectification and registration, enhancement and classification. Some of these categories have been used in the earlier studies.

Classification technique, not explored so far, is a pattern-based process of assigning individual pixels in an image to cover land classes or different objects on the basis of spectral reflectance. Such classification could be supervised or unsupervised.

Supervised classification is very much controlled by humans. In this process pixels which correspond to recognised patterns and features are identified with the help from collateral data. Representative training areas are determined which are then used to train the computer to identify features elsewhere in the image. The collateral information can be from aerial photographs or ground descriptions of nuclear facilities. If none of them is available, clustering results could be used.

Unsupervised classification (clustering) is primarily a computer process for selecting natural groupings or patterns of pixels with similar spectral characteristics. In this process the analyst has minimum input. A specified set of parameters are used by the computer to uncover statistical patterns that are inherent in the image data. This method is usually used when less is known about the site under investigation. After such classification, the analyst can give interpretation to the resulting classes.

Pattern recognition is a technique of finding known patterns in an image which can be extracted through spectral classification or by geometrical shapes. By spatially and spectrally enhancing an image, pattern recognition can be performed by humans or, automatically by a computer system; spectral recognition can be performed automatically. Also if, for example, some common shapes of nuclear facilities are determined, it is possible to train a computer to seek out such patterns in an image. While automatic pattern recognition is by no means an easy task, it is important that a method is found for recognising, using computers, various elements of a nuclear fuel cycle. In this, the newly agreed Protocol for the Application of Safeguards is important. Under the provision of exchange of information, a party is required to give "A general description of each building on each site, including its use and, if not apparent from that description, its contents. The description shall include a map of the site."(Article 2.iii) Armed with such information, the use of digital elevation model (DEM) techniques could be a very useful tool as it would enable the Agency to create three dimensional pictures of the site to be visited and give it a better sense of what and where to look for different activities. The site diagrams would also make automatic pattern recognition task more feasible.

Change detection is a process in which differences in the status of an object or a phenomenon are identified by observing them at different times. The main idea is that changes in buildings, infrastructure etc. must result in changes in grey level values of the relevant pixels. Several methods

can be used to detect changes: image differencing (or other arithmetic operations), multitemporal classification or post-classification comparison as well as linear transformations.

Geographic information systems (GIS) is yet another powerful tool which enhances the interpretability of images acquired from space. Normally image interpretation is carried out in isolation without actually integrating, with a satellite acquired image, any other external information. An important starting point is to geocode the image. This is carried out by re-sampling each data set to a uniform pixel size which is registered to a geographic co-ordinate system. A GIS is a system for collecting, storing, organising, integrating, manipulating and analysing and displaying a set of geographic data. These could be digital maps or non-spatial information such as tabulated demographic information.

2.3 Methods of data recording and retrieval

The Russian high resolution data are recorded on films and the whole satellite with its photographic content is physically recovered and, therefore, in this case the question of data transmission does not arise. All other satellites transmit their data electronically to the ground stations. However, this has limitation because the satellite has to be in line of sight of a ground station to retrieve the data. For this reason, a number of ground stations spread round the globe have been established by the operators of the US Landsat and the French SPOT satellites. The distribution and the coverage of these stations need to be assessed.

Generally at present information gathered from space is recorded on an on-board tape recorder to be played back when the satellite is over a ground receiving station. However, not all satellites have tape recorders on board and in any case tape recorders tend to be unreliable because they are mechanical devices which could get damaged during the launch phase. Recently, this is overcome by deploying solid state data storage devices on board satellites. Such capabilities should be assessed.

Data can be transmitted via communications satellites to the ground station but this is not generally available. It is therefore, important to investigate whether the current generation commercial communications satellites are capable of handling the data rates resulting from civil observation satellites. For example, the US Landsat-5 transmits the TM data at a rate of 83 MB/s. While the French SPOT satellite has a tape recorder on board, its data transmission rate is 50 MB/s and that for the European ERS-1 is 100 MB/s. It is, therefore, important to investigate the capabilities of commercial communications satellites to determine whether they are capable of handling such high data rates. It might be useful to discuss this with a number of civil communications satellite operators such as the Inmarsat. A more promising method may be the use of mobile ground-based receiving stations for retrieving satellite data.

3 OBSERVATIONS OF SOME NUCLEAR FACILITIES FROM SPACE: CASE STUDIES

The Sites and type of data examined are listed in Table 3.1.

Table 3.1. Nuclear sites investigated

Site location	Satellite	Data format	Date of images	Facility/location*
Baghdad (Iraq)	KVR-1000 SPOT Pan	Film CCT	27/06/1991 12/05/1991	Reactors and reprocessing at Tuwaitha and enrichment at Tarmiya/33.20N,44.26E
Dimona (Israel)	SPOT	CCT Pan/10	08/10/1991	Nuclear complex
PINSTECH (Pakistan)	SPOT KVR-1000	CCT Pan /10 Film positive/2	18/02/1992	Nuclear research centre
Yongbyon (North Korea)	SPOT Landsat	CCT Pan/10 XS/20 TM/30	19/09/1989 11/06/1986 01/06/1992	Nuclear complex
Kyshtym (Russia)	Landsat	CCT TM/30	01/08/1987 13/05/1993	Plutonium production
Sellafield (UK)	SPOT Landsat	CCT PAN/10 XS/20 TM/30	19/03/1990 30/06/1986 10/02/1989	Repoarring facility
Almelo (Holland)	Landsat	CCT TM/30	19/07/1992	Enrichment facility
Gronau (Germany)	Landsat	CCT TM/30	19/07/1992	Enrichment facility
Hanau (Germany)	Landsat	CCT TM/30	03/07/1991	Fuel fabrication facility
Russian facility	Landsat XS data ERS-2 SAR	CCT CCT	1/08/1987 and 13/05/1993 7 May 1993	Reactors
Dungeness (UK)	SPOT XS ERS-2 SAR	CD-ROM CD-ROM	9 December 1986 7/11/1995 20/02/1996 30/04/1996 4/06/1996 9/07/1996 26/11/1996 31/12/1996	Power reactor
Gorleben (Germany)	Landsat KVR-1000	CD-ROM CD-ROM	24/08/1984 31/08/1989 Date unknown	Interim spent fuel element and low-level radioactive waste storage; a pilot conditioning facility; exploratory mine

*Degrees and minutes of latitude and longitude.

Besides SPOT panchromatic and SPOT multispectral there are Landsat TM5 multispectral images analysed. Moreover, KVR-1000 panchromatic and ERS-2 SAR radar images are also analysed.

3.1 Iraqi Tuwaitha nuclear facilities

Around Baghdad there were two important nuclear complexes, Al Tuwaitha to the south and Al Tarmiya to the north of the city. In the former, examined in this report, Iraq had constructed three nuclear facilities which it had declared under its safeguards agreement with the IAEA. These were the Russian IRT-5000 5 MWth reactor fuelled with highly enriched uranium, the Tammuz-2 500 kWth French reactor, and small fuel fabrication and storage plants. Near Al Tarmiya, an enrichment facility using electromagnetic isotopic separation (EMIS) method had been under development.

On 15 May 1997, the Board of Governors of the IAEA approved new measures to strengthen its safeguards procedures under an additional protocol. Under this, a State Party will be committed to provide the Agency a general description of each building on a site with a map of the facility as well as other relevant information. The usefulness of such maps is illustrated below.

Consider the Al Tuwaitha facility. A site diagram[20] of the complex is shown in Figure 3.0. An extract from a panchromatic image (10m pixel resolution) acquired over Baghdad by the French SPOT satellite on 12 May 1991 (i.e. after the Gulf War in February 1991) is shown in Figure 3.1. Security building (a), chemical research laboratory (b), the site of the Tammuz-1 and -2 research reactors (c), and an unidentified building 43 (d) are marked in the Figure and discussed below. Using the Adobe Photoshop[21] image processing software, the site diagram was corrected for size and orientation and was then overlaid on the satellite image as shown in Figure 3.2, in which at A, a number of buildings can be seen on the image but they do not appear on the site diagram.

On 27 June 1990, before the Gulf War, a Russian Cosmos satellite carrying a KVR-1000 high resolution panchromatic camera (about 2m photographic resolution) took a picture of Baghdad. An extract from the full scene is shown in Figure 3.3. The image in this figure was obtained by scanning a small section of the original positive transparency using an Agfa Arcus 2 flat bed scanner. The resolution of the scanned image is 2,400 pixels/inch.

While the resolution of the original data was degraded somewhat, this facilitated comparison between the Russian analogue image and the digital one obtained by the SPOT satellite. As before, the line drawing of Figure 3.0 was overlaid on this image as shown in Figure 3.4. A number of the unregistered buildings can be seen in the image (marked A) indicating that these buildings have been there for at least one year. Also, new buildings have been constructed between 27 June 1990 and 12 May 1991. Examples of these are marked by B in Figures 3.2 and 3.4. Some of the other differences between these images were identified by eye and they are highlighted in Figure 3.5.

[20] Adopted from Kokoski, R., "Technology and the proliferation of nuclear weapons", 1995, (SIPRI, Oxford University Press, 1995), pp. 105-116.

[21] Adobe Photoshop version 3.0 manufactured by Adobe Systems Incorporated, Mount View, California, USA.

Figure 3.0. A map of the Tuwaitha nuclear complex.

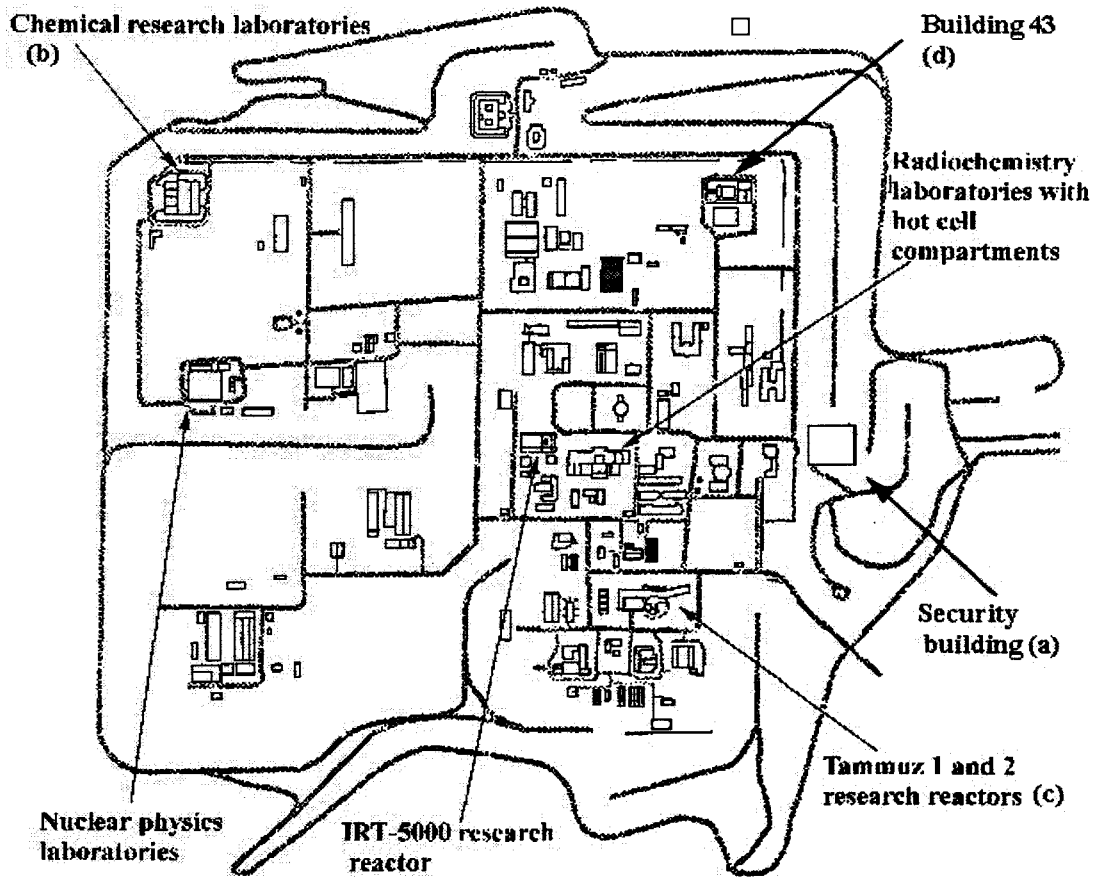

From the site diagram, it can be seen that a number of buildings do not appear on the diagram but they can be seen in the satellite image. This illustrates a method that can be used to check the initial data a Member State might supply the Agency under the new Additional Protocol. For example, under the Article 2, the Party is required to give a general description of each building on each site as well as a map of the site.

A possible quantitative measure was investigated for determining changes in a scene. First the two images acquired at different times are co-registered so that they match exactly and then they are subtracted one from the other. However, this process changes the original pixel values in one image which would then make the interpretation of the results difficult. This is particularly true when spectral analysis is to be carried out on a multispectral image. Also, if this method were used in the present case, the KVR-1000 image would have to be re-sampled in order to match its resolution with the SPOT image. This would change the pixel values of this image even more. In addition, corrections due to radiometric differences resulting from different atmospheric conditions (e.g. position of the Sun, humidity, etc.) have to be applied. Thus, it was necessary to use another method of comparing the images without changing their pixel values.

Figure 3.1. An extract from a full scene (10 m pixel resolution) acquired by French SPOT satellite over Baghdad on 12 May 1991 showing the Iraqi nuclear reactor complex at Al Tuwaitha after the Gulf War. Security building (a), chemical research laboratory (b), the site of the Tammuz-1 and -2 research reactors (c), and an unidentified building 43 (d) are identified from Figure 3.0.

Source: CNEC/SPOT Image.

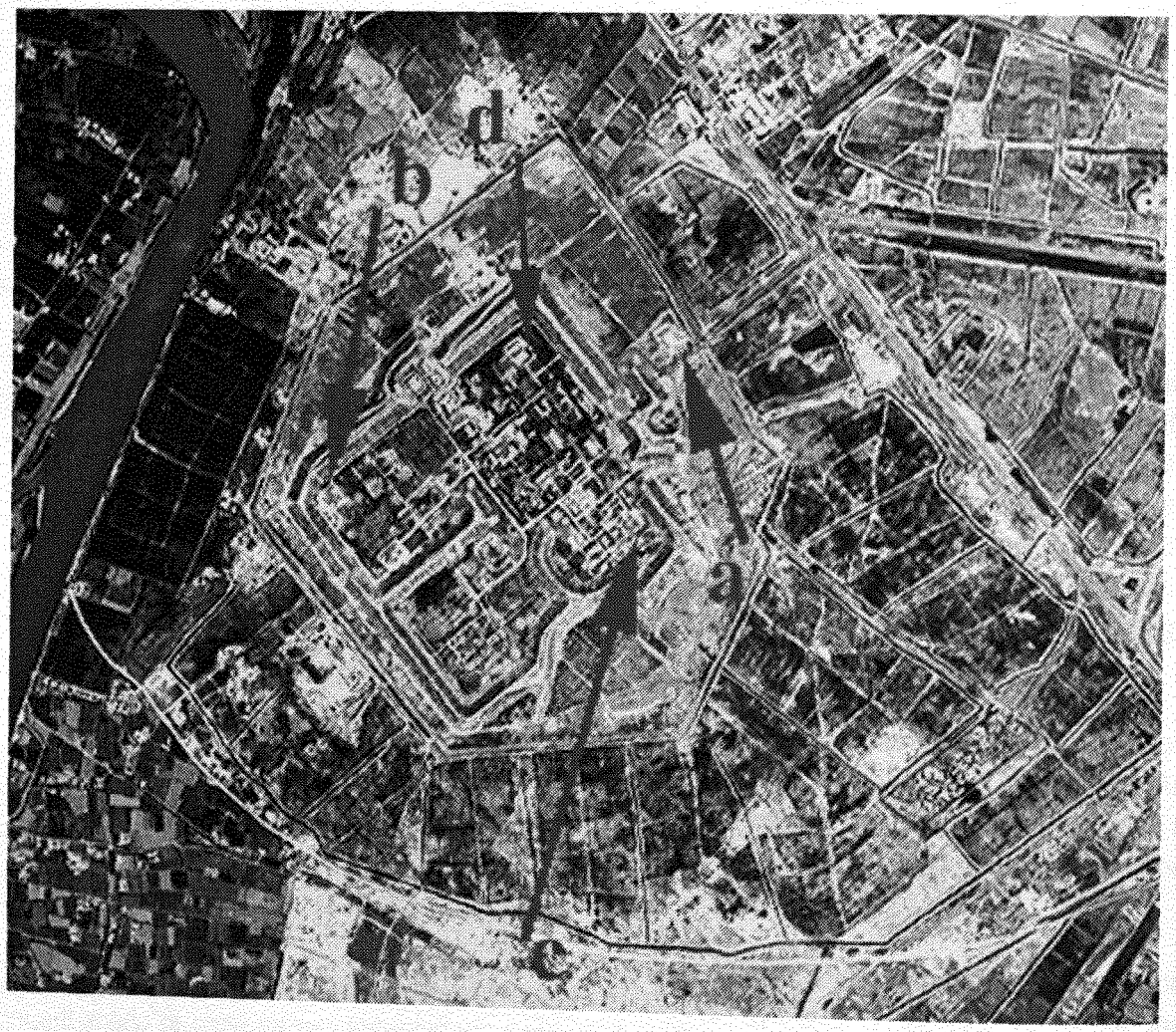

In the example, the changes to be detected were due to some of the buildings being damaged or destroyed during the Gulf War. A satellite image is usually available in the form of digital data with its pixels attributed minimum and maximum reflectance values 0 (for black pixels) and 255 (for white ones). Values in between represent different grey levels. Buildings tend to be highly reflective compared to the soil so that a destroyed building will appear darker than a normal one. Thus, for example, if the distribution or histogram of the grey levels as a function of the number of pixels is examined, it is found that the maximum will be located near the high values of grey levels if the buildings were neither camouflaged nor destroyed. This is used in the following analysis.

It had been reported that, at the Al Tuwaitha site, a number of buildings were damaged by bombing during the 1991 Gulf War.[22] Two such sites at **b** (a chemical laboratory) and **c** (a building near the location of the Tammuz-1 and -2 reactors), from Figures 3.1 and 3.3 respectively, were extracted. Also

[22] ***Ibid***. Kokoski, p. 109.

from these figures, it can be seen that the site **a** has not changed significantly. This is not unreasonable as the site seems to be a security building at the entrance gate to the complex. Also the building at **d** appears unchanged in both images. The distributions of the reflectance values as a function of the number of pixels were plotted for these small extracts (see Figures 3.6 to 3.9).

Figure 3.2. Site diagram of Figure 3.0 overlaid on the satellite image of Figure 3.1 (12 May 1991). Buildings that are not marked on the site diagram are indicated by A. B indicates possible new constructions. Compare these with the images in Figures 3.3 and 3.4.

Figure 3.3. An extract of a full scene acquired by Russian Cosmos satellite KVR-1000 sensor (2 m photographic resolution). The image was acquired on 27 June 1990, i.e. before the Gulf War. Security building (a), chemical research laboratory (b), the site of the Tammuz-1 and -2 research reactors (c), and an unidentified building (d) are identified from Figure 3.0.

Source:KVR-1000

Although two sensors with different spatial resolutions were used to acquire the images, their spectral characteristics are very similar; 0.51-0.73μm for SPOT and 0.58-0.72μm for the Russian KVR-1000 camera. The images were acquired in 1990 and 1991 at nearly the same time of the year (see Figure 3.5). Thus, any differences in the characteristics of the extracts from the two images are likely to be due to the changes at the site, i.e. structural changes of the buildings, and not because of the atmospheric, seasonal or lighting conditions. There are effects, such as radiometric differences due to ageing of buildings or structural changes such as reconstruction of a flat-topped to a sloping or glass from a tiled roof building, which may change the reflectance values. To avoid atmospheric and seasonal variations, relative changes in the extracts from the same image were examined and the histograms were compared for the two images. The histograms should be similar for buildings from the same image unless they have been physically changed, for example, due to destruction.

Figure 3.4. Site diagram of Figure 3.0 overlaid on the Russian satellite image acquired on 27 June 1990, before the Gulf War. Buildings that are not marked on the site diagram of Figure 3.0 are indicated by A. Compare these with those in Figure 3.2.

Figure 3.5. The KVR-1000 image acquired on 27 June 1990 (1) and the SPOT image acquired on 12 May 1991 (2) show some of the changes, identified by eye, that occurred during this period. Some of these are highlighted by square brackets.

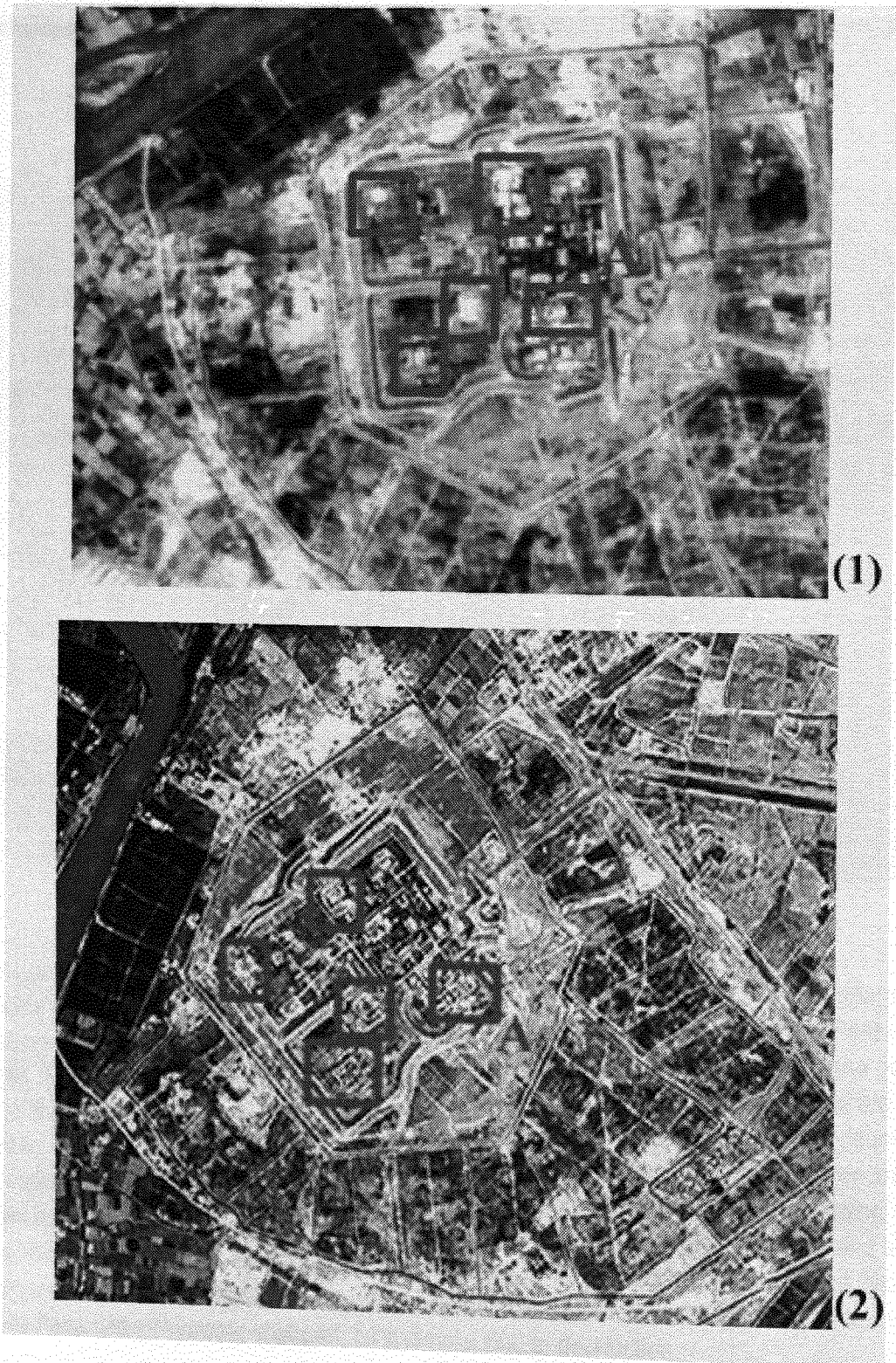

Histograms of the distribution of reflectance as a function of number of pixels for all the four sites in each of the two images (Figure 3.1 and 3.3) were determined. Figure 3.6 shows the four histograms for the different building sites in the Russian KVR-1000 image. It can be seen that, except for the building at **c**, all the other three histograms are very similar, suggesting that in 1990, i.e. before the Gulf War, no camouflage had been used. On the other hand, building at **c** is less reflective. This is confirmed by the

mean values of the pixels for the three similar sites being similar and higher than the site at **c**. Therefore, it is concluded that the roof of building **c** may be made of a different material.

A similar analysis was carried out using extracts of the same sites from a SPOT image. These are shown in Figures 3.7, 3.8 and 3.9. In Figure 3.7, the histogram for the site of the building at **c** in Figure 3.1 is compared with that for the gate at **a**. As before, the mean value for the building site is lower than that for the gate. Similar observation can be made for the site **b**. These suggest that changes at these sites have occurred. It should be remembered that comparisons of various buildings are made between buildings in the same image and not between those from images acquired on different occasions.

Thus, it can be seen that comparison of histograms could be a useful quick way to detect changes in a facility. This method needs to be explored further. The advantage of a high resolution image, such as the Russian KVR-1000, is also clear. For example, the identification of facilities is easier from an image such as Figure 3.3 than from Figure 3.1. The former, because of its higher resolution would retain the definition when enlarged compared with the latter in which case it will begin to show pixels. This is in spite of the fact that the image in Figure 3.3 had already lost some quality because, for this study, it was obtained by scanning the original photographic image. Also multispectral images would help to determine changes in the spectral characteristics of objects on the ground. Not only this but detection of changes could be easier with such data. This is investigated below.

Similar analysis was carried over the Al Tarmiya EMIS enrichment site. Figure 3.10 shows panchromatic images acquired by the Russian KVR-1000 sensor and the French SPOT satellite. On a site diagram[23], the EMIS machine housing was identified. This is indicated at **(a)** in Figure 3.11. It can also be seen from Figures 3.10 and 3.11 that the buildings at **(b)** and **(c)** have been changed. The one at **b** divided into three sections may be a result of damage caused as a result of the Gulf War or it may have resulted from the IAEA's dismantling process. The site at **c**, not identified in the map, appears to be damaged also. Whether this was the result of the 1991 war or the dismantling process is difficult to determine from these images, but it is clear that with the use of a site diagram it is simpler to see where changes may have taken place at a site and where information on a site might have been withheld.

Figure 3.6. Histograms of the four extracts (a, b, c and d) from the image in Figure 3.3.

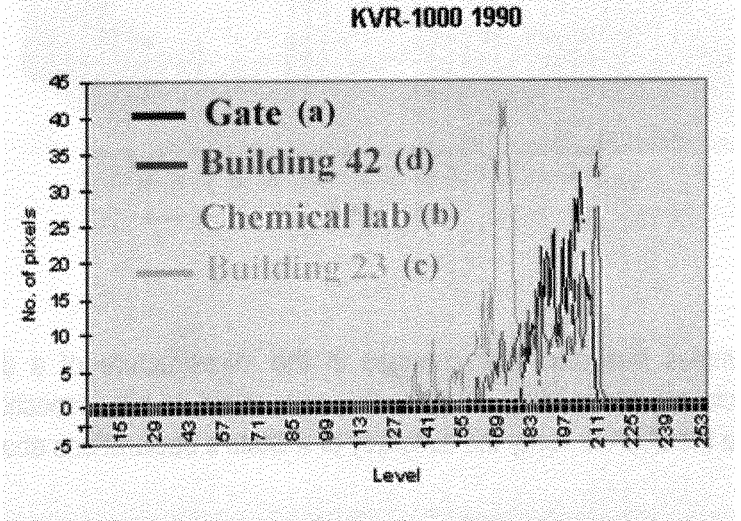

[23] ***Ibid***. Kokoski, p. 110.

Figure 3.7. Histograms of the two extracts (a and c) form the image in Figure 3.1.

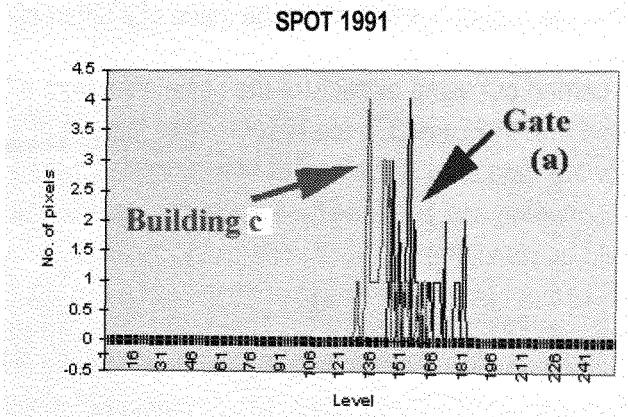

Figure 3.8. Histograms of the two extracts (a and b) from the image in Figure 3.1.

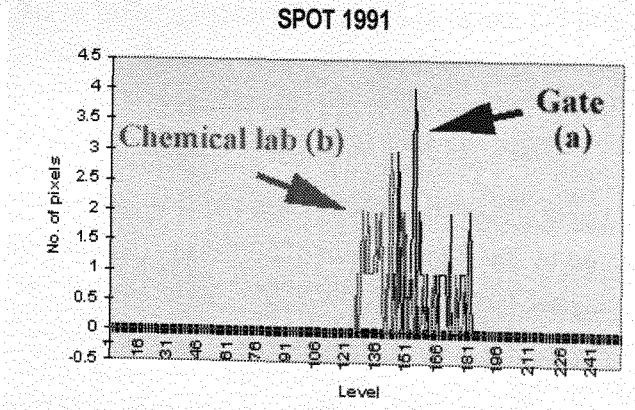

Figure 3.9. Histograms of the two extracts (a and d) form the image in Figure 3.1.

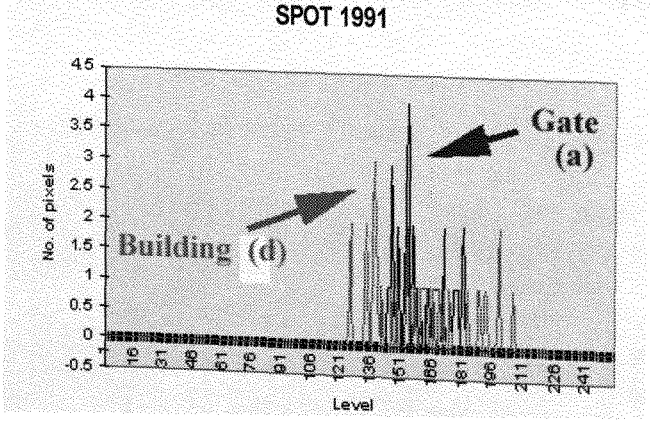

The above examples illustrated that changes in the infrastructure of a declared site can be detected by commercial remote sensing satellites that may avoid on-site inspections. Moreover, such imagery would unable the IAEA to verify the accuracy of a State's declarations about the facility.

Figure 3.10. Extracts from the full scenes over Baghdad acquired by the Russian KVR-1000 sensor (top) on 27 June 1990 (before the Gulf War) and the French SPOT satellite (lower image) on 12 May 1991. (a) is the site of the EMIS machine housing; (b) an un-identified building which appears to have changed in 1991 (see the lower SPOT image); and similarly changes have occurred at c.

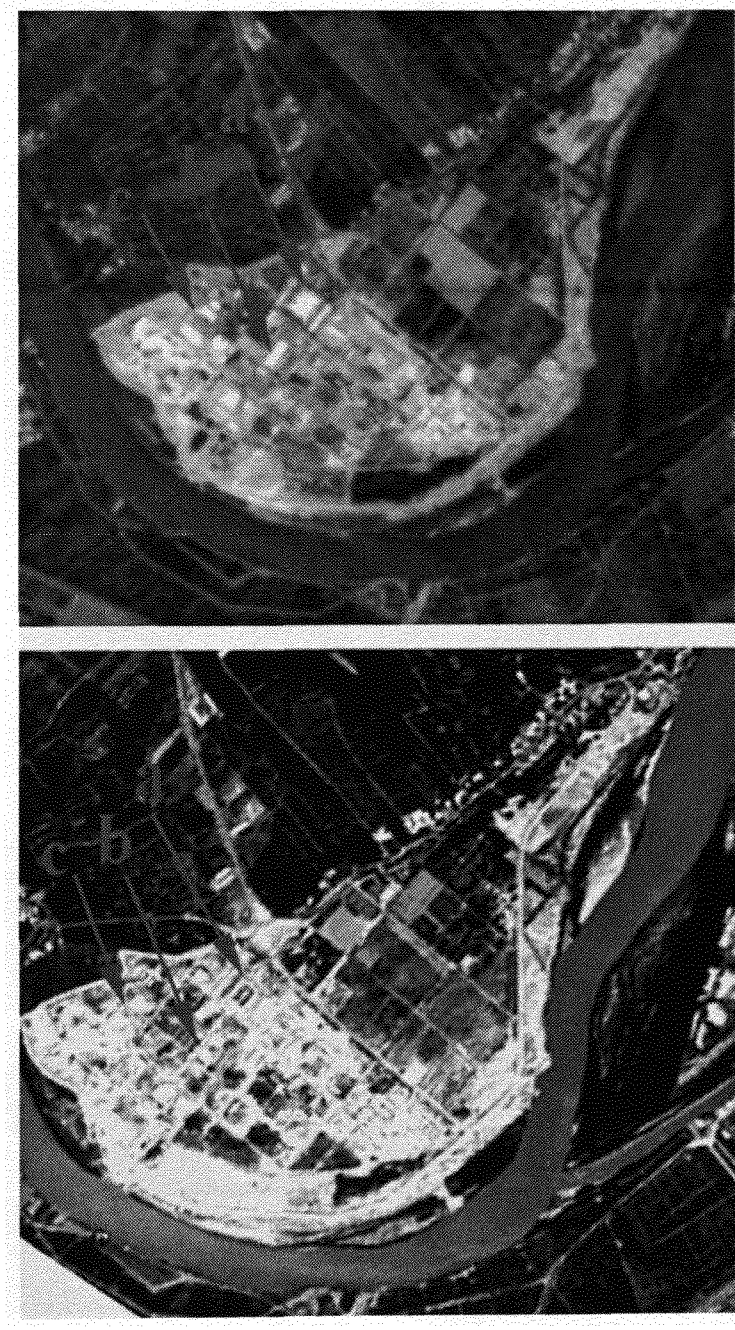

Figure 3.11. A map of the Al Tarmiya is superimposed over the extracts from the full scenes from Russian KV-1000 (top) sensor image and the French SPOT (below) satellites.

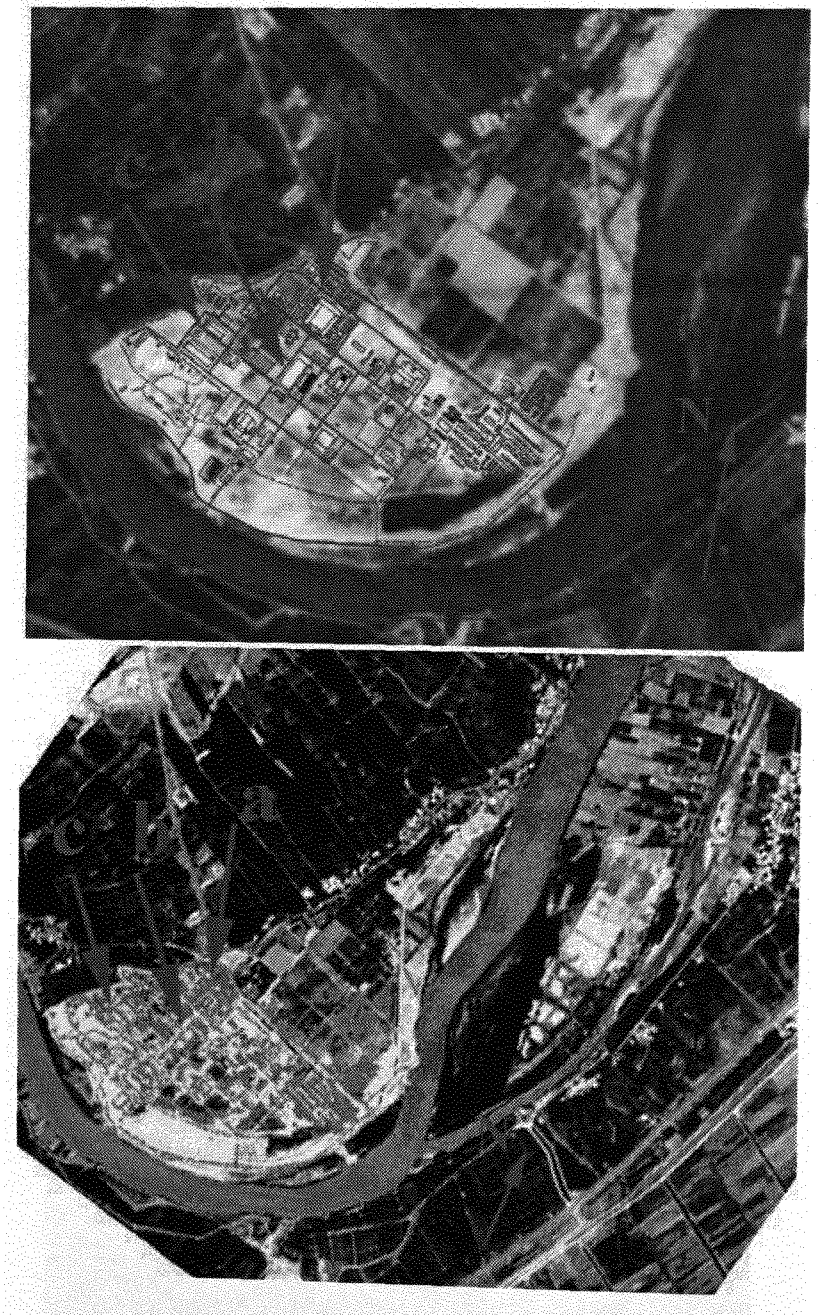

3.2 Israel's Dimona reactor complex

In 1957 France agreed to supply Israel a nuclear reactor and a chemical facility for the separation of plutonium from the irradiated fuel in the reactor.[24] The site for the reactor was some 15km south-east of the town of Dimona in the Negev desert (see Figure 3.12). Although the existence of the facility became known publicly in December 1960, it was probably detected in 1958 by a US U-2 reconnaissance aircraft.[25] An agreement between the atomic energy organisations of the two countries

[24]Perrin, F., (the scientific head of the French Atomic Energy Commission from 1951 to 1970), an interview in the Sunday Times (London), 5 October 1986.

[25]Spector, L.S., **The Undeclared Bomb**, (Ballinger Publishing Company, Cambridge, USA, 1988), p. 170.

was signed on 17 September 1956.[26] Officially France was to deliver its EL-3 experimental reactor to Israel. This is a tank-type reactor fuelled with 1.35 per cent enriched uranium and cooled and moderated by heavy water. The reactor, with a nominal power of 15 MWth, was designed for fundamental research, structural materials testing and isotope production.[27]

Figure 3.2. A full SPOT panchromatic scene over the Dimona reactor complex and its environment; (1) Beersheba; (2) Military airfield north west of the Dimona reactor complex; (3) a large ammunition storage site with possibly nuclear weapons; (4) Dimona reactor complex; (5) possible phosphate mining areas, both linked by rail and road to the Dimona complex; (6) military airfield south west of the Dimona reactor complex; (7) there are two possible air defence sites; and (8) town of Dimona. Scale: 1:250,000.

Source: CNES/SPOT; image processed at the Defence Research Agency, Farnborough, UK.

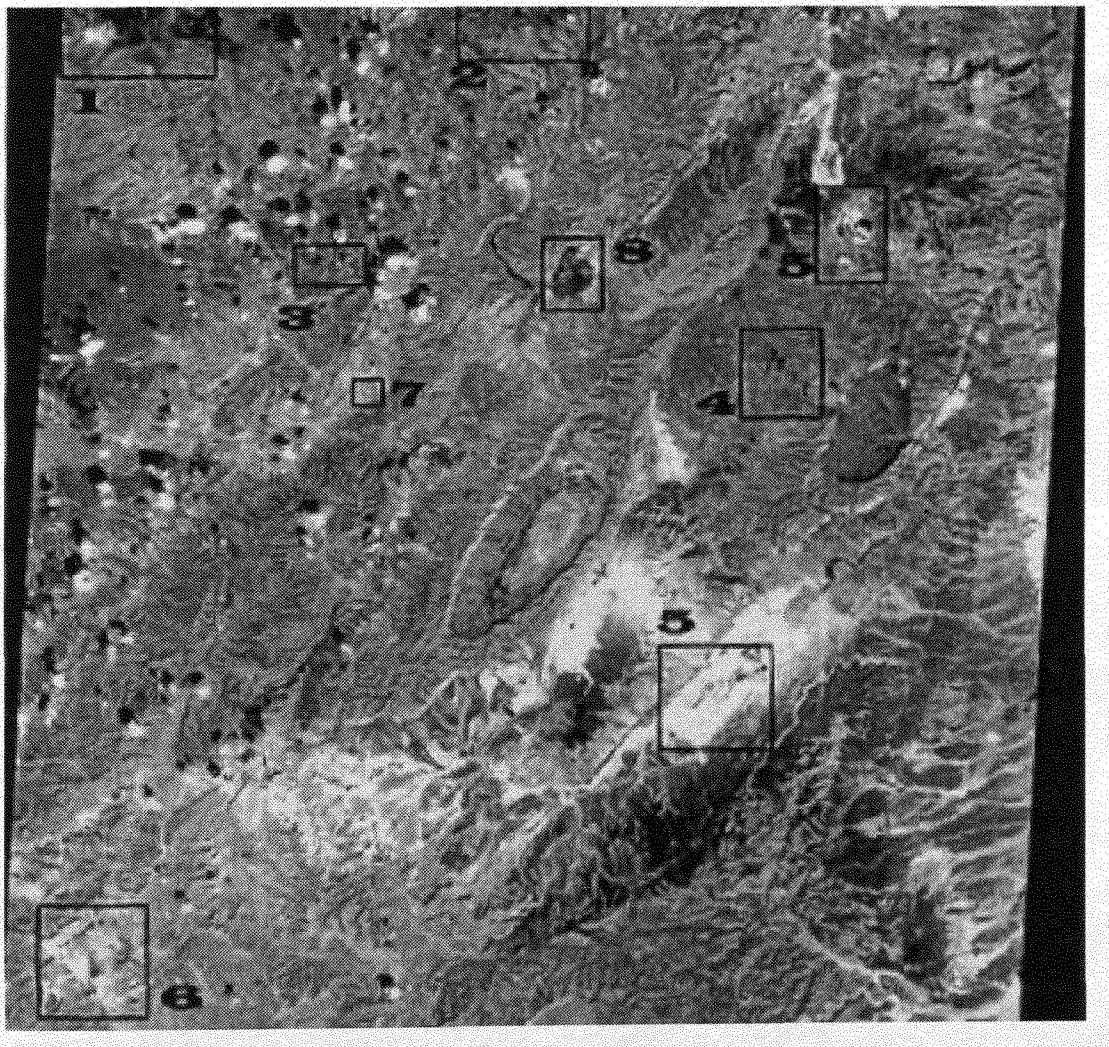

The Dimona reactor, IRR-2, is a heavy-water moderated natural-uranium reactor upgraded to operate at 40-70 MWth.[28] The IRR-2 may be similar to the French G-1 plutonium production plant at Marcoule. This is a natural uranium, graphite moderated, air cooled 38 MWth reactor.[29] The dimensions of the G-1 reactor together with its shield are 14m length, 24m wide and 18m high. An enlargement of

[26] *Ibid.*
[27] **Directory of Research Reactors**, vol. II, 1989, (IAEA, Vienna), pp. 294-300.
[28] Péan, P., **Les Deux Bomber**, (Fayard, Paris, 1981).
[29] **Directory of Nuclear Reactors, vol. IV, (IAEA, Vienna), pp. 177-182.**

the reactor complex is shown in Figure 3.13 in which the reactor is reported to be at **A**.[30] However, the dome of the reactor building is not very clear. Since the reactor is not a power reactor, the heat carried away by the air coolant is not used to drive turbines. Thus, it must be dissipated in some way so that some of this heat must escape to the atmosphere. This would be detected by a Landsat type satellite in the thermal band. In Figure 3.14 a small pond can be seen at **H** just outside the outer perimeter fence. The function of this is not clear from the panchromatic SPOT image.

Plutonium is separated from irradiated fuel elements by chemical means. A plutonium separation plant, completed by about 1966, is built underground in the reactor complex.

Figure 3.3. Enlarged Dimona reactor complex in which the possible reactor site and the plutonium separation plants are at (A) and (B) respectively. A fuel fabrication plant may be located at (C). A possible underground storage facility is located at (D). Scale 1:28,350.

Source: CNES/SPOT; image processed at the Defence Research Agency, Farnborough, UK.

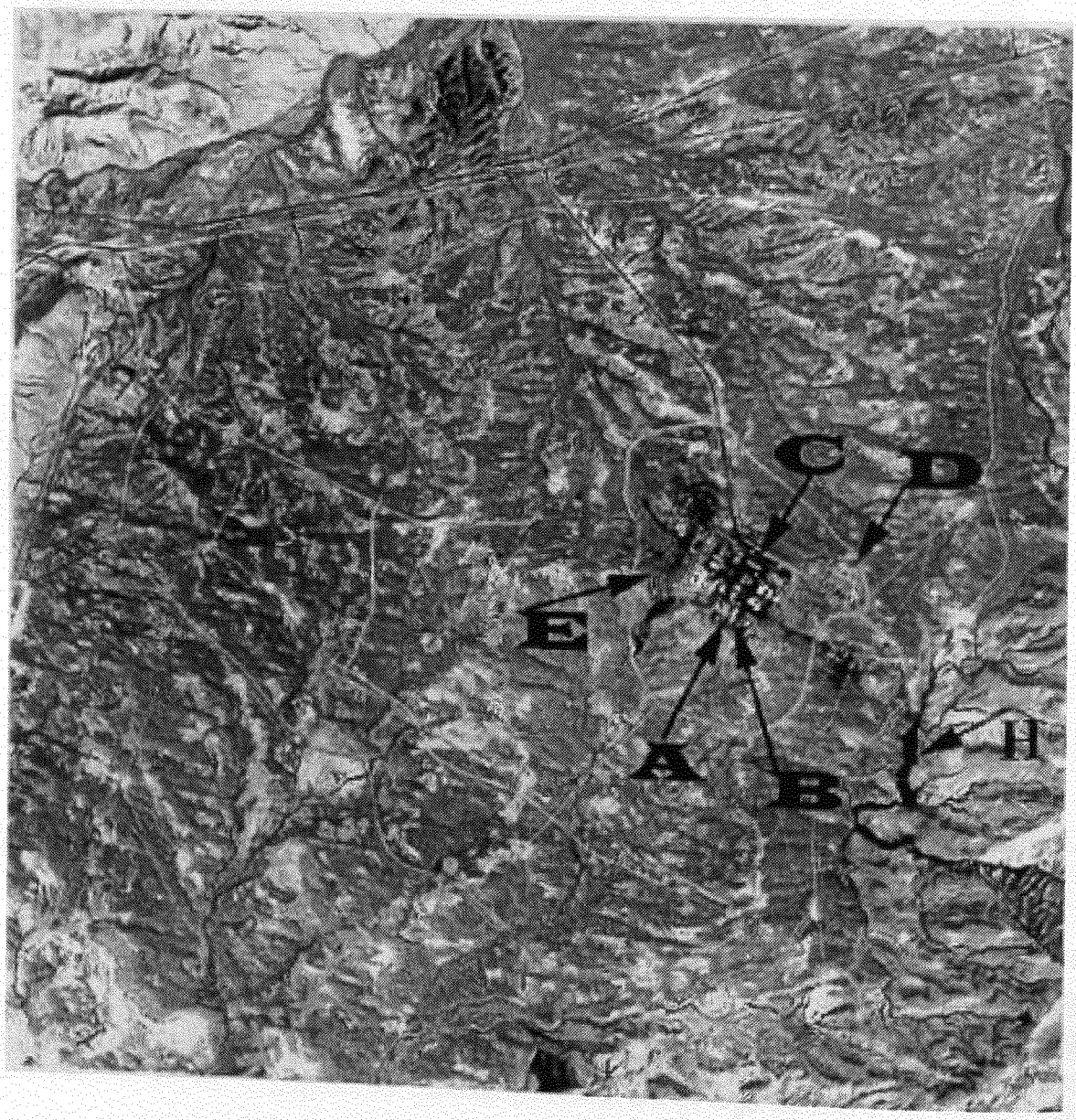

[30] **Space Media Network**, Stockholm, Sweden, private communications.

Figure 3.4. An enlarged sections (4) and (5) of Figure 3.12 showing the Dimona reactor complex (A) and the possible northern phosphate mine (B). The town of Dimona (C) can also be seen to the left of the Dimona site. The security fences (D, E, & F) protecting the reactor complex are clearly visible and marked in black. A road (G) linking the mine and the reactor facility can also be seen clearly. Scale: 1:85,000.

Source: CNES/SPOT; image processed at the Defence Research Agency, Farnborough, UK.

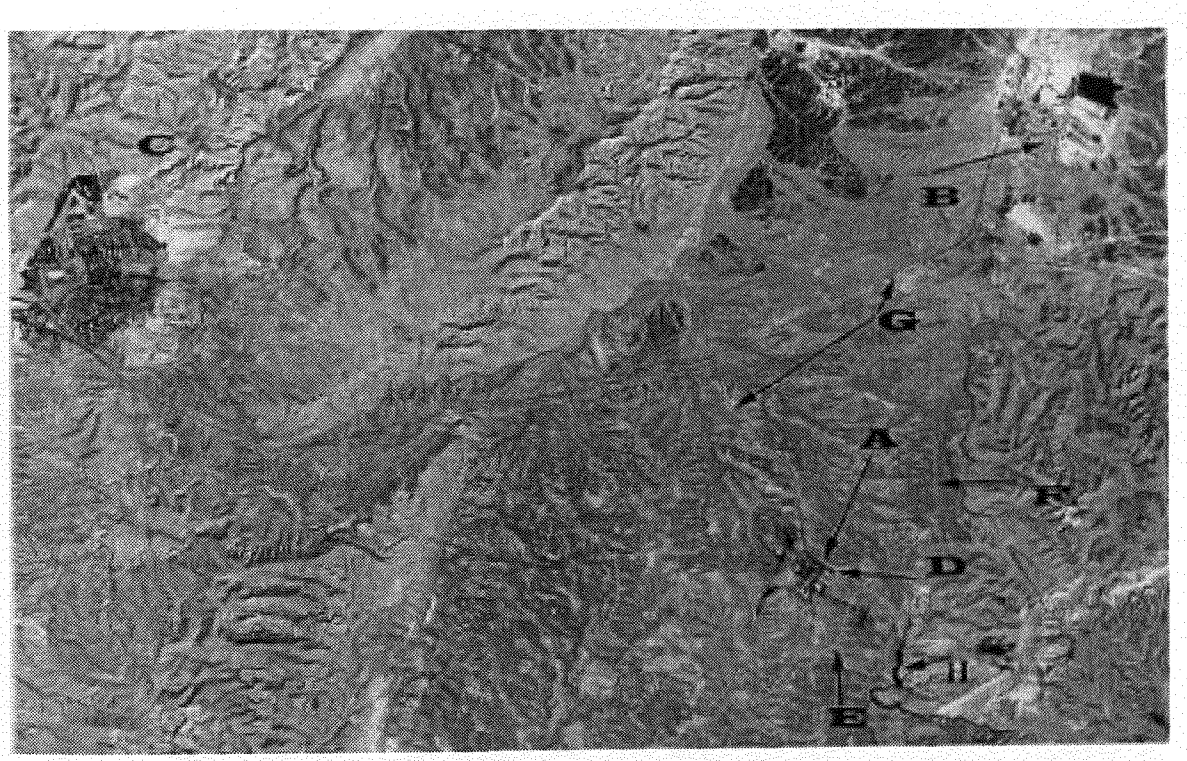

The plutonium production rate has been some 40kg per year.[31] Generally plutonium extraction plants are long buildings. It is possible that the building at **B** in Figure 3.13 may be such a plant.

The critical element in a nuclear fuel cycle is uranium. Israel has acquired this by various means. Its indigenous source is from phosphate mines in the Negev desert near Beersheba.[32] In Figure 3.12, two mining areas at **(5)** are identified. An enlarged section of the reactor complex and the northern mine are shown in Figure 3.14. It can be seen that the mine is linked to the town of Dimona (at **C**) by road and rail. The road also leads to the northern part of the reactor complex and to a long building (**C** in Figure 3.13) which may be where the fuel for the reactor is produced. The building is 140m long and 40m wide.

Covert facilities are generally very heavily secured by perimeter fences. The Dimona reactor complex is no exception. In fact three such fences can be seen in Figure 3.14. The outer most ring is a double fence. It may be argued that an ordinary industrial complex may also have perimeter fences as a defence against, for example, un-authorised intruders or terrorists, obviously a danger in this area. However, the use of three fences would indicate a possible high value facility. In addition to these, at **E** chevron like scars or planted trees can be seen. These may be planted for additional protection from any observers of the complex from the roads on the north and north-western sides of the reactor complex. A closer examination of the image in Figure 3.12 shows active defences, such as anti-aircraft

[31] *Ibid*, Perrin.
[32] *Ibid*, Spector, L.S., p. 191.

guns or missiles. Two possible anti-aircraft defence sites have been identified at (**7**) in Figure 3.12. Moreover, two very large military airfields are situated to the north and the south of reactor complex, which may well act as further active defences, although this may not be the only purpose for these airfields. In Figure 3.15, enlarged section **6** in Figure 3.12 shows one of these airfields. A conventional ammunition and a possible nuclear weapons storage sites can also be identified at **A**.

Figure 3.5. An enlarged section (6) of Figure 3.12 shows the second southern military airfield. At A, a possible high explosive or nuclear weapons storage area can be seen. Scale 1:28,350.

Source: CNES/SPOT; image processed at the Defence Research Agency, Farnborough, UK.

Often near such nuclear facilities high explosives and or nuclear weapons are stored. This does not appear to be the case for the Dimona site. However, to the north west of the complex some 25km (area **3** in Figure 3.12) in the mountains a large ammunition storage site was detected. It is possible that some nuclear weapons may be stored here. This is seen in the enlarged section in Figure 3.16 at

A. The bunkers that may be housing nuclear weapons are widely spaced compared to those at **B**. Also the whole area is bounded by a security fence.

Figure 3.6. Enlarged section (3) of Figure 3.12 shows the large conventional ammunition storage site at (B) with possible nuclear weapons storage area at (A). Scale 1:28,250.

Source: CNES/SPOT; image processed at the Defence Research Agency, Farnborough, UK.

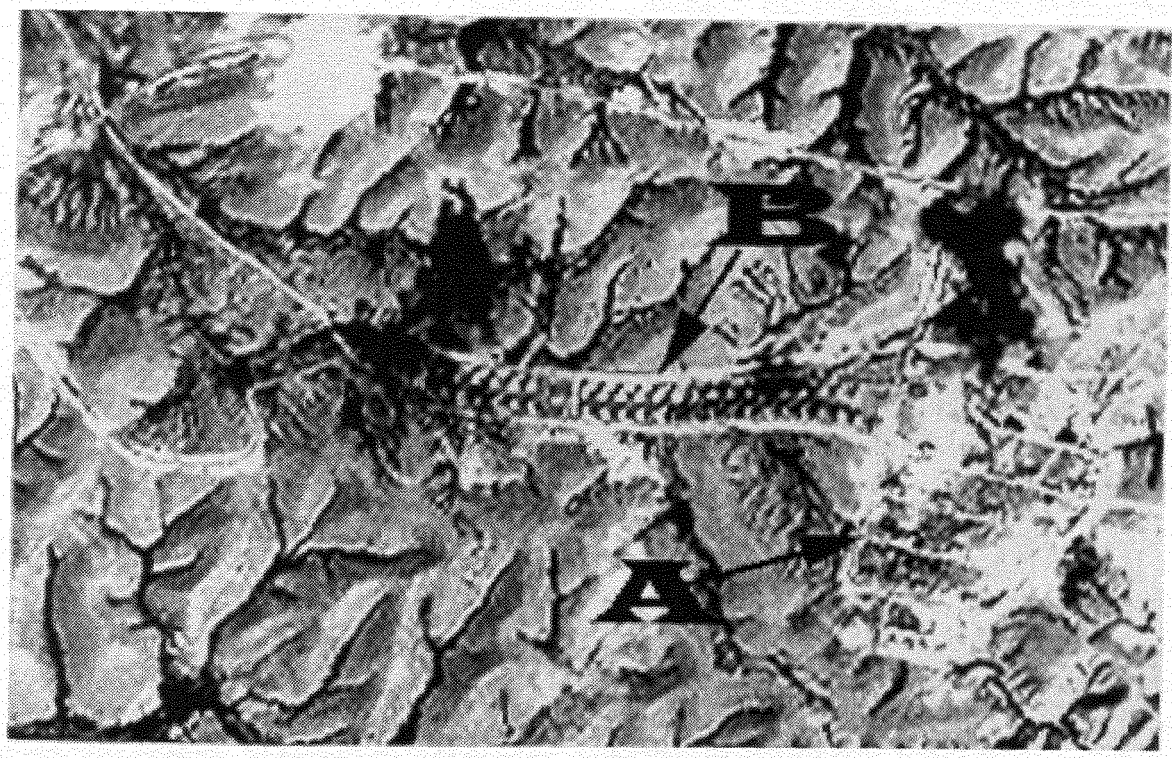

3.3 Pakistani nuclear facilities

Pakistan's sole known source of unsafeguarded fissile material is from its uranium enrichment plant at Kahuta. The first prototype centrifuges were manufactured at Sihala where blue prints for the construction of the Kahuta plant were also made.

Whilst the pilot centrifuge began operating in about 1979 at Sihala, it was not until 1984 that the first batch of partially enriched uranium was produced. High enrichment of uranium was achieved in 1986.[33] It is reported that there are between 1,000 and 14,000 centrifuges, which have produced about 100kg of the highly enriched uranium by early 1988.[34] The production rate is reported to be for two to three bombs per year.[35] However, Pakistan recently stated that the Kahuta enrichment plant has not been producing highly enriched uranium for some time and there are no plans to do so at present.

[33] "Scientist Affirms Pakistan Capable of Enrichment, Weapons Production", Nawa-I-Waqt (Lahore), 10 February 1984, (translated in Joint Publication Research Service/Nuclear Proliferation and Development, 5 March 1984, p.36.

[34] Senator Alan Cranston, "Nuclear Proliferation and U.S. National Security Interests", **Congressional Record**, 21 June 1984, p.S7901; and "Inside Kahuta", **Foreign Report**, 1 May 1986.

[35] **Nuclear Weapons and South Asian Security, Report by the Carnegie Task Force on Non-Proliferation and South Asian Security (Washington, D.C., Carnegie Endowment for International Peace, 1988).**

The Pakistan Atomic Energy Commission's main research centre is at Pakistan Institute of Nuclear Science and Technology (PINSTECH) at Nelore in Islamabad. This is located at (**1**) just outside Islamabad as shown in Figure 3.17 in an image acquired from a Russian satellite in April 1991. An experimental reprocessing plant has been developed at PINSTECH (see Figure 3.18). Another facility at Chashma is capable of reprocessing 100,000 kg/a of spent fuel. In the Dera Ghazi Khan area, mining for uranium is being carried out. Also at this site, uranium is converted to uranium hexafluoride for enrichment process. The capacity is just over 190,000 kg of hexafluoride per year.[36] The Atomic Research Reactor facility in the Kahuta area is detected at (**1**) in Figure 3.17 and enlarged in Figure 3.18. The geographical location of this site computed from the SPOT image is 33^0 39' 7" north and 73^0 15' 30" east. The image in Figure 3.18 was compared with that obtained from a SPOT image. As expected, the two metre (photographic) resolution reveals considerable details. For example, buildings at the complex **A** are resolved in Figure 3.18. As this complex has a strong perimeter fence, it is possible that the experimental reprocessing plant mentioned above may be located here. Also, individual bunkers in the ammunition storage area are resolved. The road **C** out of the Research Reactor Centre leads to a dam, north-east of this site, (**2**) in Figure 3.17.

Finally, Pakistan has only one commercial nuclear power plant, the 125MWe KANUPP (Karachi Nuclear Power Project) reactor near Karachi. It also has two small research reactors, Pakistan Research Reactor, PARR-1 and PARR-2. Both these are under the IAEA safeguards.

The two images over Islamabad were acquired at two different resolutions; 10m (pixel) SPOT satellite and about 1m (equivalent pixel) Russian KVR-1000 sensor with the hope of detecting Pakistan's enrichment activities in the Kahuta area. The present analysis indicates that the Kahuta enrichment facility is not covered by either of these two images. However, the Russian image reveals many details on the defence related activities south of the Atomic Research Reactor. It can be seen from Figure 3.18 that the PINSTECH complex has a perimeter fence. Pakistan's enrichment plant, not in either of the two images analysed, is located to the south-east of the Research Reactor Centre complex. At a first glance, the security round these facilities seems very light. However, the Russian image, which covers larger area south of Islamabad, revealed a military airport at (**3**) south-west of the Research Reactor complex in Figure 3.18. Moreover, to the south of this a surface-to-air missile site was also detected at (**4**).

[36]Weissman and Krosney, The Islamic Bomb, (New York: Times Books, 1981), pp. 81, 219.

Figure 3.7. The full panchromatic scene over Islamabad (A) acquired by a Russian satellite in April 1991 where PINSTECH and Pakistan's Atomic Research Reactor near Kahuta area are located at (1); a large dam at (2); a military airfield at (3); and a missile site at (4) can also be detected. Scale: 1:220,000.

Source: Transasia, UK.

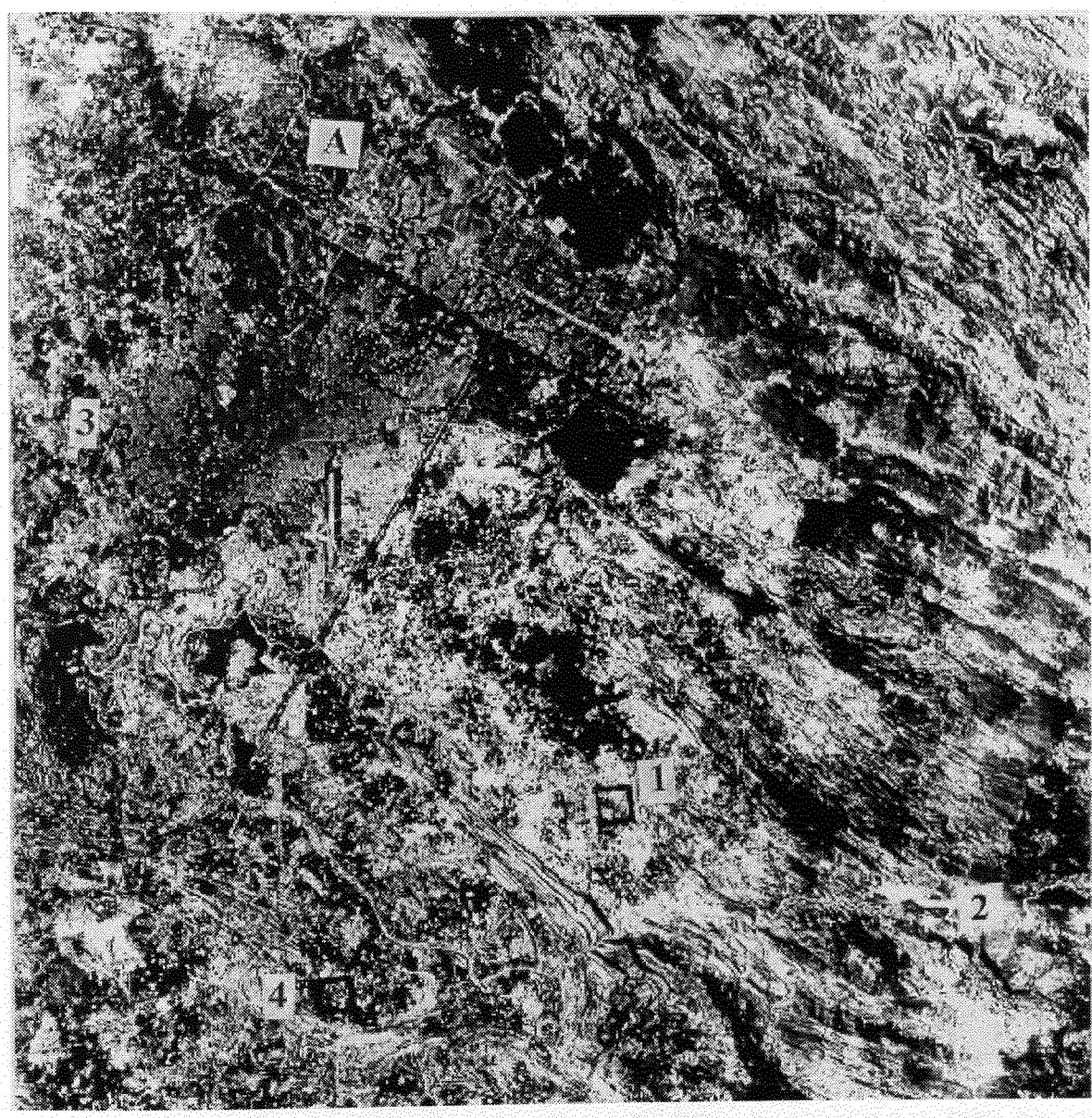

Figure 3.8. An enlarged section (1) from Figure 3.17 showing the Atomic Research Reactor facility. Buildings at (A), and the ammunition storage areas at (B) are seen more clearly than those in a SPOT image. Also the sites at (A) and (D) have perimeter fences indicating a sensitive area. Scale: 1:20,000

Source: Transasia, UK.

3.4 The DPRK's nuclear facilities

On 4 May 1992, the DPRK in its initial report to the IAEA submitted a list of nuclear facilities and material that would come under the IAEA's safeguards. These are summarised below [37].

There are four locations where some of the important facilities are situated or are under construction. These are:

1. PYONGYANG:

- where a Soviet supplied IRT pool type 8MWth research reactor is located; it is fuelled with 80% enriched uranium supplied by the former USSR; it is used for isotope production, neutron scattering experiment, neutron radiography, nuclear chemistry and for training purposes. The facility, under the IAEA safeguards, measures 6 x 10 x 10m high and it has been in operation since 1965[38];

- hot cells, supplied by the former USSR, are also located at the Institute of Nuclear Physics, Kim Il Sung University; they were supplied during 1960s or 1970s; pilot studies on ^{239}Pu separation have been carried out;[39]

2. *YONGBYON* where at least three important facilities are located:

- 5MWe experimental gas-graphite reactor in operation since 1985 or 1986; capable of producing some 4 to 7kg of ^{239}Pu per annum;

- a larger 50MWe reactor, capable of producing some 40 to 60kg of ^{239}Pu per annum, has been under construction;

- a fuel fabrication plant;

- a reprocessing plant, some 180m long and six stories high, appears to be completed;[40]

- Soviet supplied 0.1MW critical assembly.

3. TAECHON , PAKCHON, & PYONGSAN:

- a 200MWe power plant is under construction expected to be completed in 1996; this could produce some 160-200kg/a ^{239}Pu; each site has uranium mine and uranium concentrate plant; and

4. SHIN PO:

- proposed site for three 635MWe power reactors.

---

[37]IAEA Newsbriefs, vol. 7, no. 3(55), June/July 1992, p.3.
[38]**IAEA Directory of Nuclear Research Reactors**, 1989, pp. 100-101.
[39]Albright, D., and Hibbs, M., "North Korea's plutonium puzzle", **Bulletin of the Atomic Scientists**, November 1992, pp. 36-40.
[40]***Ibid.***

It can be seen that the major nuclear facilities are at Yongbyon. It has been reported that DPRK has based the design of its nuclear power reactors on that used for the Calder Hall reactors in the UK.[41] The cooling water from the condenser is allowed to fall in a spray into a pond in the cooling tower. As the water falls it is cooled by the current of air forced up through the cooling tower by convection. It may, therefore, be possible to detect this in the Landsat image in the thermal band.

Two images acquired over this area by the French SPOT satellite were examined. These were a multispectral image with 20m pixel resolution taken on 11 June 1986, and the other a panchromatic image with 10m pixel resolution taken on 19 September 1989. A Landsat 4 image of the same area was also acquired on 1 June 1992 in order to see whether it is possible to pin-point the location of the 5MWe reactor from the detection of possible emission of heat or a cloud of condensed air from the cooling tower of the reactor.

A panchromatic full scene over Yongbyon is shown in Figure 3.19 in which the town of Yongbyon is identified at **B** and the nuclear facilities at **A**. Whilst no active defences such as anti-aircraft gun or missile sites were found, three military airfields were identified at **C, D** and **E**. At **F** a large ammunition storage site was found. The equivalent area **A** in the SPOT multispectral and panchromatic images was enlarged and are shown in Figures 3.20 and 3.21 respectively. At these resolutions, it is difficult to identify the nature of the facilities in the area except to indicate that the area is isolated and some facilities have security fences indicating the military nature of the activities. However, over the period 11 June 1986 and 19 September 1989, the areas south and south-west of Yongbyon have been considerably developed. A more extensive road network has been laid and natural vegetation has been cleared around various sites for further development. The panchromatic image enabled detection of a possible railway line which links complexes **A, C** and **E** (Figure 3.21) from north-west coming from south of the site **A**, crossing the river before passing through the site **C**. In the 1986 image, site **A** is the only one that is well developed. Some construction had started at sites **C, D**, and **E**, while the ground at site **F** had been prepared but little construction had taken place (compare Figures 3.20 and 3.21).

[41]"North Korea's nuclear power programme revealed", **Nuclear Engineering International,** July 1992, vol. 37, no. 456, pp.2-3.

Figure 3.9. Full SPOT panchromatic scene over Yongbyon (B), North Korea. The nuclear facility is identified at (A) and three military airfield are at (C), (D) and (E). At (F) a large ammunition storage area was identified. The image was acquired on 19 September 1989. Scale: 1:340,000

Source: CNES/SPOT; image processed at the Defence Research Agency, Farnborough, UK.

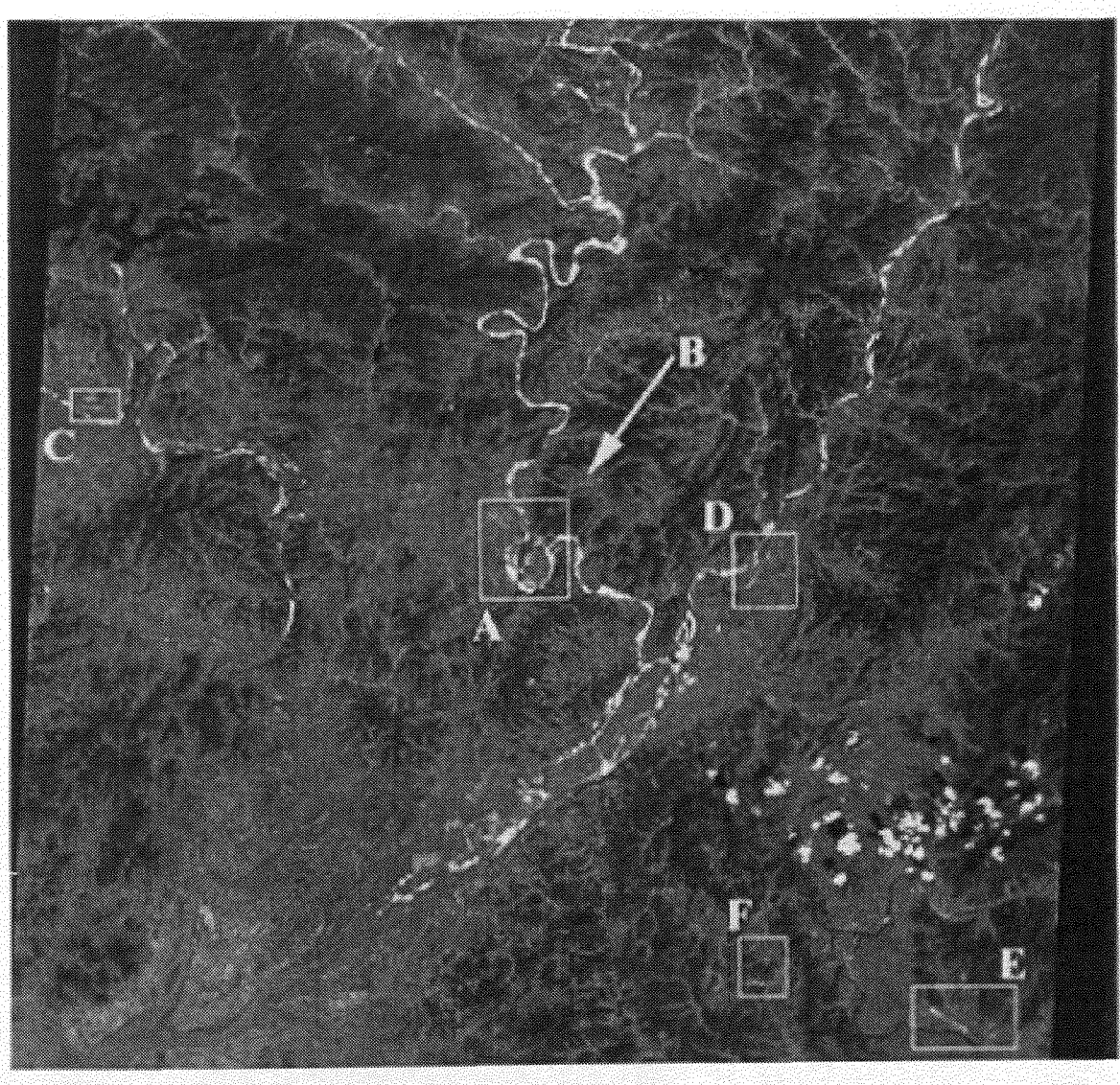

Figure 3.10. An equivalent area (A) in Figure 3.19 is enlarged from a SPOT multispectral image acquired on 11 June 1986 where band 1 is green, band 2 blue and band 3 is red. The Soviet supplied reactor may be at (A). Area (B) is a residential area. See the text for sites (C), (D), (E), and (F). Scale: 1:45,000

Source: CNES/SPOT; image processed at the Defence Research Agency, Farnborough, UK.

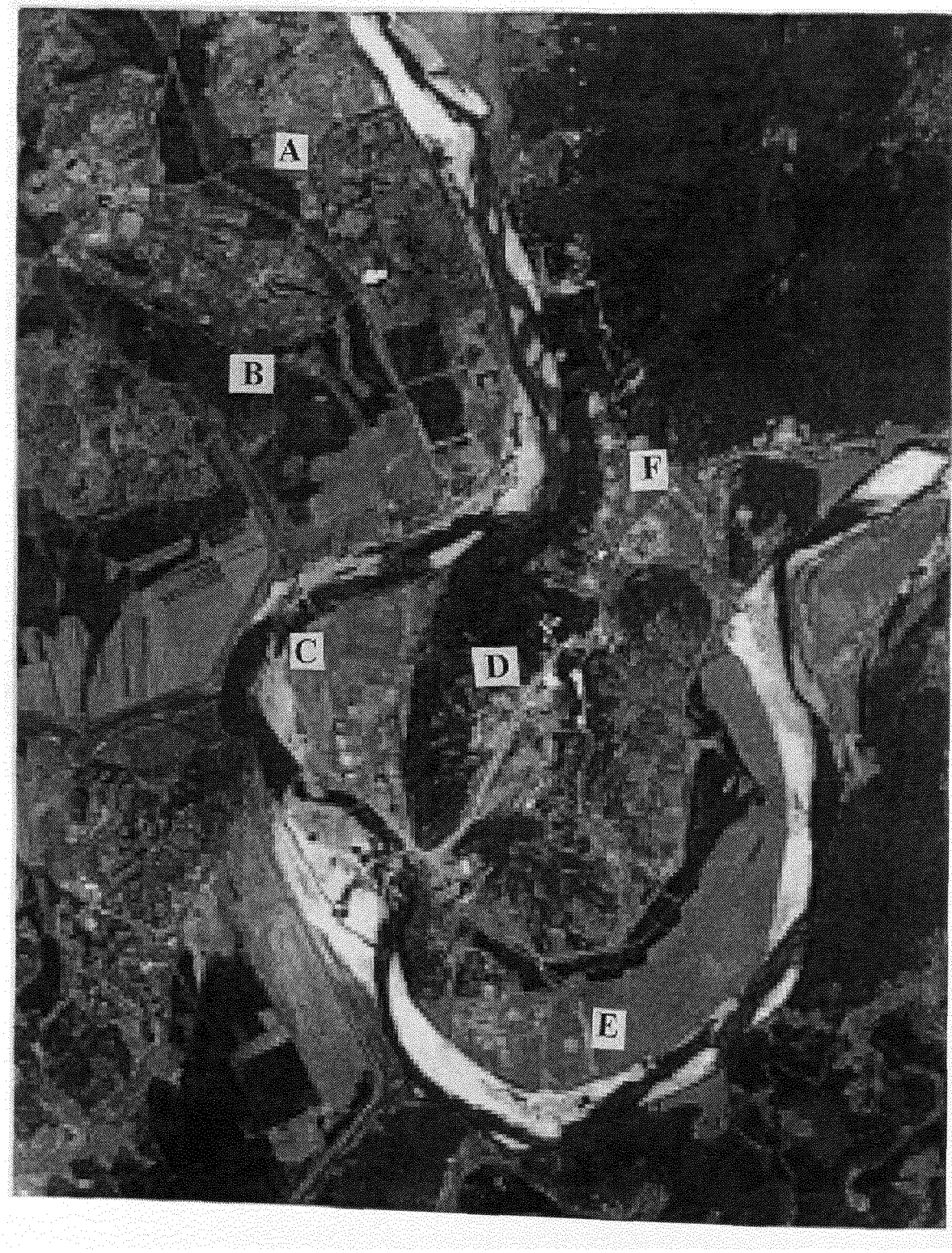

Figure 3.11. Enlarged section (A) from Figure 3.19. Comparing with Figure 3.20, it can be seen that considerable development has taken place between 11 June 1986 and 19 September 1989. For various sites, see the text. Scale: 1:28,300

Source: CNES/SPOT; image processed at the Defence Research Agency, Farnborough, UK.

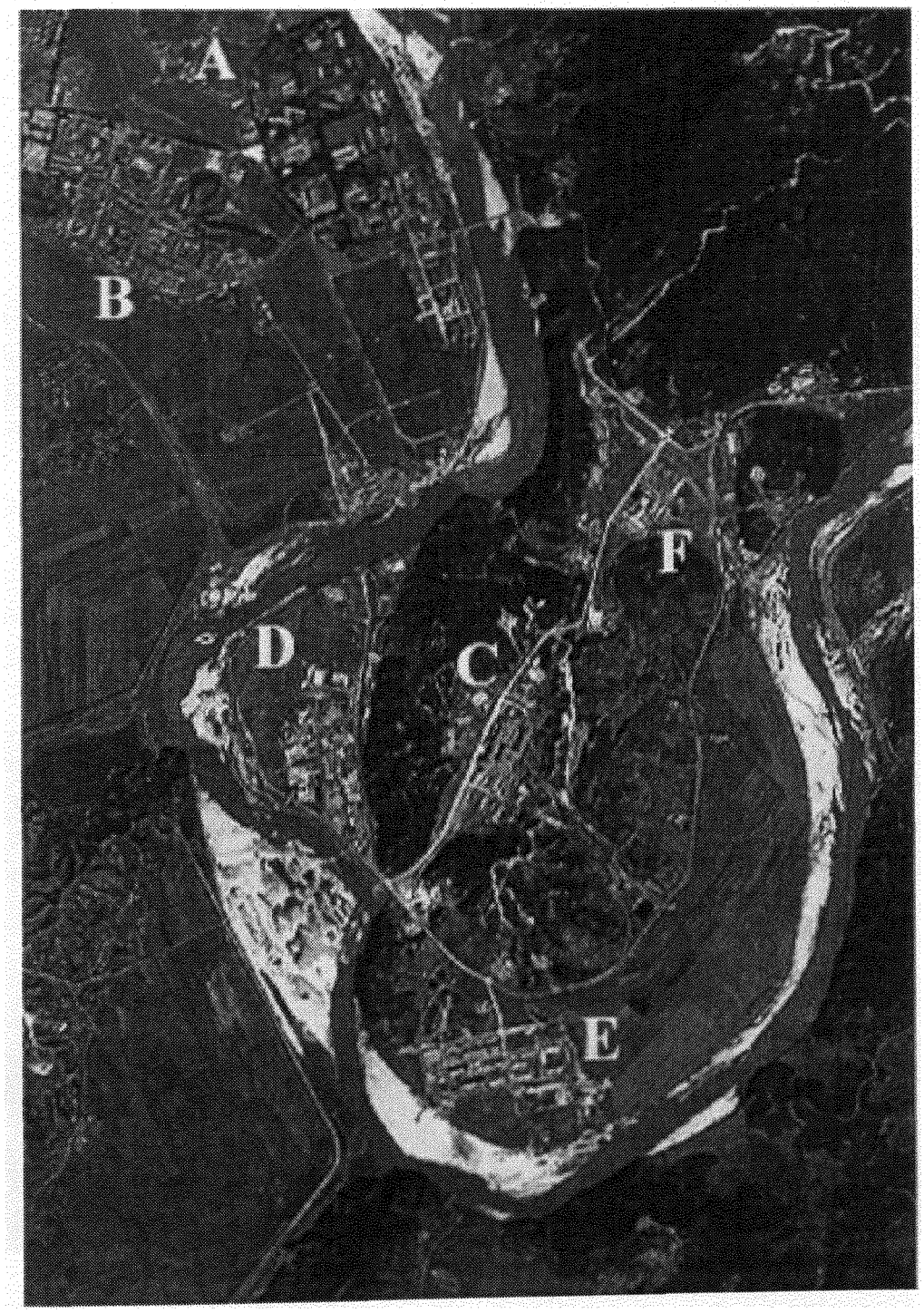

Thus, it is reasonable to assume that site **A** is where the Russian supplied research reactor and the sub-critical facilities are located. These facilities were acquired from Russia in 1965. It is the largest area within the complex divided into two by a road running north-west to south-east. The site on the right close to the river is divided into about seven sections each containing large buildings. This probably is the research area with the nuclear installations and some support facilities and administration buildings. The complex **B** to the left of the road may be the accommodation units arranged in rectangular pattern. The complex is linked to site **F** east side of the river by a possible rail bridge constructed between 1986 and 1989. An attempt was made to locate and determine the operational characteristics of the 5MWe reactor using the Landsat 4 thermal band. An enlarged section of the nuclear facility is shown in Figure 3.22 which is a combination of bands one (blue), two (green) and three (red). This shows that much of the area that was undeveloped in June 1986 is developed by 1992.

Radiation from various parts of a similar extract from the thermal band was examined. The image was unstretched in order to avoid changes in the pixel values. It was found that maximum response was obtained at **1** and **2** (Figure 3.22). This may be because the buildings are new and, therefore, reflecting light in the visible range of the electromagnetic spectrum. However, as this area was not developed in 1986, it is fair to assume that the reactor cannot be located here because it did not become operational until some time in 1986 or 1987. The next intense responses were from areas **3, 4** an **5** but these have been found to be bare land on the SPOT satellite's high resolution image. It is possible the land has been prepared for building constructions and foundation may have been laid. Other high spots were detected at **6** and **7**. These buildings were constructed by 1986 so one of these may be the 5MWe reactor. The heat source may be a cooling tower. It should be remembered that the sensor on board the satellite measures the surface temperature only and not the body temperature. Also the software used, (IDRISI and Photoshop) convert the data in the thermal band into blackbody temperature. In order to obtain the real surface temperature it is necessary to apply a correcting factor given by the emissivity of the surface being sensed. In the present study this conversion has not been attempted. Nevertheless, the blackbody temperature measurements can be useful as relative values. The temperature values at **6** and **7** were 23.6°C and 24.4°C respectively. In this way temperatures of various other buildings in the complex were also determined. They were all found to have temperatures within the range 22.7±0.5°C. Clearly a high resolution image would clarify this.

Another indicator of the operation of a reactor is the discharge of hot water into a nearby river or a lake. In the case of the Yongbyon complex, it is built on the west bank of the River Kuryong. Therefore, it is possible that some warm water from, for example, the turbine condenser, may be discharged into the river.

Figure 3.12. A section from a US Landsat 4 multispectral image acquired on 1 June 1992 showing the North Korean nuclear complex. The image is a combination of bands one (blue), two (green) and three (red). Scale: 1:143,000

Source: EOSAT/Landsat; image processed at the Defence Research Agency, Farnborough, UK.

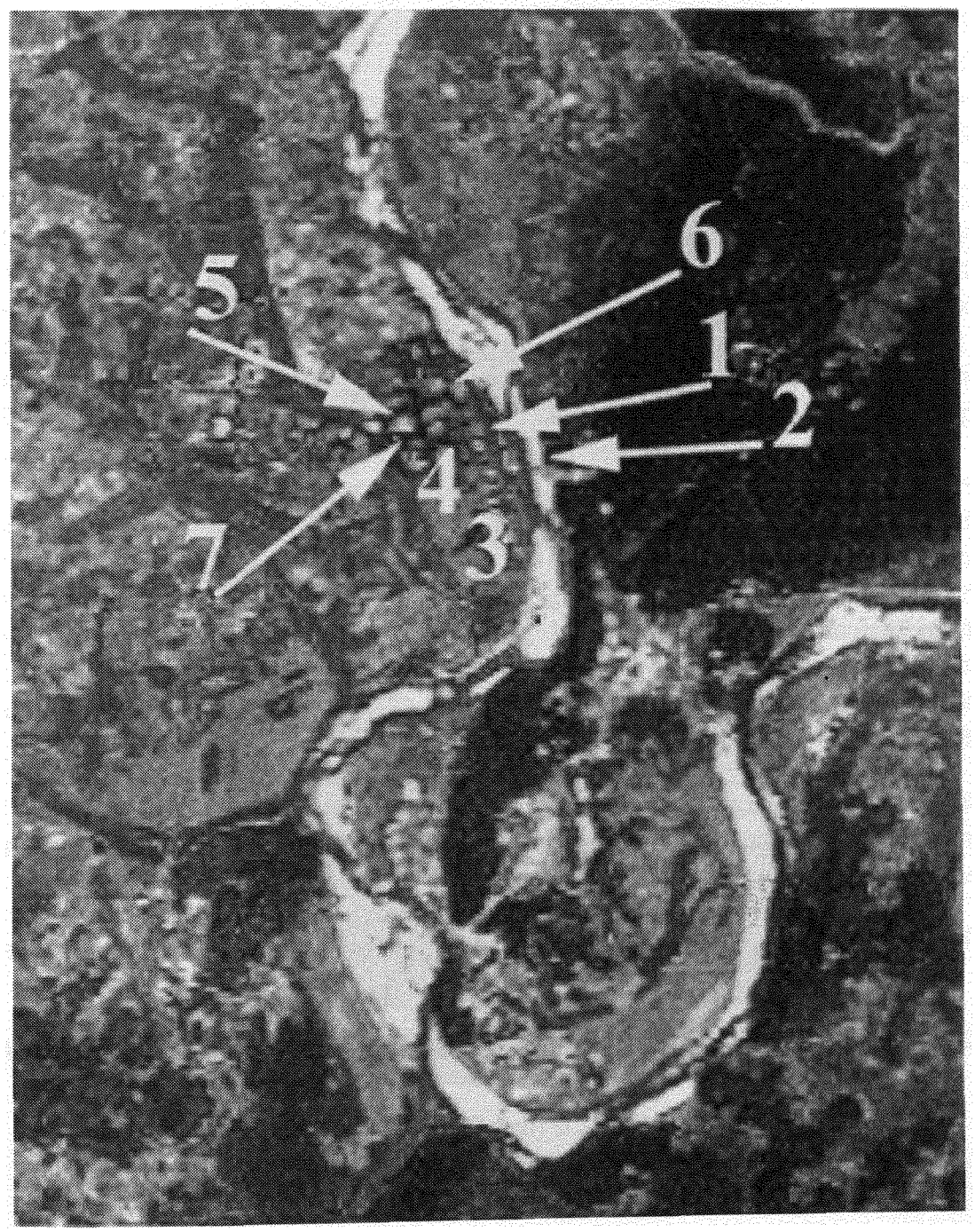

An attempt was made to detect this in the river using the thermal band of the Landsat image. Using the band five, as it gave a very clear image (lack of atmospheric effects), a line was drawn on screen interactively through the middle of the river shown in Figure 3.22. This vector drawing was then transferred to the image from the thermal band and the corresponding pixels were examined for transmitted radiation. Different values of radiance were assigned different colours to generate a density sliced image shown in Figure 3.23. It can be seen that radiation emission is generally evenly distributed. In other words the colour distribution does not look very different at **A** in the vicinity of the nuclear complex, than that produced along the northern part of the river before it reaches the nuclear complex.

One problem here is that the river is narrow with respect to the spatial resolution of the sensor. For example, at its maximum width is about 115m and it can be as narrow as some 60m. The resolution of the thermal band is 120m. Thus, considerable uncertainty can be introduced in the temperature measurements since a single pixel may or may not cover the water alone. Over the narrow parts of the river, it is possible that only half a pixel comes over the river and the other half will be over the land. The radiance in this case will be the result of an integrated response over the land as well as over the river. It might be suggested that when temperature detection and measurements are involved, it might be more useful to acquire images at night local time or even to use radar (SAR). A second complicating factor is the varying depth of the river which may affect the thermal characteristics. In fact the SPOT panchromatic image indicated that the river is shallow in the region of the suspected reactor facility and becomes deep towards the southern part of the river. These factors make it difficult to interpret the thermal images when the operational characteristics of a facility are studied. It has been suggested that the "radiochemical laboratory" is located at **C** (Figure 3.21).[42] The buildings here consist of four main rectangular blocks, the largest of which measures 120m x 80m and several other smaller support-type buildings. There is little evidence for major expansion in this area. Resolution limitations preclude the identification of any security fences or other security measures.

In the report of the Director General of the IAEA to the member states, it is stated that "it was essential to obtain access to, and take samples from, two sites which the Secretariat has reason to believe are nuclear waste-related:

1. The site which Agency officials had visited on 14 September 1992 and which was located east of the radiochemical Laboratory; and

2. A site on the opposite side of the road from a nuclear waste storage site shown to Agency inspectors."[43]

[42]de Selding, P., "Photos indicate N.Korean growth in nuclear ability", Space News, vol. 1, no. 9, 12-18 March 1990, pp.1 20.
[43]*Ibid*, **INFCIRC/419**, p. 5.

Figure 3.13. The line represents the middle portion of the river Kuryong. All the pixels from the image from the thermal band along this line are represented in this drawing. The different amount of radiation was assigned a different colour. There are no signs of concentration of a particular colour in the vicinity of the reactor complex.

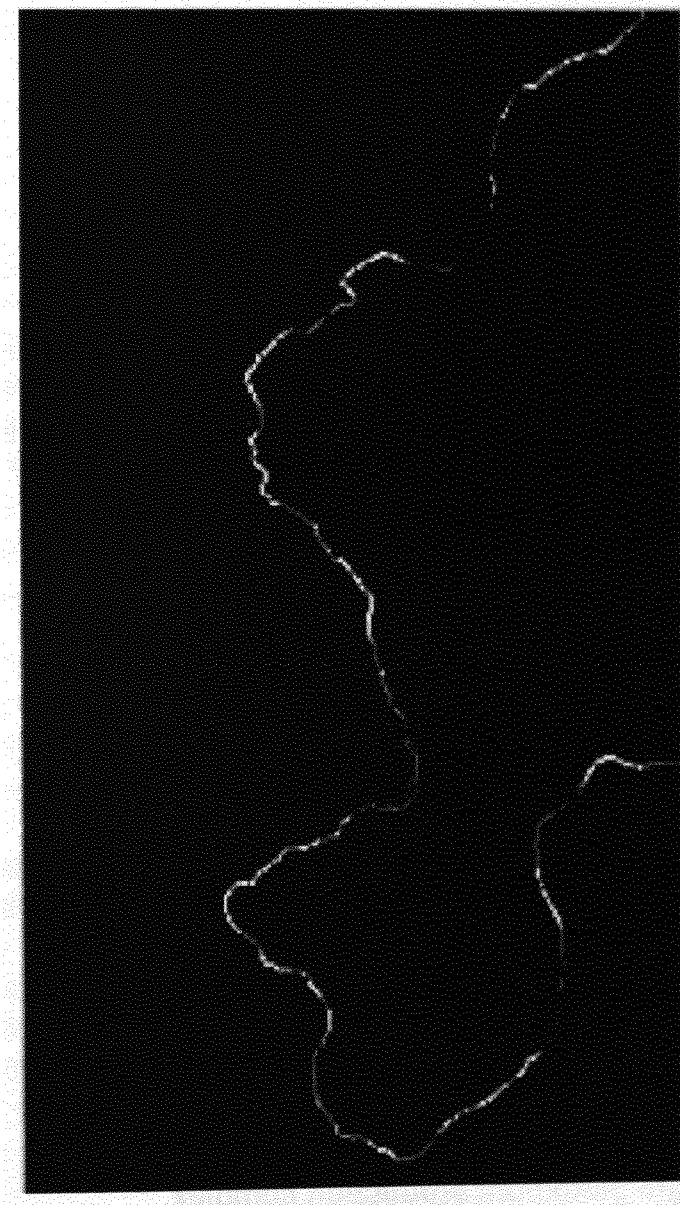

This may be referring to buildings on the eastern side of the road dividing the complex. While there are some large buildings here, they are not multi-storey ones (as suggested by lack of long shadows).

Site **D** is east of site **C** separated by hills. Two large building dominate the centre of the site. The multi-storey buildings, as indicated by long shadows, are of "I" and reverse "L" shapes and are approximately 190m x 20m and 180m x 20m respectively. Their form suggests large administration or research buildings. Again, no security fencing can be identified. To the eastern side of the road, which bisects the site, are a further group of buildings that extend back into the natural vegetation on the hillside.

It has been suggested that the 50MWe power plant is located in the southern part of the complex at **A**.[44] The complex consists of five to six rectangular multi-storey buildings, with the largest to the south east and west of the site. Those in the south-east measure approximately 180m x 30m, whilst those in the west are 70m x 30m and 150m x 30m. The largest building might be a reactor as a possible water inlet and outlet run from the south-east corner of the complex to the open river. The inlet was not apparent in 1986 due to extensive sediment deposition on the meander. Either of the other two buildings may be the reprocessing plant under construction. The site has been considerably expanded since the 1986 image with a new internal grid pattern roadways. There is little evidence of an electricity transmission yard, pylons or other infrastructure associated with power generation, nor are there any signs of an active plant.

Site at **G** in Figure 3.20 consists of a cluster of buildings to the north of the main complex on a hill. It is linked to site **F** to the south by a road constructed after 1986. The purpose of this site in not clear. It may be some kind of observation post as the whole complex can be viewed from this site.

The site **F** has grown to be the hub of the new road network. It probably controls the access to the whole complex. The site has remained at a similar size to the 1986 image. No major development has taken place.

The above analysis indicates the usefulness of low resolution images for detecting changes in an area. Not only this but relatively low spectral resolution of the SPOT sensor (compared with the Landsat satellite) can be useful.

3.5 Russian Kyshtym plutonium production complex

In this section the Russian plutonium production plants at a complex east of the town of Kyshtym in Chelyabinsk Province is studied using two Landsat 5 TM images acquired on 1 August 1987 and 13 May 1993. The site, Chelyabinsk-65, formerly referred to as Chelyabinsk-40, is the first of the four sites where the Russian plutonium has been produced. The other three facilities are at: (2) Dodonovo, on the Yenisey River north-east of Krasnoyarsk in Siberia; (3) the "Siberian plant" is located near Troitsk or Tomsk; and (4) at Beloyarskiy, near Sverdlovsk.[45] A recent Russian reference lists only three locations where plutonium production plants are located. These are the Chelyabinsk-65 (the above mentioned

[44] *Ibid*, de Selding.

[45] Cochran, T B., Arkin, W M., Norris, R S., and Sands J I., **Nuclear Weapons Databook-Soviet Nuclear Weapons**, vol IV, 1989, pp.79-83, (Natural Resources Defense Council/Harper & Row, Publishers, New York).

first facility) with five reactors, Tomsk-7 (number 3 mentioned above) with five reactors and Krasnoyarsk-26 (number 2 mentioned above) with three reactors.[46]

The first plutonium production reactor (AV-1) at Chelyabinsk-65 achieved criticality in June 1948 and produce plutonium for the first Soviet nuclear test in August 1949.[47] This and four other reactors subsequently built at the Chelyabinsk-65 complex were graphite-moderated, natural-uranium-fuelled water cooled reactors. A fuel reprocessing plant with a capacity of 500tHM/a and a pilot vitrification plant were also built in the same complex.[48] The former was built to reprocess fuel from the power reactors as well as that from the propulsion reactors of ice-breakers and submarines.[49] Water from the Lake Kyzyltash (see map in Figure 3.24) was used to cool the reactors. Between 1949 and 1950, storage tanks for the high level nuclear waste were built some 1.5km from the reprocessing plant. In 1957 one of these tanks began to leak and in September 1957 the tank exploded causing wide spread contamination of the area.[50] It has been reported that, since 1949 low and medium level waste has been discharged in the River Techa (see the map in Figure 3.24). By about 1955 or 1957 the river became so polluted that inhabitants some 150km downstream had to be evacuated and two dams, one of these can be seen in an extract of the Landsat image (Figure 3.25) of the area in Figure 3.24, and artificial reservoirs were built to stop the flow of the river. Despite the fact that the Lake Kyzyltash, the River Techa and the reservoirs were heavily polluted, the water from them continued to be used for cooling the reactors.[51]

Figure 3.25 shows a false colour combination of bands 2 (red), 3 (blue) and 4 (red) of the 1993 Landsat image with the main features of the Chelyabinsk facilities interpreted. Complex 1, south of the Lake Kyzyltash appears to be the site of the early reactors. The site of the new reactors is shown as complex 2, which is north of the reservoir constructed on the River Techa. The two sites are clearly linked by a road. Within complex 1 a large, long building can be detected due to its high reflectance properties in the visible bands of both Landsat images. A large area of deep shadow appears next to the building which indicates that it is considerably taller. The physical appearance of this building suggests that it may be a plutonium reprocessing plant. A number of other buildings can be distinguished within the complex but their roles are more difficult to interpret. However, there appears to be a feature which links complex 1 and Lake Kyzyltash which is possibly the route of cooling water pipelines. If this is the case, then the buildings where the pipelines originate may be the reactors. Within each of bands 1 to 4, there is evidence of a fence extending around the perimeter of the complex. A false-colour composite of bands 4, 3 and 2 defines this feature more clearly.

[46]Diakov Anatoly, "Plutonium", Nezavisimay Gazette, 12 May 1994.
[47]*Ibid*, Cochran et al.
[48]Barker, K., "Reprocessing and HLW management in the USSR", **Nuclear Engineering International**, vol. 36, no. 440, March 1991, p.42.
[49]Bibilashvili, Yu. K., and Reshetnikov, F. G., "Russian nuclear fuel cycle", **IAEA Bulletin**, vol. 35, no. 3, September 1993, pp. 28-33.
[50]Medvedev, Z., "Bringing the skeleton out of the closet", **Nuclear Engineering International**, vol. 35, no. 436, November 1990, pp.26-32.
[51] *Ibid*, Medvedev.

Figure 3.14. Map showing the Chelyabinsk area. The nuclear complex studied is near Kyshtym. The area covered by the image is also indicated.

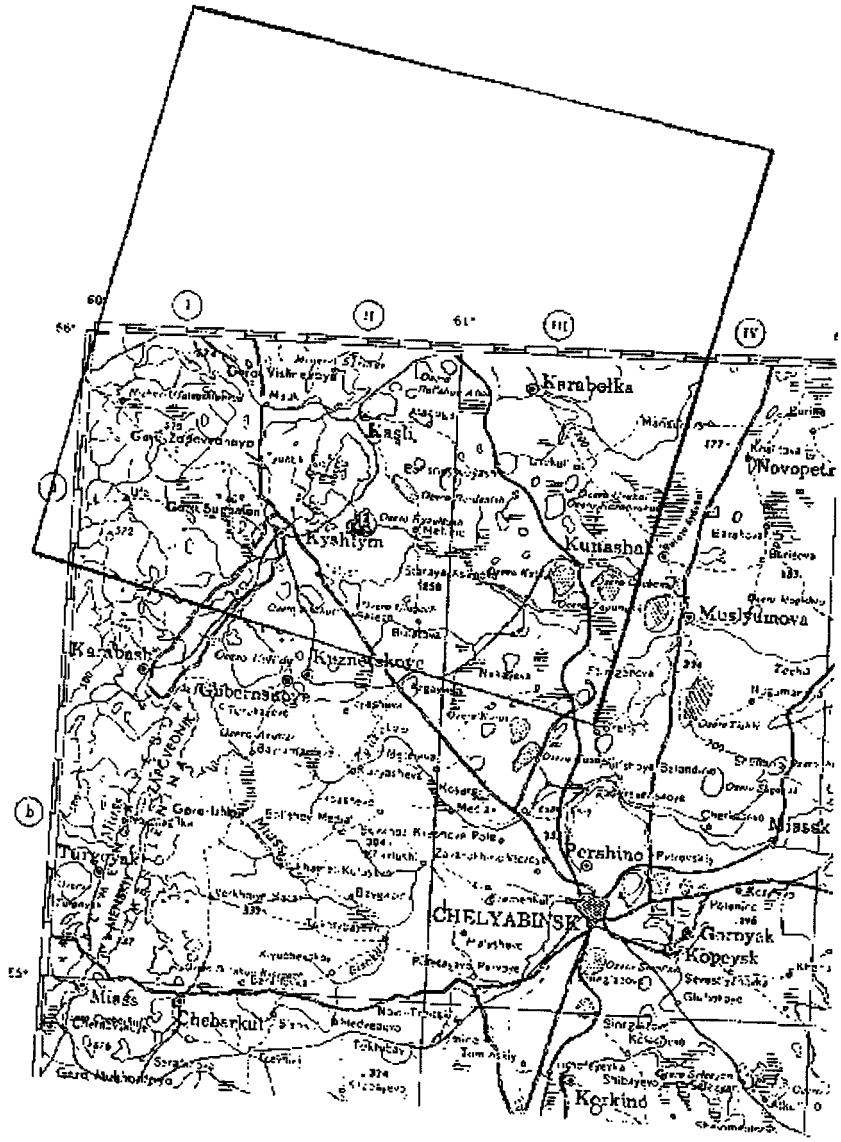

Figure 3.15. Bands 2 (blue), 3 (green) and 4 (red) of Landsat TM multispectral image acquired on 13 May 1993 with some features interpreted. Scale: 1:143,000

Source: EOSAT/Landsat; image processed at the Defence Research Agency, Farnborough, UK.

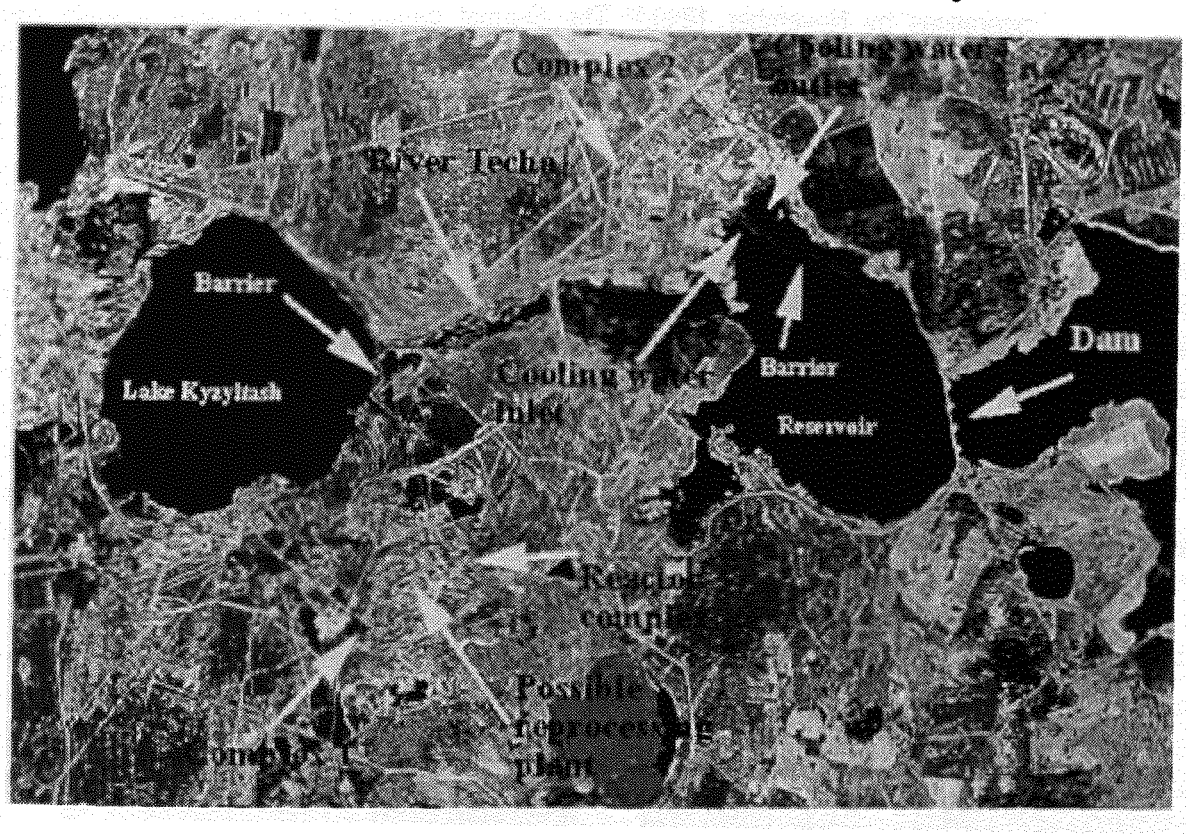

There is little evidence of any changes taking place within or around complex **1** between 1987 and 1993. In contrast, at complex **2** a large number changes in the physical characteristics of the facility can be identified through differences between the 1987 and 1993 images, particularly in the visible and near-infrared bands. Such changes can be identified using these bands individually (e.g. Figure 3.26), but false-colour composites of bands 4, 3, and 2 for each date help to enhance the images for visual interpretation. The 1987 images appears to show a number of disturbed, un-vegetated surfaces within the complex, which are indicative of an early phase of construction. By 1993 the individual buildings within the complex can be more clearly identified and several areas and roadways which had formerly been used for construction activities now appear to be re-vegetated. One notable difference between the two dates is that in the 1987 image a feature can be clearly identified which links the complex with the reservoir. In the 1993 image there is no evidence of this feature in any band. It is suspected that this is a channel along which pipelines have been laid for transporting cooling water between the complex and the reservoir. Once installed, the pipelines have been covered over and the area re-vegetated. Both the 1987 and 1993 images show evidence of a railway line extending north-east of complex **2**. No railway line appears to be associated with complex **1**.

In addition, the images show evidence of active defences such surface-to-air missile (SAM) sites and ammunition bunkers similar to those identified in images of Dimona and Baghdad nuclear sites. For example, two possible SAM sites are located to the south of the reactor facility. A large missile field is found north of Kyshtym. Also there at least two military airfields located to the north-east and south-east

of the reactor complex. Moreover, to the east of this site a very large ammunition storage facility was found.

In June 1989 two of the five reactors at Chelyabinsk-65 were shut-down and the remaining ones stopped their operations by November 1990.[52] The thermal bands of the Landsat images were analysed in order to investigate the use of water from Lake Kyzltash and the artificial reservoir by the facilities for cooling purposes. Within IDRISI and the Photoshop the algorithms called Thermal and Black body respectively were used to convert the digital number values in band 6 of each image to black-body temperature values in degrees Celsius. The images shown in Figure 3.27 were created by using band 4 to create a mask which delineated the Lake Kyzyltash. This mask was then applied to the thermal images. In the 1987 thermal image, a plume of warm water can be clearly seen extending north for a considerable distance along the eastern fringes of Lake Kyzyltash. The surface temperature of the water within this plume is a maximum of 10°C warmer than the bulk of water in the lake. The plume of warm water enters the lake from behind a barrier constructed in the lake which, presumably, is used to separate the inlet and the outlet of the water used for the reactors.

Figure 3.16. This shows the complex 2 in false colour composite of bands 1 (blue), 2 (green) and 3 (red) of Landsat TM multispectral image. The left image was acquired in 1987 and the one on the right in 1993. Scale: 1:143,000

Source: EOSAT/Landsat; image processed at the Defence Research Agency, Farnborough, UK.

If the plume of warm water is a discharge of cooling water effluent from complex **1** then it can be suggested that the reactors at this site were operating at the time of acquisition of the 1987 image. This observation confirms the reported operational status of this complex for this date. However, an examination of the 1993 thermal image of Lake Kyzyltash shows that the warm plume of effluent water is still evident, and it is in fact larger in spatial extent and thermal magnitude, being a maximum of 15°C warmer than the bulk of water. Thus, contrary to some reports that the reactors at complex **1** ceased operation in November 1990, the imagery indicates that the facility was still in operation in May 1993.

[52]Sutyagin, I., private communications.

However, this finding is in line with one recent report of the status of these reactors.[53] The warm water is probably resulting from the reactors which may still be producing electricity but not plutonium. Some cooling may still be required after shut down but perhaps not enough to account for these temperatures.

It has been reported that at complex **2**, the construction of three breeder reactors had started but this was halted in 1987 as a result of the Chernobyl accident.[54] Nevertheless, the cooling water appears to be taken in from the reservoir and the warm water is discharged into the reservoir also. This is evident by a barrier constructed to separate the inlet and the outlet of the water used for the reactors (Figure 3.25).

The thermal properties of the reservoir adjacent to complex **2** were also examined using the thermal bands of the Landsat images. As in Lake Kyzyltash, a barrier has been constructed in the reservoir to separate inflow and outflow waters. Figure 3.28 shows the surface temperature variations within the reservoir in 1987 and 1993. These were created using the same masking procedures as in Figure 3.27. In the 1993 thermal image the surface temperature of discharged water to the right of the barrier is approximately 2°C higher than that of the water to the left of the barrier and in the middle of the reservoir. In contrast to the situation in Lake Kyzyltash, the plume of water which is warmer than the bulk of water in the reservoir does not extend beyond the confines of the barrier, but the area within the barrier is much larger than that within the barrier in Lake Kyzyltash. In the 1987 image there appears to be no difference in surface temperature between the bulk of the reservoir and the water within the barrier. Thus on the evidence from the thermal imagery, complex **2** appears to be operating in May 1993 but not in August 1987. The smaller temperature differential of the plume in 1993 suggests that a smaller reactor may be responsible for this effluent. This is in agreement with a suggestion that complex **2** contains a tritium production reactor rather than a power reactor or plutonium production plant.[55] Lake Kyzyltash appears to be warmer than some of the others in the vicinity. This may be because of silting. One source of the water is from a small river which flows into the Lake Silach to the north of the Lake Kyzyltash. Lakes Silach, Irtyash and Kyzyltash are linked by small rivers. Because of the dams built on the River Techa after Lake Kyzyltash, it is suggested that the flow of water has stopped causing considerable amount of silting to occur in the Lake Kyzyltash making it shallow. This would affect the depth and thermal properties of the water.

[53]**World Nuclear Industry Handbook**, 1994, p.34.
[54]Ruokola E, and Vilkamo S., "All change at Chelyabinsk" **Nuclear Engineering International, vol. 36, no. 438, January 1991, p.18.**
[55]*Ibid*, Sutyagin.

Figure 3.17. Band 6 of a Landsat TM multispectral image showing the surface temperature variations of the Lake Kyzyltash in 1987 (left) and 1993 (right).

Source: EOSAT/Landsat; image processed at the Defence Research Agency, Farnborough, UK.

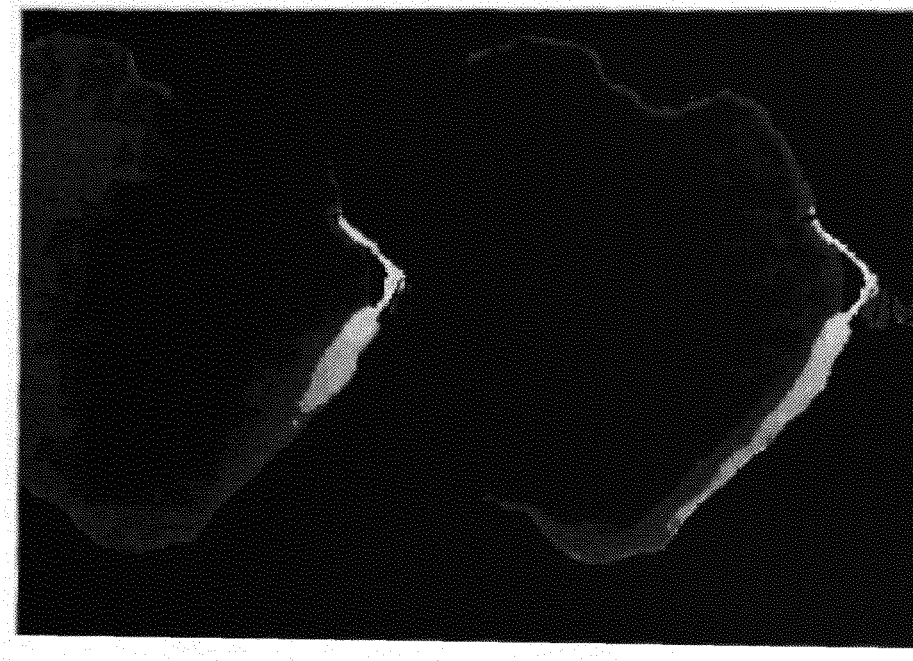

Figure 3.18. Band 6 of a Landsat TM multispectral image showing the surface temperature variations of the reservoir in 1987 (left) and 1993 (right).

Source: EOSAT/Landsat; image processed at the Defence Research Agency, Farnborough, UK.

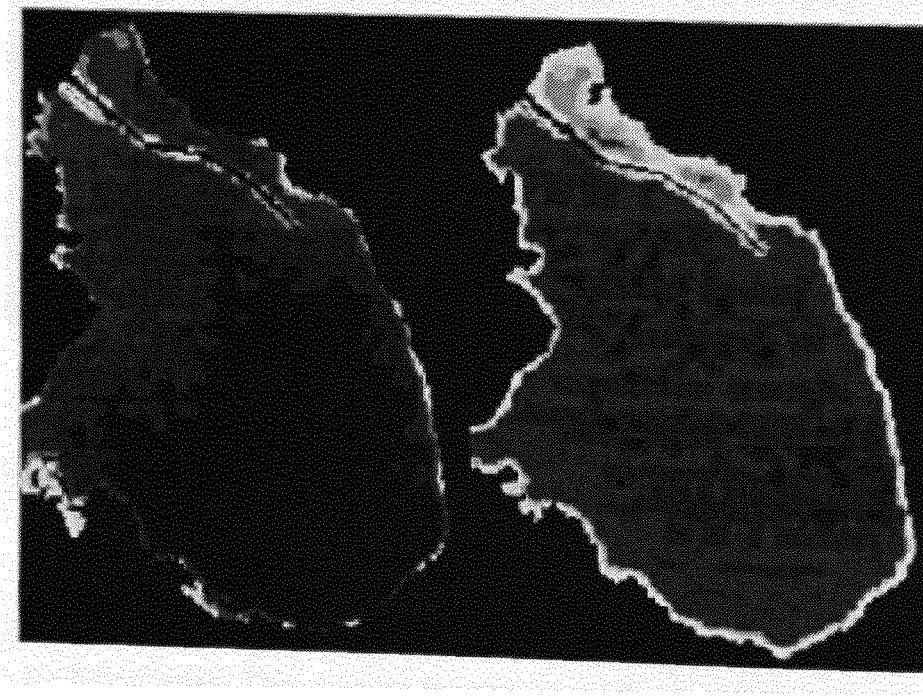

3.6 Sellafield complex in the UK

Three images over the UK's main fuel reprocessing plant (the Thermal Oxide Reprocessing Plant - THORP) at Sellafield, formerly known as Windscale, and electricity producing reactors at Calder Hall in Cumbria were examined. These were acquired by the French SPOT satellite in June 1986 (multispectral) and again in March 1990 (panchromatic) and the US Landsat TM in February 1989. Sellafield is of considerable interest because a number of early plutonium and dual purpose plutonium and electricity production reactors were built in this area. The area is also being considered as a potential underground nuclear waste storage site. However, as was announced by Douglas Hurd, the then Foreign Secretary, at the NPT Review and Extension Conference held in New York in 1995, the production of plutonium by Calder Hall nuclear reactors for explosive purposes has ceased.[56]

The proposal to build the Windscale site was announced in July 1947 and the work to develop the facilities began in September of the same year. Two reactors were built in late 1950 for the production of plutonium for the UK weapons programme. Both were graphite-moderated air-cooled reactors. The reactor cores were cooled using a once-through forced air which was then discharged through 137m chimneys with filters placed at their tops. The latter were used to prevent radioactive nuclides escaping into the atmosphere. In October 1950, the first Windscale pile became critical. A chemical separation plant at Windscale was completed in April 1951. In the same month, the first pile began operation at normal power level and the second one became critical in June. The latter plant was commissioned in October 1951. The chemical separation plant took the first fuel for processing in January 1952. The two reactors were in operation until July 1958 when the first one was closed down followed by the second one only three months later in October. A prototype advanced gas-cooled reactor (AGR) was built at Windscale and commissioned in December 1962. It produced 28 MW of electricity and formed the basis of the future civil nuclear power programme. The AGR was shut down in April 1981.[57]

However, considerable demand existed for plutonium for the UK weapons programme so that by 1953 a generation of dual purpose reactors were designed at Harwell to produce plutonium as well as electricity.

The reactors, still in operation, are graphite-moderated and cooled by pressurised carbon dioxide. The hot gas from the reactor is first allowed to pass through a heat exchanger in which steam is produced. The latter is then used to drive the turbines to generate electricity. The cooled gas is then re-circulated into the reactor core. The steam from the turbine exhausts is condensed by passing it over tubes through which cold water is flowing. In order that the resulting hot water can be used again, it is taken to cooling towers to be cooled. It is interesting to note that the quantity of water circulating round a plant is about 150,000,000 gallons a day of which about 3,000,000 gallons are lost in evaporation. This has to be made up from rivers or other sources.

The construction of the first two such reactors at Calder Hall site at Sellafield began in August 1953. The first reactor became critical in May 1956 and commenced its operation three months later in August. The Calder Hall 2 became critical in 1957 and began to generate electricity in February 1957. The location of the Calder Hall 1 and 2 reactors are shown on a map in Figure 3.29 and their layout[58] in

---

[56]Statement made by the UK Foreign Secretary during the Non-Proliferation Treaty Review and Extension Conference, 18 April 1995, United Nations, New York.

[57]**Windscale 1957 - Anatomy of a nuclear accident,** by Arnold, Lorna, 1992, (Macmillan, 1992).

[58]**Calder Hall,** by Jay, Kenneth, 1956, (Methuen & Co Ltd., London, 1956).

Figure 3.30. In June 1954 a decision was taken to construct two more reactors at Calder Hall to meet the increasing demand for plutonium for defence use. Calder 3 began the production of electricity in 1958 and the fourth reactor began producing electricity in April 1959. These reactors are expected to continue to produce electricity through to 1999 when Calder Hall 4 may be shut down.[59]

Figure 3.31 shows the full panchromatic scene acquired by the French SPOT satellite on 19 March 1990 over the west coast of Cumberland in UK. From the map in Figure 3.29, the Sellafield site can be confirmed at A in Figure 3.31. This is enlarged in Figure 3.32 in which the four Calder Hall reactors and the THORP reprocessing facilities can be seen clearly at [1] and [2] respectively. From the layout diagram of the Calder Hall facilities shown in Figure 3.30, the four cooling towers at (3), the four reactors at (4) and the two turbine houses at (5) can be identified in Figure 3.20. Using the aerial photograph shown in Figure 3.33, the three buildings (6), (7) and (8) in Figure 3.32 can be identified as the receipt and storage facility, the head end plant and the chemical separation plant respectively. The sites marked 9 and 10 in Figure 3.32 are probably the old reprocessing facility and cooling ponds respectively for the spent fuel from the Calder Hall reactors.

While the SPOT multispectral sensor has a lower spatial resolution (20m pixel), a multispectral image acquired on 30 June 1986 over the Sellafield area was used to see the extent of development that took place between 1986 and 1990. The image of Figure 3.32 was combined with the multispectral image of the same area (Figure 3.34). While several smaller changes can be detected, the large development that occurred between June 1986 and March 1990 can be clearly seen at (1) and (2) in Figure 3.34. More subtle changes can be detected by subtracting one image from the other. However, for this it is preferable to have images with the same resolution since in the case of images with different resolutions, inevitably re-sampling occurs which would change the original values of the pixels in the re-sampled image.

A false colour composite of bands 2 (blue), 3 (green) and 6 (red) is shown in Figure 3.35. This was to confirm that the canal joining the River Calder and the sea was not used to carry discharged water used for cooling the reactors. No hot water plum was detected at the outlet of the canal linking the sea but some water vapour from the four cooling towers can be easily seen. This would suggest that at the time of the image on 10 February 1989 all the reactors were in operation. While, in the absence of hot water plums in the sea or lakes, this method is a useful one to detect whether a reactor is operating or not, it is not completely satisfactory. The water condensation from cooling towers depends on the atmospheric temperature. For example, condensation outside the towers is not visible in Figure 3.34 because the SPOT multispectral image was acquired in the month of June when the atmospheric temperature is likely to be warmer. However, as the cooling towers are observed from vertically above, a bright signature over each of the towers is detected indicating that some condensation may be occurring inside the towers. This would suggest that the reactors are operating. As the image in Figure 3.32 was acquired in March, some condensation is expected to occur. In the image it can be seen that around the top two towers, vapour condensation is occurring but not around the two lower ones; at least it appears to be considerably less in one of them (the upper tower). This may be either both the reactors are operating at a lower power levels than normal or one of them (the upper reactor) has been shut down. British Nuclear Fuels plc. (BNFL) confirmed the above interpretation of the status of the reactors in June 1986 and February 1989 and indicated that on 19 March 1990, the Calder Hall Reactor 2 was shut down for refuelling. Thus, the above interpretation of events from the images is in reasonable agreement with what was happening on the ground.

[59]**World Nuclear Industry Handbook 1993**, (Nuclear Engineering International, 1993).

Figure 3.19. Map of the Sellafield area and its surrounding.

Source: Davies, A.W., "Deep geological disposal of radioactive waste - assessing the environmental impact", Nuclear Energy, vol. 33, no. 2, April 1994, p. 105.

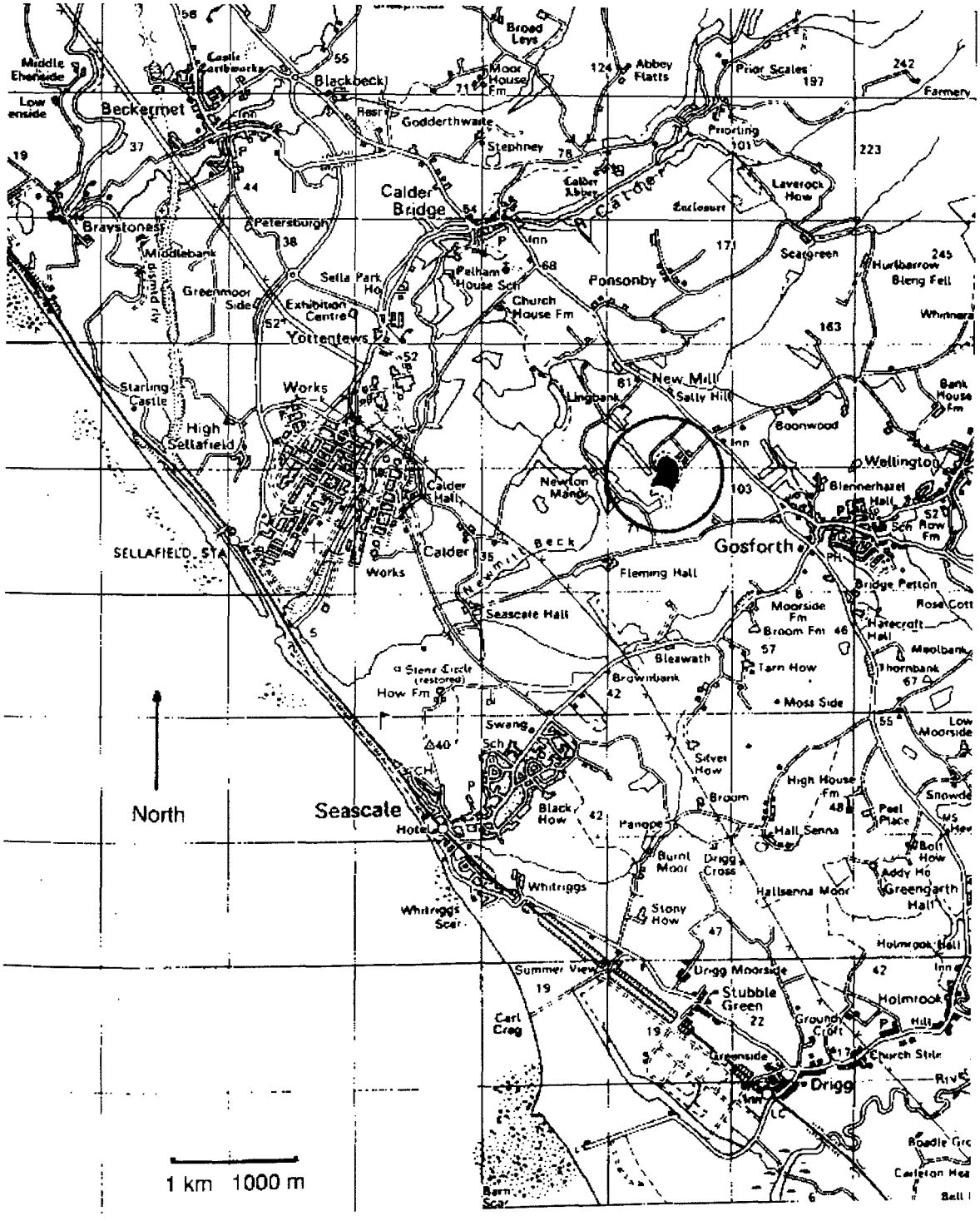

Figure 3.20. The layout of the Calder Hall 1 and 2 reactors.

Source: *Calder Hall*, by Jay, Kenneth, 1956, (Methuen & Co Ltd., London, 1956).

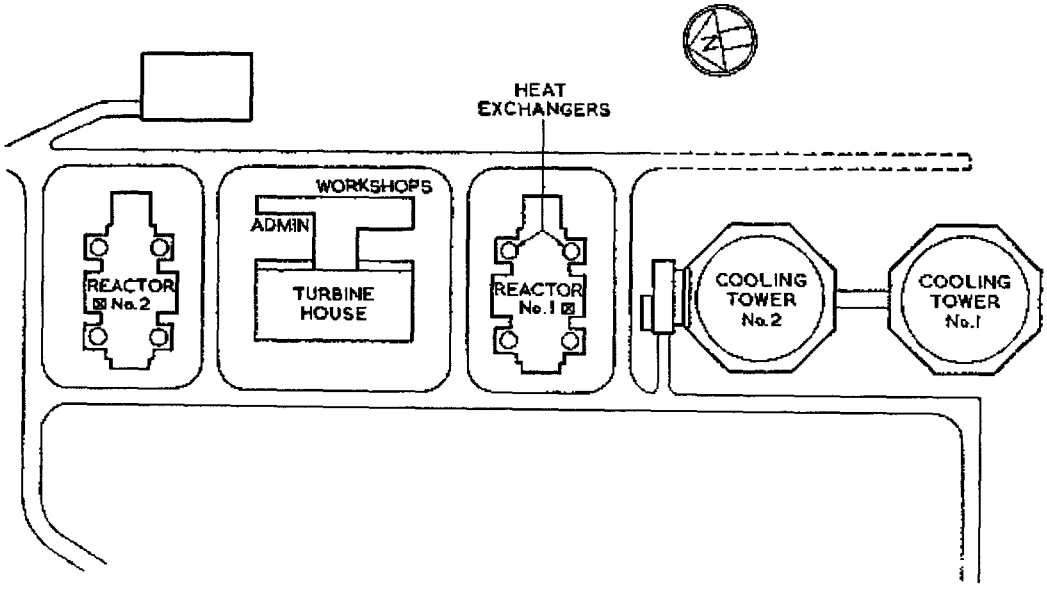

Figure 3.21. Full SPOT panchromatic scene (March 1990) over the Sellafield site in UK. The THORP reprocessing plant and the four Calder Hall reactors are located at (A). Scale: 1:233,830

Source: CNES/SPOT; image processed at the Defence Research Agency, Farnborough, UK.

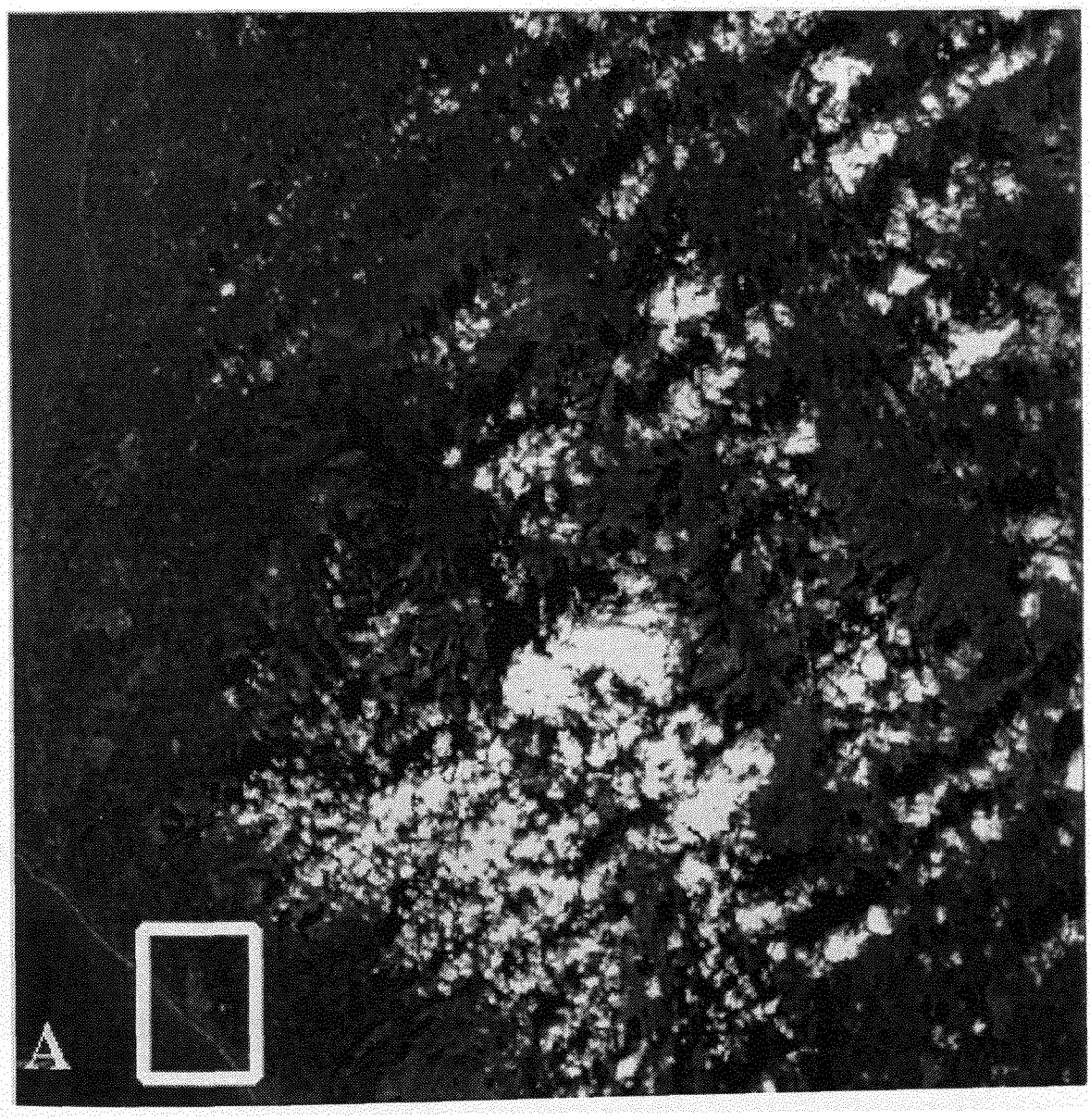

Figure 3.22. Enlarged section (A) of Figure 3.31 shows the details of the Calder Hall reactors (1) and the THORP reprocessing plant complex at (2). Scale: 1:17,000

Source: CNES/SPOT; image processed at the Defence Research Agency, Farnborough, UK.

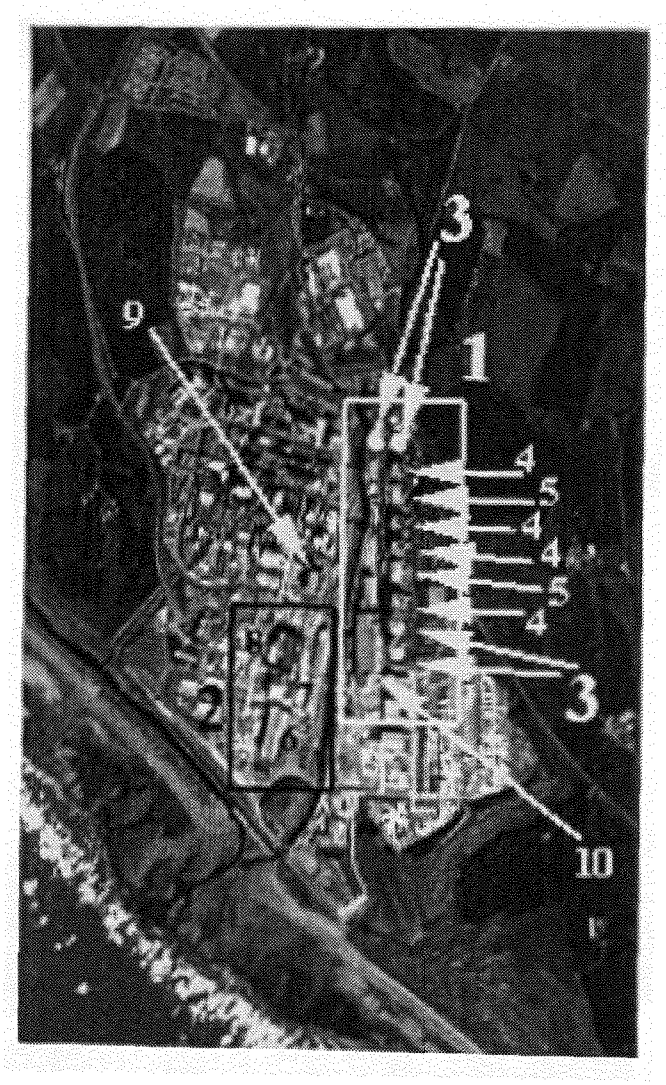

Figure 3.23. An aerial photograph of the THORP reprocessing plant in UK.

Source: The Thermal Oxide Reprocessing Plant - THORP, British Nuclear Fuels plc 1992.

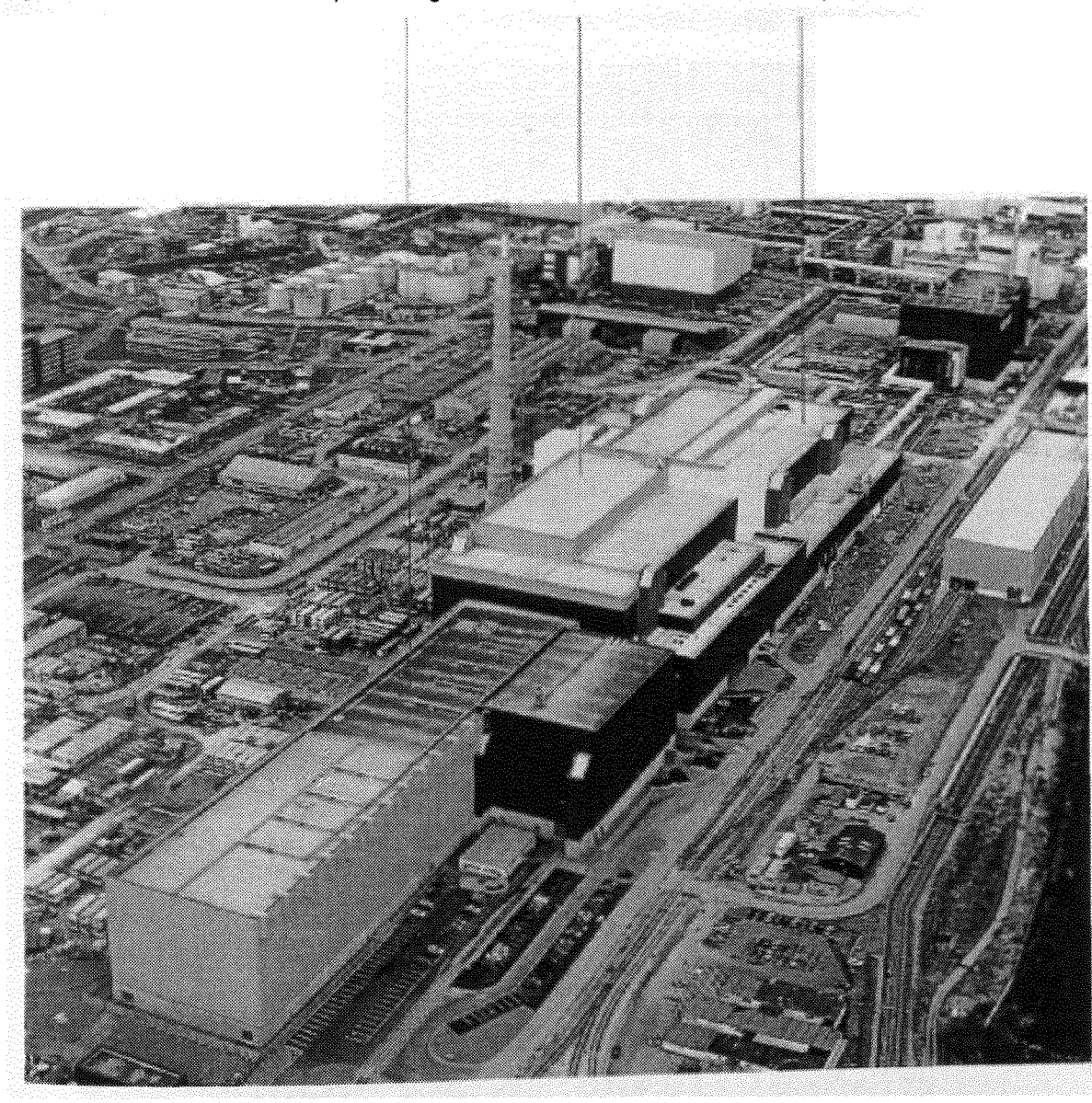

Figure 3.24. This shows the same area as that in Figure 3.9 but as a combination of the SPOT multispectral and panchromatic images acquired on 30 June 1986 and 19 March 1990 respectively. In this way the changes taken place between June 1986 and March 1990 can be detected. These are indicated in red. Major developments at (1) and (2) can be seen. Scale: 1:17,000

Source: CNES/SPOT; image processed at the Defence Research Agency, Farnborough, UK.

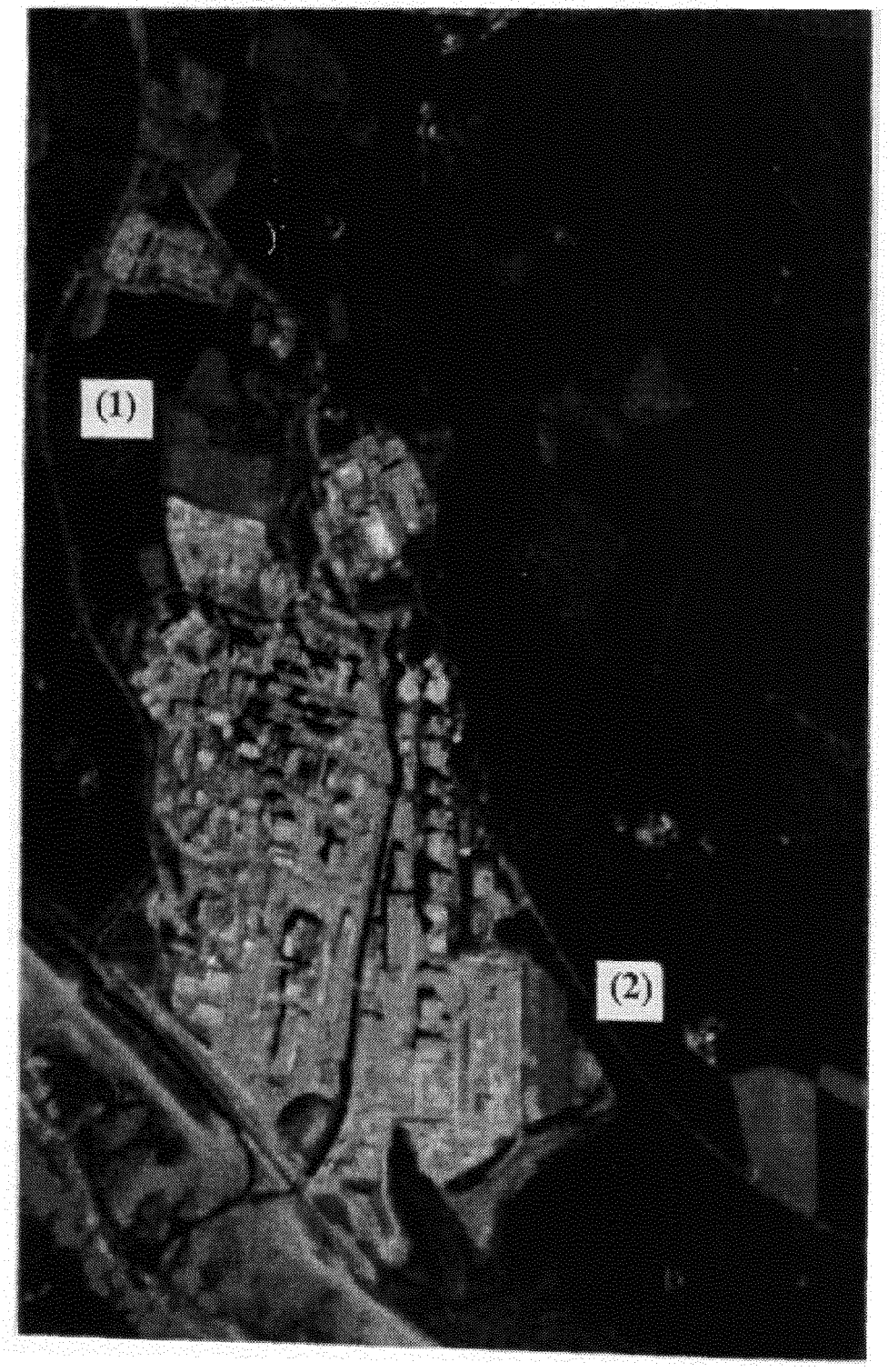

Figure 3.25. A false colour composite of bands 2 (blue), 3 (green) and 6 (red) of a Landsat multispectral image acquired on 10 February 1989 over the UK Sellafield site. This is an extract from the full scene. Scale: 1:62,000

Source: EOSAT/Landsat image processed at the Defence Research Agency, Farnborough, UK.

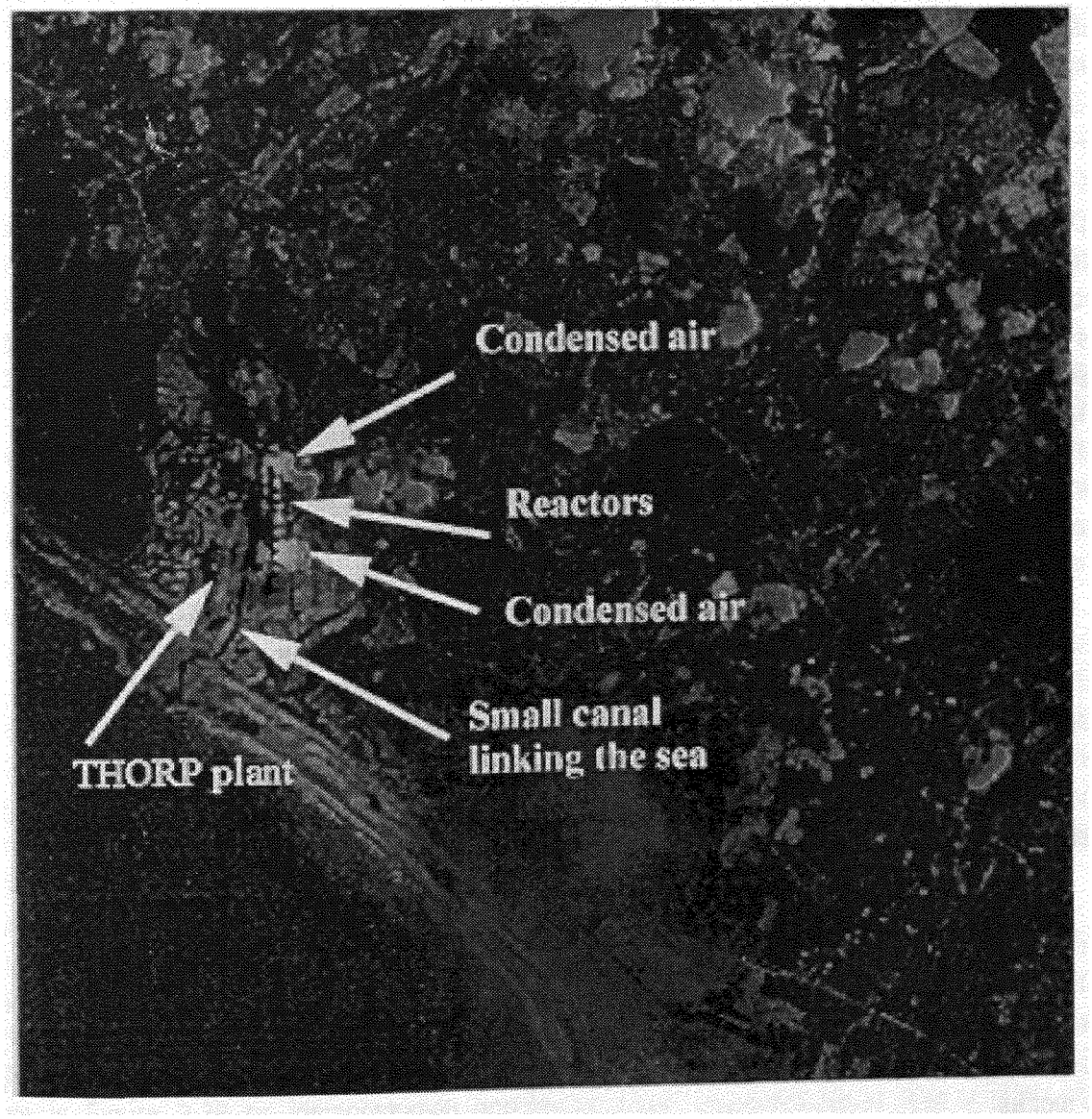

3.7 Enrichment plant at Almelo in the Netherlands

Research and development programmes on enrichment of uranium by centrifuge process were being pursued simultaneously in Germany, the Netherlands and in the UK. It was soon recognised that considerable commonality existed in all the three processes. As the technique showed promise, a joint company, Urenco, was formed in March 1970 by the three under the Almelo Treaty. Urenco was registered as a private limited company under English law on 31 August 1971 with three shareholders, BNFL plc, Ultra-Centrifuge Nederland NV (UCN) and Uranit GmbH. A sister company, Centec GmbH was also created in 1971 to hold, jointly on behalf of all partners, the patents and other intellectual property of the participating companies. The Urenco organisation expanded in the 1970s with the establishment of partnerships to own and operate the enrichment plants. Initially, two enrichment plants were constructed, one at Capenhurst in the UK and the other at Almelo in the Netherlands. The latter was a joint Dutch/German facility. The third plant was built later at Gronau in Germany. The last two facilities are discussed below.

Urenco centrifuge plants are similar in construction and layout. Basically a plant consists of a T-shaped building. The top horizontal bar of the "T" consists of the UF6 feed, product and tail handling areas, the control room and the plant rooms for the centralised services of electrical power, refrigeration, cooling water and compressed air. The vertical bar of the "T" is a distribution corridor for the centralised services. It consists of such equipment as desublimers for primary product and tail collection, heat exchangers and cooling water pumps, and low voltage transformers associated with each of the cascade hall which are attached to the vertical bar of the "T". With such a design, it is possible to add cascade halls as the demand increases. Generally the horizontal bar of the "T" is about 200m long and some 40m wide. The vertical portion can be about 200m wide and the length will depend on the number of centrifuges deployed. The design has also been adopted by Japan[60] but not all enrichment plants are necessarily "T" shaped.

Almelo plant is located south-east of the town of Almelo some 25km from the Dutch-German border and less than 30km from Gronau, the site of the German facility. The initial pilot plant of nominal 25 tSWU/a capacity began operating in 1972/73. While this facility is still operational, a commercial demonstration plant with a capacity of 200 tSWU/a was constructed and became operational in 1976. This is made of four units each of 50 tSWU/a capacity. The overall area of such a facility is about 100 x 100 metres.

A Landsat image over Almelo was acquired on 19 July 1992. The Almelo enrichment facility can be seen at (A) in the colour composite of bands 1 (blue), 2 (green) and 3 (red) shown in Figure 3.36. The size of the image (a quarter scene) was such that the German enrichment facility at Gronau is also in the same scene at (B). The locations of both the plants were determined first using such criteria as the presence of passive security fences, roads and railway lines. These were subsequently confirmed by acquiring openly available maps used for public relations by Urenco showing the locations of the two enrichment plants. For example, such a map for the Almelo plant is shown in Figure 3.37. Compare this with the satellite image of the facility shown in Figure 3.38. The shape of the boundary is very similar to that drawn in the map in Figure 3.37. In this study the maps were scanned and digitised using an Agfa Arcus flatbed scanner. While it has an optical resolution (horizontal x vertical) of 600 x 1200 dots per

[60] Heriot, I.D., "Uranium enrichment by gas centrifuge", 1988, **Nuclear Science and Technology, Report for the Commission of the European Communities, EUR 11486EN**, p.37.

inch (dpi), the maps were scanned at 300 dpi. The images were then copied on a CD-ROM using Kodak PCD 200 Writer.

The next task was to check the above interpretation by superimposing a line drawing of the facility from the map on to the satellite image. Before this could be done it was necessary to correct the satellite image geometrically taking the map as a reference. The numbers on the map indicate the same features identified in the satellite image. These were then digitised and two vector files created using the IDRISI programme. A "correspondence fill" was created which was then used to transform the satellite image to the same grid system as the map by re-sampling the image. The process consists of creating a new grid and a set of polynomial equations to describe the spatial mapping of data from the old grid into the new one. This task is performed by the software. The re-sampling options include a "nearest neighbour", and a "bilinear interpolation". The former was used in which the new grid value is the same as that in the nearest cell in the old grid. The geometrically corrected image of band 4 is shown in Figure 3.39. This band was chosen because features such as the canal, roads and the building were more pronounced as they appeared darker than other features. From the map in Figure 3.37, the areas encompassing the enrichment facility and the buildings within it and roads and a railway line were drawn and new vector files created. These features were then superimposed over the satellite image as shown in Figure 3.39. While various features align reasonably well, the method is very cumbersome. This is due to the limitation of the software. More sophisticated image processing programmes can perform such tasks more efficiently. Here, simple techniques are used to illustrate the concepts.

An enlarged view of the Almelo plant is shown in Figure 3.38. Using the overlay of the line drawing created using the above method, some interpretation of the Landsat image is attempted. The main buildings housing the centrifuges have been identified and their sizes determined from the overlay. These and roads and railway lines are indicated in Figure 3.38. It is interesting to note that even with the relatively poor resolution, the railway line and a large fence consisting of trees can be detected in the image. However, these do not become very obvious in any other band combinations.

The building labelled "smaller enrichment plant" in Figure 3.38 measures about 120m x 120m. A large scale industrial plant with a capacity of about 850 tSWU/a became operational by 1981. A typical 1,000 tSWU/a capacity may be housed in a 260 x 165 metre building. The size of the larger of the two buildings labelled "Two enrichment plants" in Figure 3.38 measures about 270m x 270m. The pilot plant shown in Figure 3.38 as "demonstration enrichment plant" measures about 60m x 60m. These dimensions are consistent with the expected sizes of such facilities.

Figure 3.26. A multispectral Landsat 4 quarter scene over Almelo (A) and Gronau (B) enrichment facilities in Netherlands and in Germany respectively. Scale: 1:80,300.

Source: EOSAT/Landsat; image processed at the Defence Research Agency, Farnborough, UK.

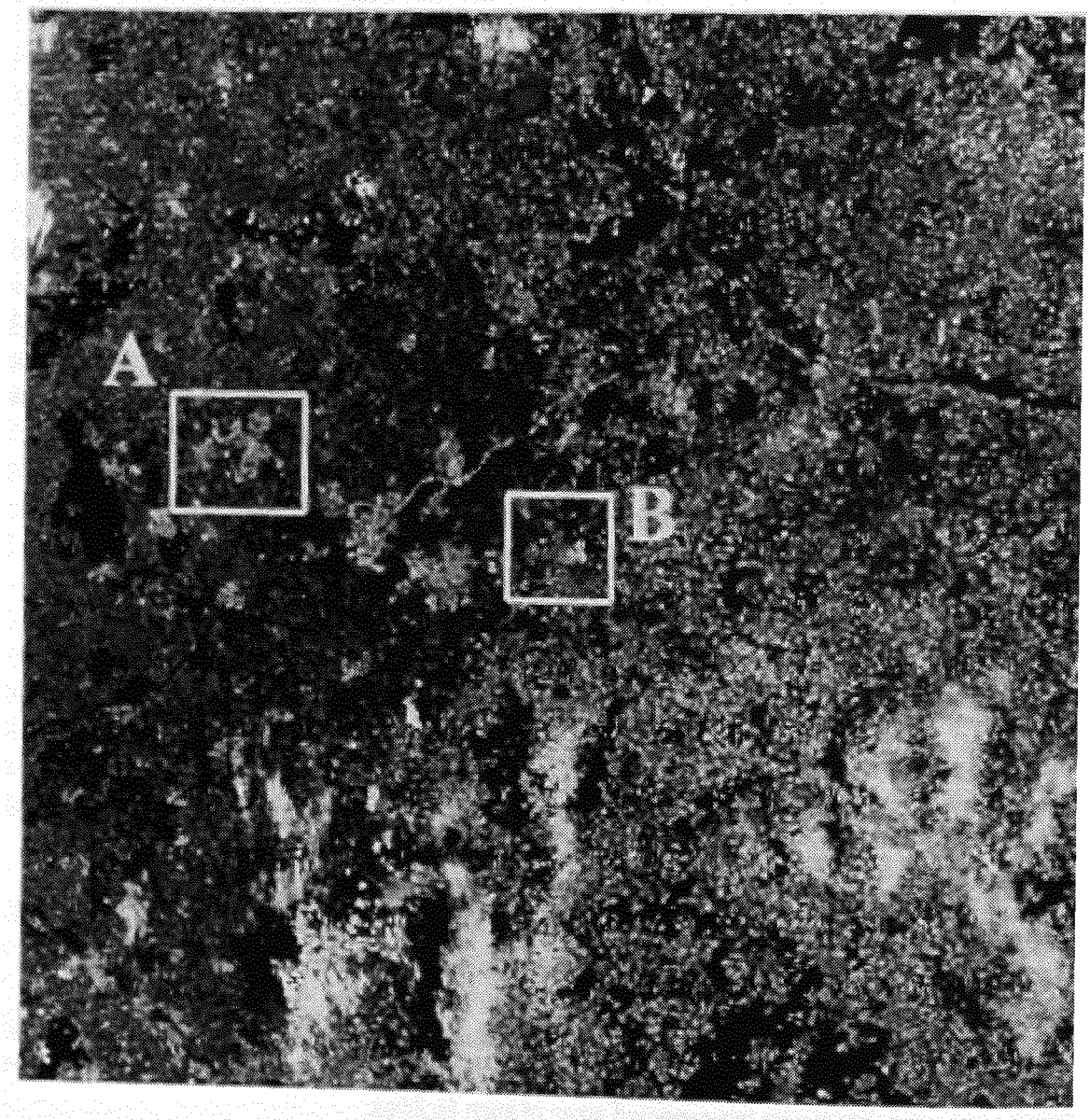

Figure 3.27. A site map of the Urenco's Almelo facility. The numbers on the map indicate the locations of points used to digitise the map. These were also identical on the satellite images.

Source: Urenco, UK.

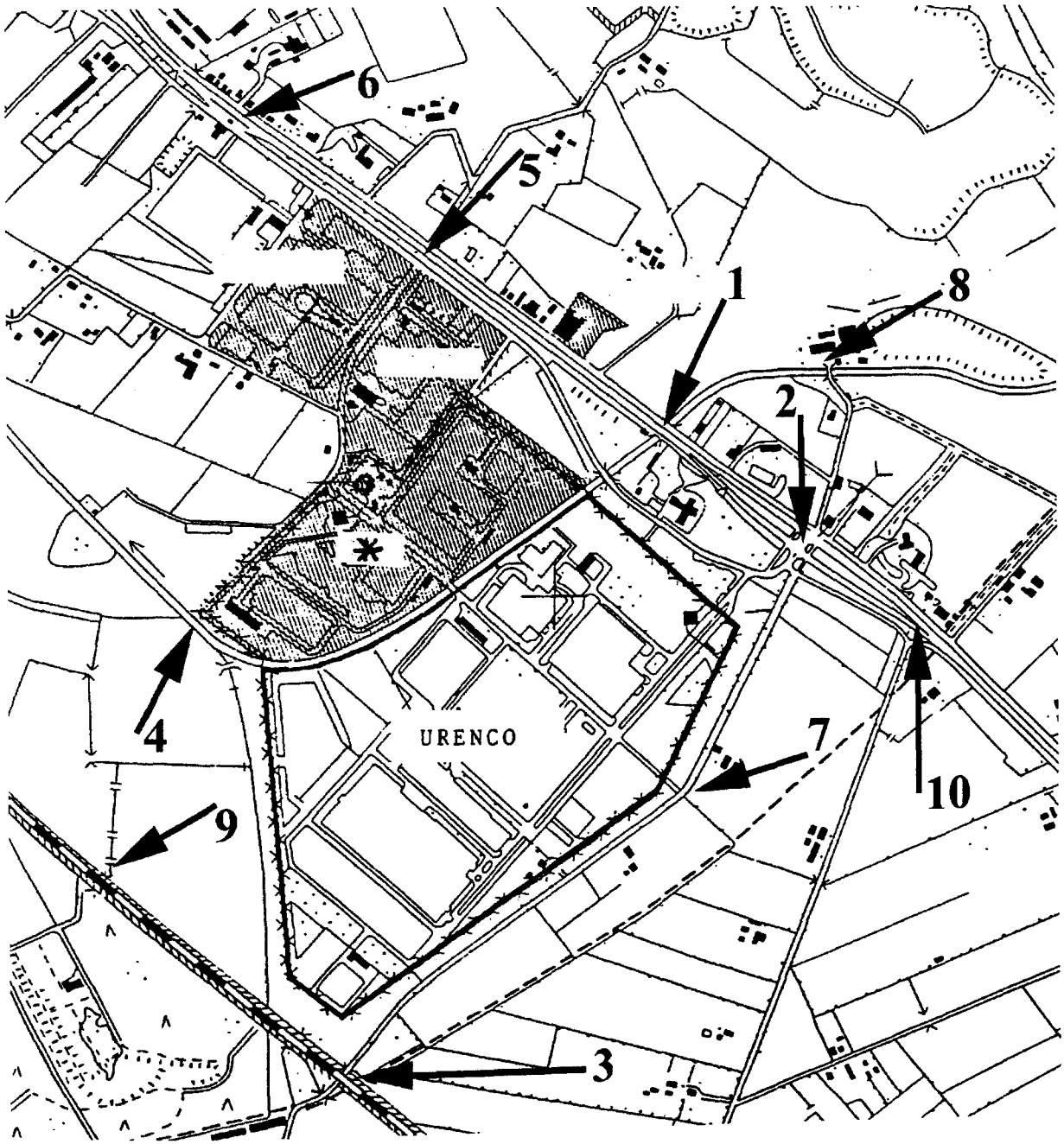

Figure 3.28. Section (A) in Figure 3.36 is enlarged showing the Almelo facility. This is a false colour composite of bands 1 (blue), 3 (green) and 4 (red). Scale: 1:80,300.

Source: EOSAT/Landsat; image processed at the Defence Research Agency, Farnborough, UK.

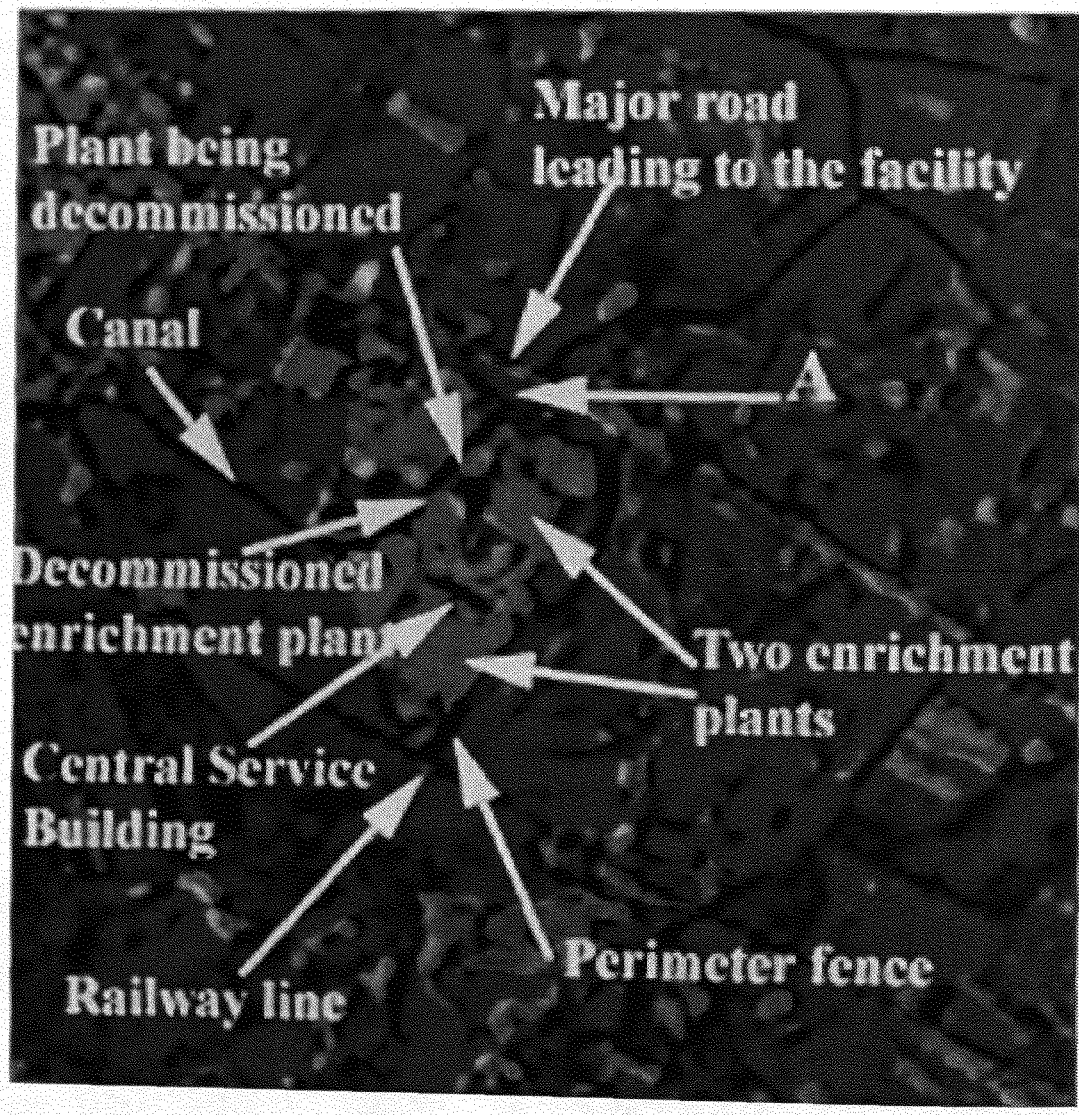

Figure 3.29. The Almelo enrichment plant observed in band 4 of the Landsat 4 scene. The features such as the boundary and the buildings, roads and the railway line are emphasised by line drawing from the map. Scale: 1:80,300.

Source: EOSAT/Landsat; image processed at the Defence Research Agency, Farnborough, UK.

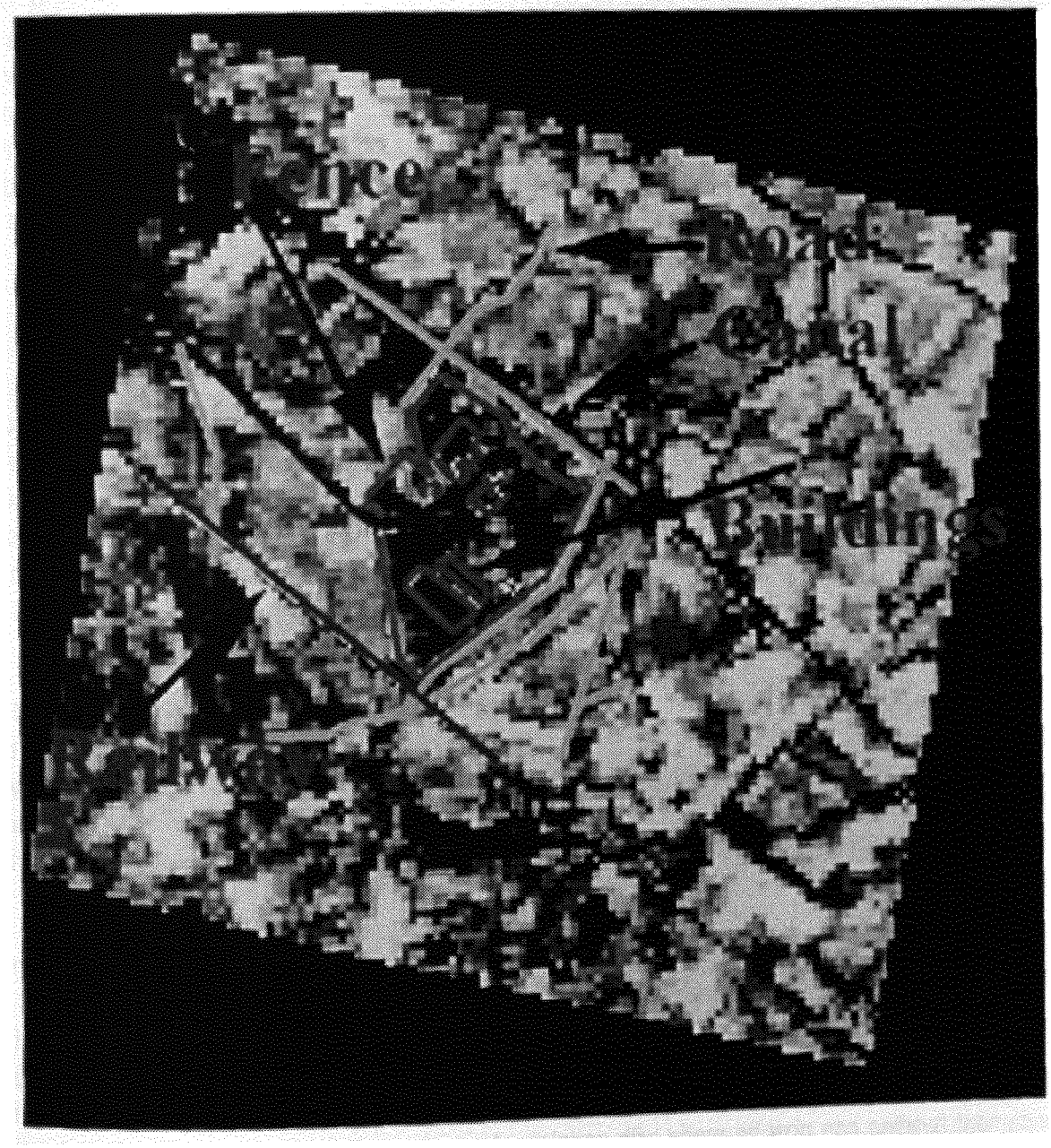

Chilled air is used to cool various systems in the plant. The final heat rejection is achieved via high capacity freon chillers discharging heat to the atmosphere via roof mounted air-cooled radiators. A typical 1,000 tSWU/a plant would dissipate about 15 MW of heat via roof-mounted air cooled radiators or a low-profile forced draught cooling tower.

The canal is very narrow so that it is not possible to detect any thermal signature in band 6 due to the discharge of hot water, if any, from the facilities. On the other hand, no thermal signature was detected over the buildings in band 6 either. It is possible that on 19 July 1992 none of the plants were working or more the likely reason may be the poor resolution of the thermal band. As noted above the temperature of the air discharged may be low and the chimneys may be small. On the other hand a considerable amount of thermal radiation over the area marked **A** in Figure 3.38 was observed. It is difficult to be certain about the origin of this thermal radiation without ground information.

3.8 Enrichment plant at Gronau in Germany

At the beginning of 1991, some 39 per cent of Germany's electric power requirement came from nuclear energy with a capacity of 22,390 MWe net. Most of the reactors producing this energy are fuelled with slightly enriched uranium for which Germany is largely dependent on foreign sources. Whilst it has hardly any indigenous uranium resources, it has developed its own enrichment capacity within the tripartite Urenco arrangement. An initial enrichment production facility was built at Almelo in the 1970. By the end of 1970s, Germany decided to build a facility at Gronau, some 30 km east of Almelo (see Figure 3.36).

The construction of the plant began in 1982. Operations began in 1985 under a licence for 400 tSWU/a. By 1987, 260 tSWU/a was achieved. In 1991 Germany had received approval to increase the capacity of its enrichment plant up to 530 tSWU/a. In 1994 the operating licence for 1,000 tSWU/a was granted and the capacity raised to 590 tSWU/a. The ultimate goal after reaching the 1,000 tSWU/a in 1998 is to achieve a capacity of 1,800 tSWU/a without construction of new buildings but employing more centrifuges.[61]

The area B in Figure 3.36 is enlarged and shown in Figure 3.40. With the aid of the site map (Figure 3.41), an interpretation is given in Figure 3.40. The size of the main enrichment building is as expected for a plant of capacity of 1,000 tSWU/a. As before, band 4 of the Landsat image over the Gronau facility was processed and the outline of the boundary of the facility and some of the roads and a railway line obtained from the map are overlaid on the image in Figure 3.42. The identification of the enrichment building can now be made with certainty. Again the thermal band was used to determine whether the enrichment plant was in operation. Whilst one or two pixels over the roof indicate slightly higher temperature than the rest of the roof, it is difficult to be certain that this represents the hot air from the facility.

[61] Private communications, Urenco, Germany.

Figure 3.40. Section (B) in Figure 3.36 is enlarged showing the Gronau enrichment facility. This is a false colour composite of bands 1 (blue), 3 (green), and 4 (red). Scale: 1:80,300.

Source: EOSAT/Landsat; image processed at the Defence Research Agency, Farnborough, UK.

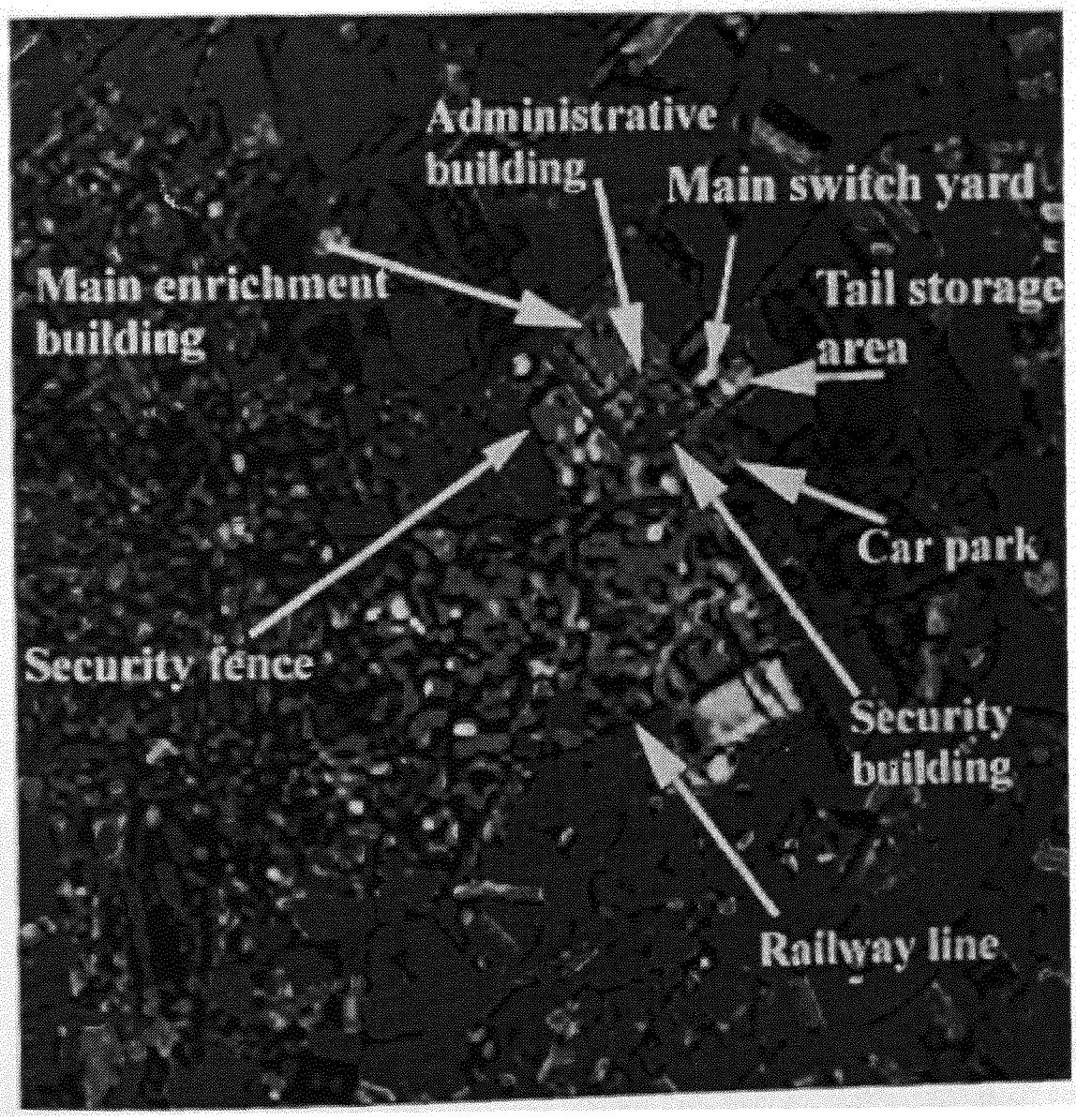

Figure 3.41. A site map of the Gronau facility. Again the numbers on the map indicate the locations of points used to digitise the map. These were also identified on t7he satellite image in Figure 3.40.

Source: Urenco, Germany.

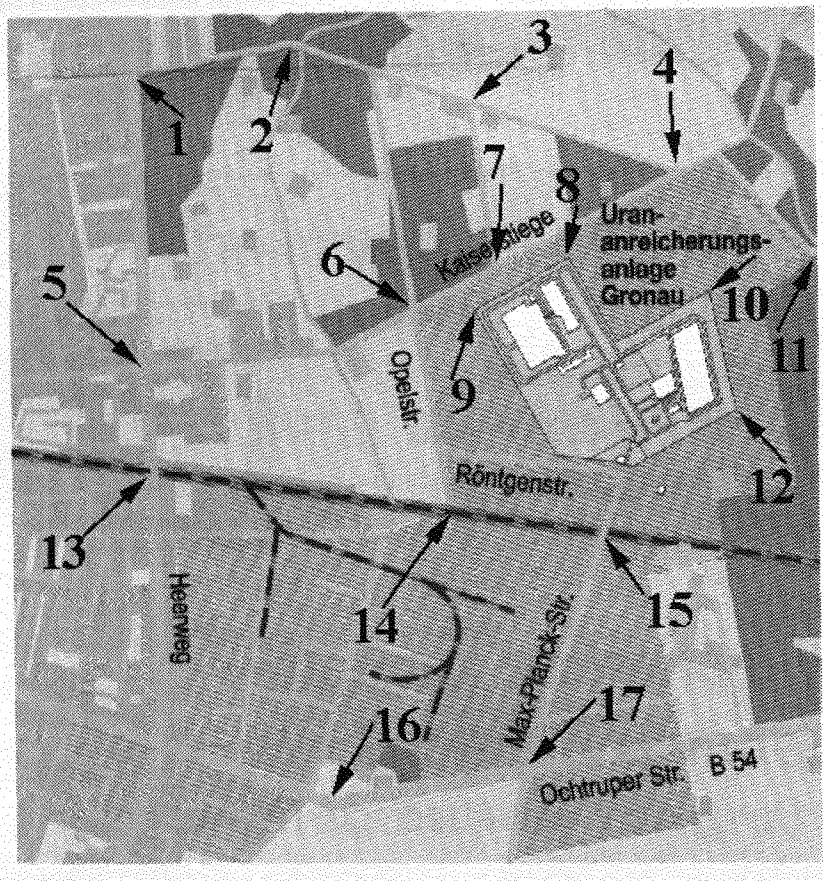

From the analysis of the two gas centrifuge plants, it can be seen that whilst there are no large power plants associated with such facilities, it is possible to detect railway tracks and the centrifuge plants could be recognised from their shapes and sizes. Perimeter fences are also detectable. It was difficult to be certain about any heat escaping from the roofs of the centrifuge buildings although there were some signs of escaping heat from the roof tops. However, this requires more rigorous analysis such as sophisticated image processing and study of images acquired at night.

Figure 3.42. The Gronau enrichment plant observed in band 4 of the Landsat 4 scene. The features such as the boundary and the buildings, roads and the railway line are emphasised by line drawing from the map. Scale: 1:125,400.

Source: EOSAT/Landsat; image processed at the Defence Research Agency, Farnborough, UK.

3.9 Fuel fabrication plant at Hanau in Germany

The Hanau fuel fabrication plant has been in operation since 1969 and current throughput is 600 MtU/a. The plant has a capacity to process up to 1,200 tonnes/a of enriched uranium fuel rods. However, pellet production for these has been suspended since the middle of 1994. Instead the plant assembled fuel pins with pellets produced in the United States. The fuel fabrication plant has now ceased to produce fresh fuel. There is considerable uncertainty over using German plutonium to produce MOX fuel at Hanau. The utilities are more inclined to use fuel produced in France and the UK for this purpose. Although the Hanau plant had been 95 per cent completed, the production of MOX fuel has been abandoned. An earlier interest in converting the Russian plutonium from nuclear weapons did not materialise. It is possible that the plant may now be decommissioned.

Whilst, with the use of a map (Figure 3.44), it is possible to determine the presence and locations of buildings within the Hanau complex, their identification is not possible at the Landsat resolution. However, some interpretation is give in Figure 3.43 which is a false colour combination of bands 1 (blue), 3 (green) and 4 (red). In Figure 3.45 the roads, railway line and the perimeter of the Hanau plant and outline of some of the buildings within it are overlaid on the satellite image (band 4) as before.

Figure 3.43. The Hanau facility at A and its surrounding area are shown in this false colour composite of bands 1 (blue), 3 (green) and 4 (red) of a Landsat multispectral image. Scale: 1:142,900.

Source: EOSAT/Landsat; image processed at the Defence Research Agency, Farnborough, UK.

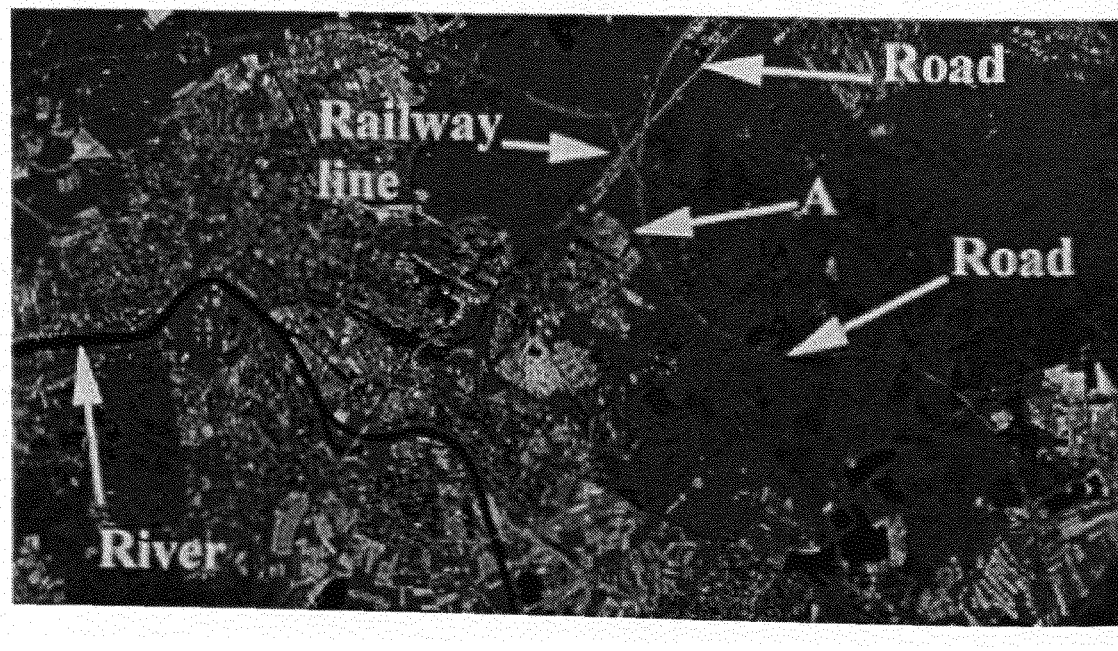

Figure 3.44. A site map of the Hanau facility. Again the numbers on the map indicate the locations of points used to digitise the map. These were also identified on the satellite image in Figure 3.43.

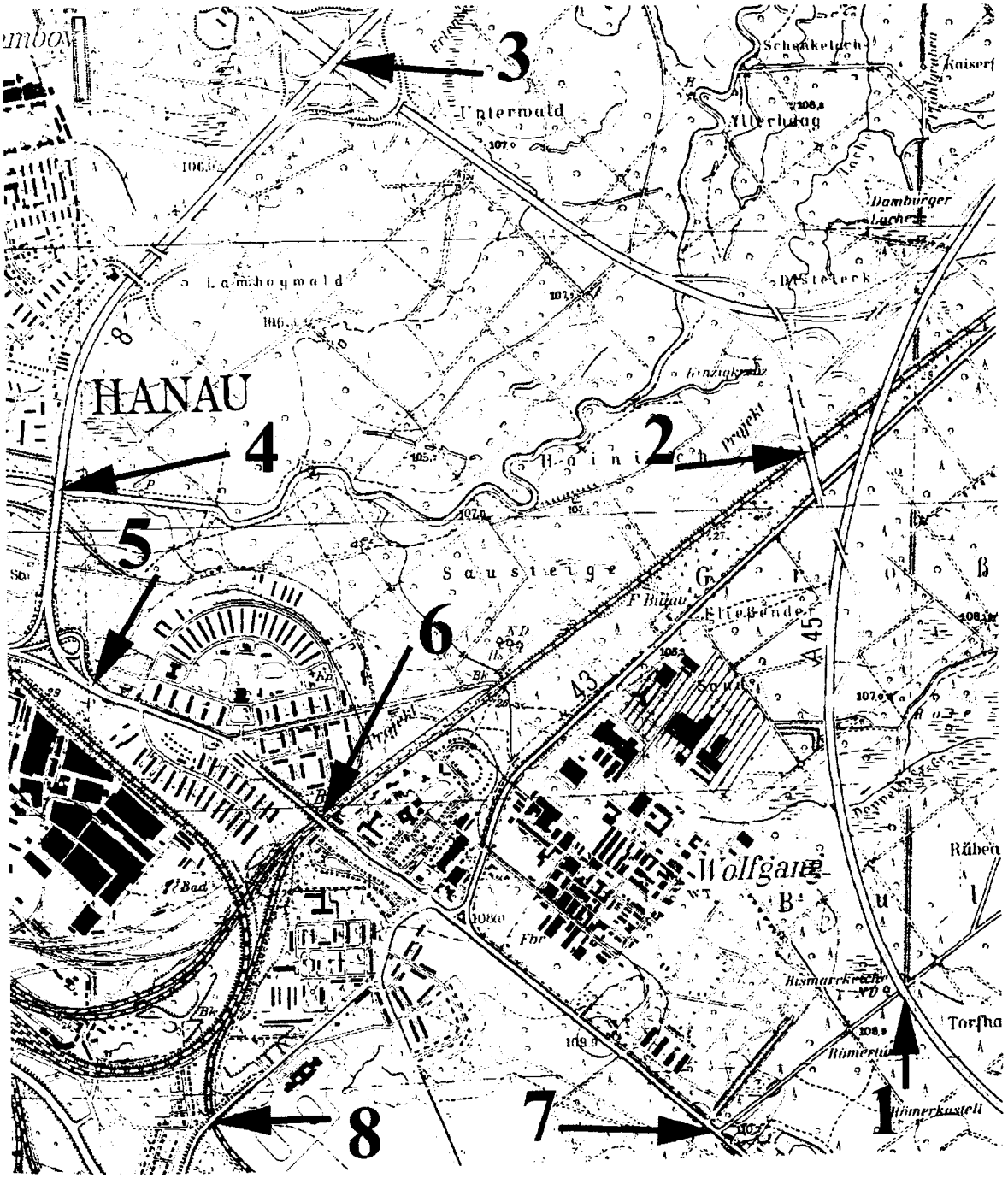

Figure 3.45. The Hanau fuel fabrication plant observed in band 4 of the Landsat 4 scene. The features such as the boundary and the buildings, roads and the railway line are emphasised by lines drawn from the map. Scale: 1:125,400.

Source: EOSAT/Landsat image processed at the Defence Research Agency, Farnborough, UK.

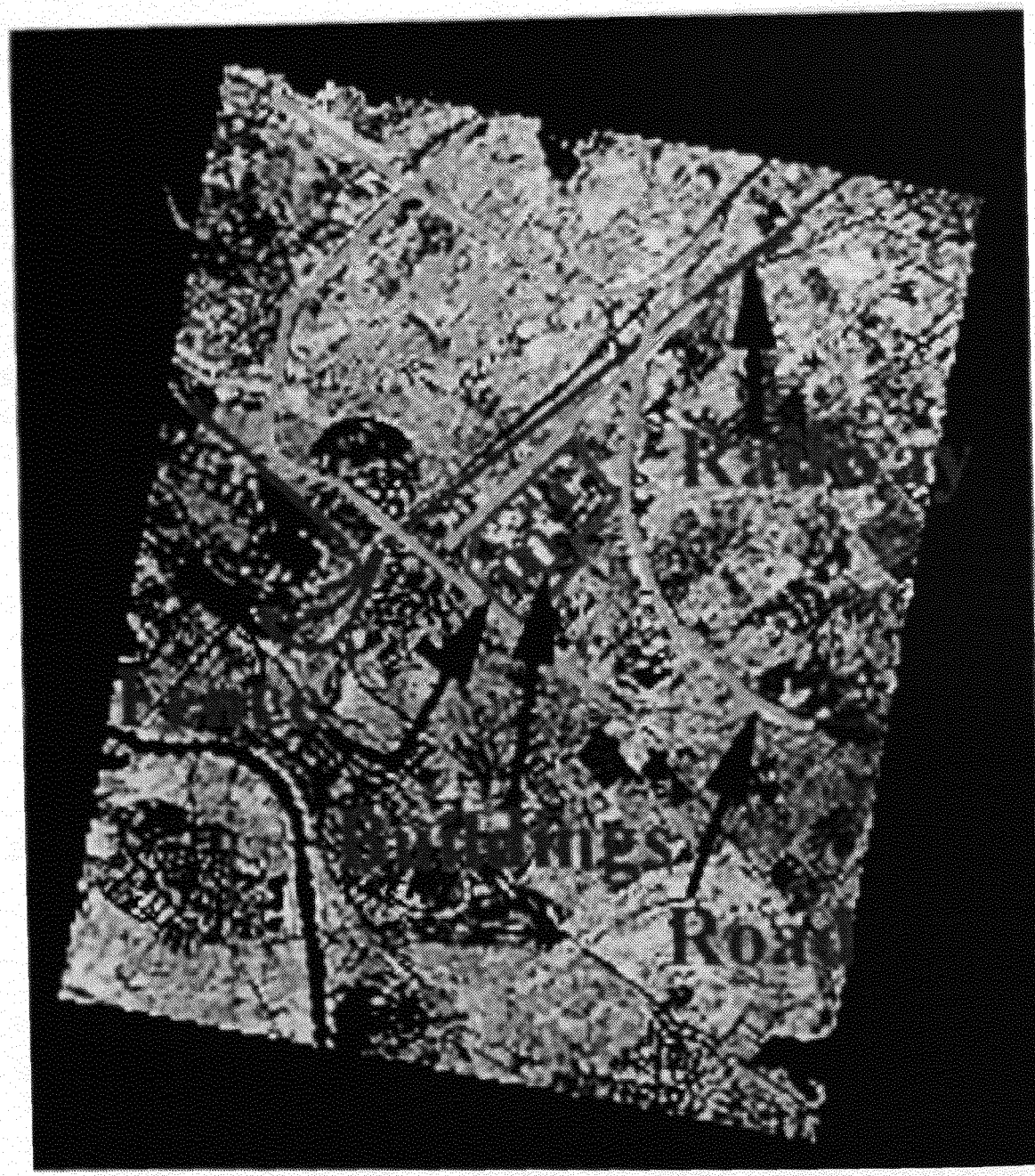

It is often argued that observations from space are severely limited because large parts of the Earth could be covered by clouds. This was true until the concept of synthetic aperture radar (SAR) was developed. Thus, in the following two preliminary test cases, SAR images were acquired over two nuclear sites. Interpretation of SAR images is less easy compared with the optical images. This is particularly true when observations of events are made over water because factors such as the wave heights, wind speeds and nature of the cost line all affect the water at the point of discharge. It is important to collect all such data when radar imagery is used routinely. In order to facilitate interpretation of the radar data in the present study, multispectral images from the French SPOT and

the US Landsat satellites were used. The optical images were enhanced using the principal component analysis (PCA) technique. These will be discussed first. Two sites were selected: the Dungeness nuclear power reactor in the UK and the reactor complex in Kyshtym in Russia.

3.10 Two nuclear facilities observed by optical and radar sensors

The need for day and night and all weather capabilities of sensors to observe earth-bound objects gave considerable impetus to the development of the SAR technology. In an active radar, the antenna of the sensor emits a burst of radiation which is reflected from the target back to the antenna, which collects the radiation just as a lens does in an optical sensor.

The returning radiation can be reflected from a diffuse, specular or a corner reflector. Thus, a SAR is sensitive to the geometrical characteristics of the surface of the object being monitored. It is also sensitive to its dielectric properties. Thus, for instance, a change in temperature of water in a lake or a river due to the discharge of cooling water, should alter the dielectric properties of water which in turn should show up in the returned radar beam. Moreover, the change in the surface structure caused by turbulence in water, for example, would also be detected in the returned radar beam. A number of SAR sensors are now in orbit operated by various countries. These are listed in Table 3.2. Wavelengths in terms of frequencies and equivalent bands are also given.

From the Table it can be seen that the resolution[62] of SAR sensors on board the current commercial satellites is better than that from the thermal sensor (120m pixel) on board the US Landsat satellite.

[62] The resolution of radar deteriorates as the distance between the antenna and the objects increases. This is because the beam fans out so that it is wider at greater distances. Moreover, the resolution is proportional to the beam width. Thus, two objects at the same range separated by a distance less than the beam width will not be resolved. The angular width of the beam generated by the radar antenna is inversely proportional to the length of the antenna. However, the size of the antenna which can be carried by a satellite is limited thus limiting the resolution of the sensor. This problem is overcome in a SAR which has a relatively short antenna which is made to behave like a very long one with a narrow beam. A long antenna can be synthesised by taking advantage of the motion of the satellite in its orbit. As the spacecraft progresses along its orbit, the short antenna of its radar transmits pulses or radiation at regular intervals towards the earth-bound objects. As the satellite approaches an object, for example, the beam of the antenna falls upon, moves across and finally leaves the object. During this time, it reflects the microwave pulses received from the radar antenna back to the antenna. The greater the distance between the object and the antenna, the longer the object remains in the beam. Seen from the object, therefore, the radar antenna appears much longer than it is and this apparent length will depend on the distance between the object and the real antenna.

The effective length of an antenna is, therefore, proportional to the range of the object. Theoretically, the resolution for an unfocused SAR is $r=1/2.\sqrt{(\lambda R)}$ where R is the slant range and λ is the wavelength. For a focused SAR with an antenna of length l, however, the theoretical resolution is given by $r=l/2$. Thus, in the latter system, the resolution of the image remains almost the same at all ranges so that high resolution images of the surface of the Earth can be obtained from considerable distances.

Table 3.2. Characteristics of some radar satellites in orbit.

Country	Sensor	Frequency (GHz)/band	Polarisation	Range resolution (m)	Azimuth resolution (m)	Repeat cycle (days)
ESA	ESR-1&-2	5.3/C	VV	26	28	35
Japan	JERS-1	1.3/L	HH	18	18	44
Canada	Radarsat	5.3/C	HH	9 to 100	9 to 100	3-24
Russia	Almaz	3.125/S	HH	15-30	15	5-7
USA	SIR-C	1.28/L 5.3/C	HH,VV,VH HV	8-30	30	-

Two sites, a UK Dungeness nuclear power reactor and a nuclear facility in Russia at Kyshtym were examined. The aim of the test is to see whether the warm water discharged into the a large body of water could be detected by radar sensor. The interpretation of radar imagery is complex because of the way in which a beam of radar interacts with object is very different than radiation in the visible part of the electromagnetic spectrum (see below). In order to facilitate the interpretation of radar images for the two case studies, images from optical sensors, the French SPOT and the US Landsat satellites, were also acquired. Therefore, in the following preliminary analysis one SPOT multispectral and six European ERS-2 radar satellite images over the Dungeness site and two US Landsat optical and one ERS-2 radar images over the Russian Kyshtym site were examined.

The optical images were enhanced by the conventional as well as the so called principal component analysis techniques. The general principle behind the latter is as follows. Much of the information in multispectral images is redundant due to correlation between the spectral bands. A digital image is made up of many small equal areas or picture elements or pixels. Each pixel has a numerical value, a digital number, which represents the intensity of electromagnetic energy received by it. This energy is collected from an area projected by the pixel on the ground. If digital numbers for TM band 1 are plotted, for example, against those of band 2, as in Figure 3.46(a), the data points are distributed in a narrow elongated band indicating that as the digital numbers increase for one band, they increase for the other band also. The largest number of digital points in the Figure are in the red band and the least numbers are in the pink area. The narrower the elongated band the stronger is the correlation between the data sets. There is a good correlation between these two bands. A similar distribution between bands 1 and 7 does not have such a narrow elongated shape (see Figure 3.46(b)) in which case the correlation has deteriorated indicating that there may be considerable redundancy between bands 1 and 2.

A straight line can be drawn through distributions along the longer dimension of the elongated Figure (i.e. along the major axis) using the method of least squares. This line is called the first principal component of the data and its length is the first eigenvalue (see the Tables 3.3 and 3.4 in which the values in columns are the component eigenvalues and variances). The parameter describing the variation of the digital numbers in a single band around the mean value is known as the variance. It can

be seen from the Figure 3.46 that along the major axis of the distribution there is a spread of data from the two bands. The parameter which shows the extent of the spread along the line is known as the covariance of the first principal component. A new co-ordinate system can be generated if this line is used as one axis and a second one perpendicular to it. This second axis is known as the second principal component. Combining the two bands in this way generates the first principal component. In this way the covariance matrix of the entire scene, the principal axes in feature space which account for the bulk of the variance, can be determined (see Tables 3.3 and 3.4). The data are then projected along the first two or three of these axes, effecting a dimensionality reduction.

Figure 3.46. The distribution of the digital numbers for the Landsat TM band 1 and band 2 (a) and band 1 and band 7 (b).

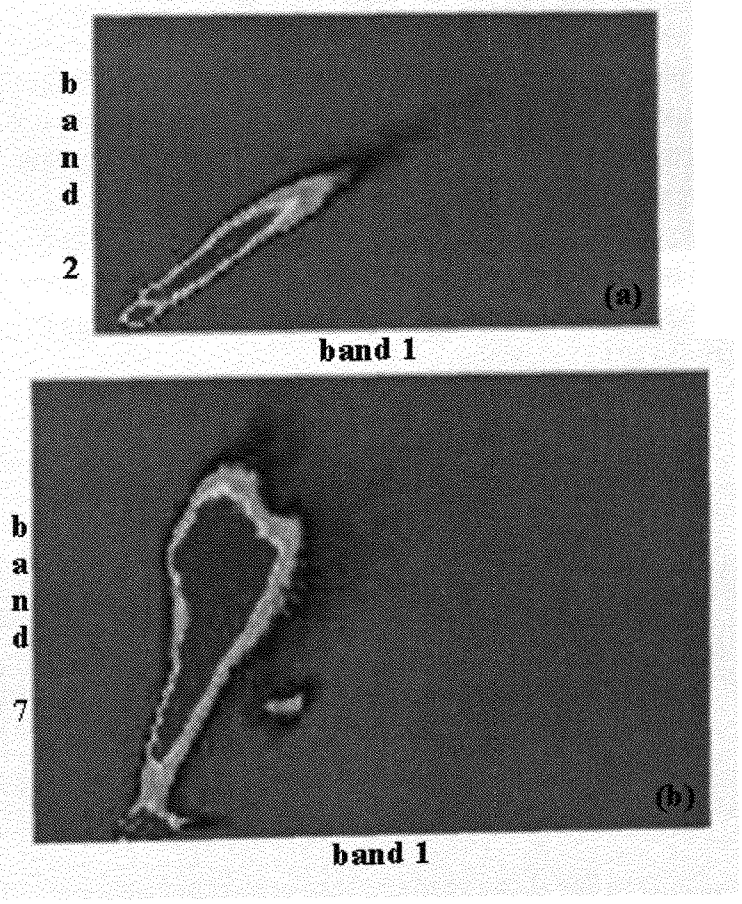

The UK Dungeness nuclear power reactor. The fuel in the early British nuclear reactors was low enriched uranium contained in magnesium alloy cans, hence the name Magnox for the reactors. A development of the early Magnox reactors is the advanced gas cooled reactors (AGR), which use slightly enriched uranium (2.3% uranium-235) contained in stainless steel containers. The AGRs tend to have smaller cores than those for the Magnox reactors and they are operated at higher temperatures. They are more efficient giving a greater power output than Magnox of similar size. At Dungeness, on the south-east coast of the UK, there are two Magnox (Dungeness A1 and A2) and two AGR (Dungeness B1 and B2) power stations. The Magnox A1 and A2, each with the power output of 285 MWe, went into operation in November 1965 and January 1966 respectively while the AGR B1 and B2, each with the power output of 660 MWe, went into operation in April 1983 and January 1986 respectively. All the four reactors are gas cooled using pressurised carbon dioxide.

In these reactors, the hot gas from the reactor core is first allowed to pass through heat exchangers in which steam is produced which is then used to drive the turbines to generate electricity. The cooled CO2 is then re-circulated into the reactor cores. The steam from the turbine exhausts is condensed by passing it over tubes through which cold water is flowing. The resultant warm water is discharged into the sea rather than being cooled in large cooling towers.

In the following preliminary test case, a multispectral image acquired by the French SPOT satellite on 9 December 1986 and six SAR images acquired on 20 February, 30 April, 4 June, 9 July, 26 November and 31 December 1996 by the European ERS-2 satellite over the Dungeness power reactors in the UK were examined. An extract of an image acquired by the SPOT satellite is shown in Figure 3.47a. The reactor site can be identified at **A.**

When the image was compared with a map of the area, a road and a railway line appear at B but these could not be detected in the image. Using the ERDAS Imagine image processing software, principal component analysis (PCA) was performed. The resulting image, a combination of the three principal components, is shown in Figure 3.47b. The road and the railway line are now visible (B). Not only this but the airfield at C can be easily detected. On the northern side of the Dungeness peninsula, the sandy coast line exposed at low tide can be seen. On the other hand, only parts of the coast line on the southern side can be seen. In the region of the power stations little sandy coast line is exposed at low tide, suggesting that the region is covered with water even at low tides making the area suitable to discharge reactor cooling water into the sea.

Figure 3.47. An extract from a full scene over the Dungeness power station in UK. The image was acquired by the French SPOT satellite using the multispectral sensor (20m resolution): (a) shows the normal band 1 (blue), band 2 (green) and band 3 (red) combination; (b) shows the combination of the three principal components PC1(g), PC2(r) and PC3(b).

Source: CNES/SPOT.

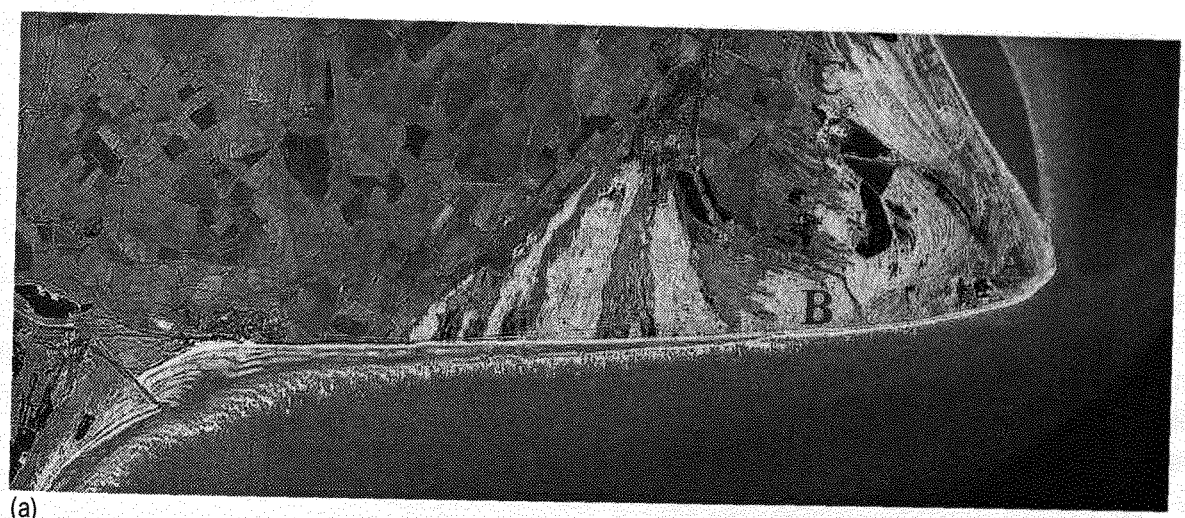

(a)

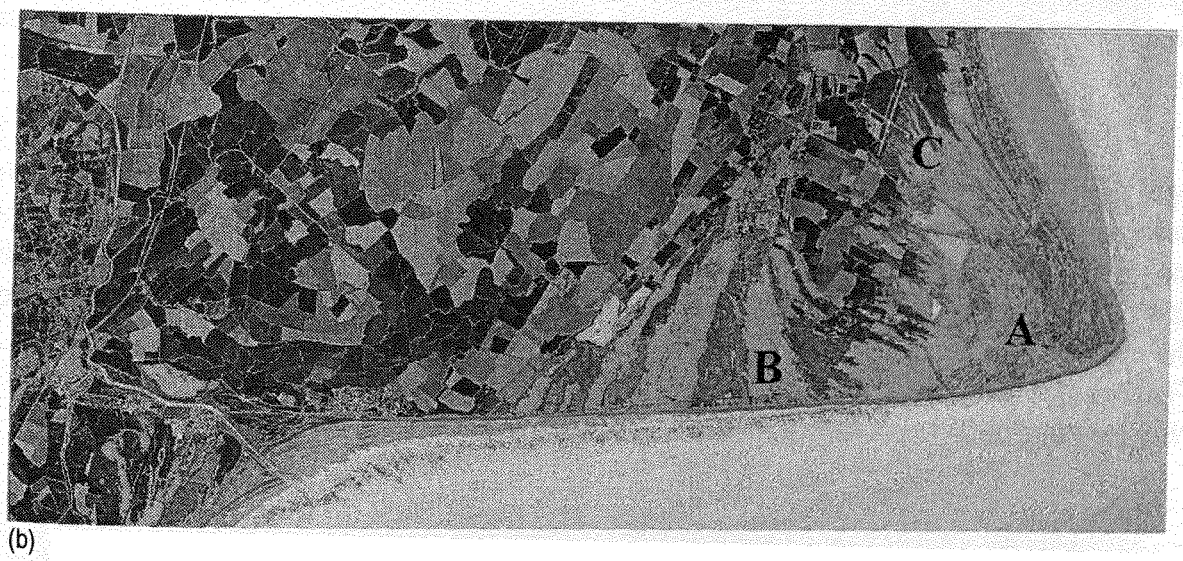

(b)

In Figure 3.48 a, b, c, d, e and f are extracts from full scenes of ERS-2 SAR images over the Dungeness power stations. The bright signature at A in the case a is due to the reactor building complex. While individual reactors can not be resolved, two distinct blocks of buildings can be identified, each of which may have the pairs of the Magnox and the AGR reactors. If the warm water from the reactors cause any turbulence on the sea surface, a bright signature might result since some of the radar radiation would be scattered back to the antenna. However, if the sea surface is calm, very little radar energy would reach the antenna resulting in a dark signature. The warm water may also change the sea surface properties causing in changes in the wave patterns, for example, dampening the waves giving dark signatures on the satellite image. The other factors that may affect the radar signature are the tides and wind speeds causing changes in wave patterns. In Figure 3.48a, the tide is low as evidenced by the broadening effect of the Dungeness peninsula. This effect can also be seen in the optical images in Figure 3.47. On 20 February 1996, the tide was low, as can be seen in Figure 3.48a and, since waves can be seen in the image, the winds may have been strong. Because of both these effects being present, it is difficult to interpret this radar image. However, just below the reactor

complex there appears to be a small dark patch at C. It is possible that this is due to the warm water in which case it may be concluded that one or more reactors are in operation. The information on the status of the reactors was obtained from the operators and it was found that two of the four reactors were in operation.

In Figure 3.48b, immediately below the reactor complex, a very dark plume can be seen spreading into the sea towards the north east round the Dungeness peninsula. The beach (B) on the northern part of the peninsula can not be seen in Figure 3.48b because of the high tide. In Figure 3.48c, again a similar dark warm water plume can be seen. In Figure 3.48d, the beach at B can be seen because of the low tide indicated by the tidal front. In this case the signature due to the discharged warm water is considerably smaller, barely distinguishable from the dark area lining the southern coast. On the other hand the plume seems to be larger in Figure 3.48e and the tide is also high as indicated by the submerged beach at B. There is no similar signature of a warm water plume at the reactor site in Figure 3.48f, at least judged by the lack of dark response. There seems to be some bright signature originating in the vicinity of the reactor site spreading towards the east. If the dark signature is due to the discharged warm water from the reactors, then the images indicate that on 20 February only some reactors may be operating, on 30 April and 4 June perhaps all four reactors were in operation, while on 9 July either all the reactors were in operation but at very low power or only some were in operation; again at low power. On 26 November, only some reactors were in operation as suggested by some increase in the discharged water. On 31 December all the systems may have been shut down because no dark plume can be detected.

Thus, it was concluded that: (1) on 20 February not all the reactors were in operation; (2) on 30 April and on 4 June possibly all reactors were working; (3) on 9 July some units were probably shut down as there was very little sign of warm water; (4) on 26 November more units were operating since the dark plume was increased in size; and (5) on 31 December again all units may have been shut down as there was no sign of the dark plume. Only some of these observations were confirmed from the data acquired from the reactor operators.[63] In fact, for example, two units were operating on 20 February and on 4 June, all were operating on 9 July, three out of four were in operation on 26 November and on 31 December and only one was in operation on 30 April.

[63] Private communications.

Figure 3.48. Extracts from four ERS-2 SAR images over Dungeness.

Source: ESA.

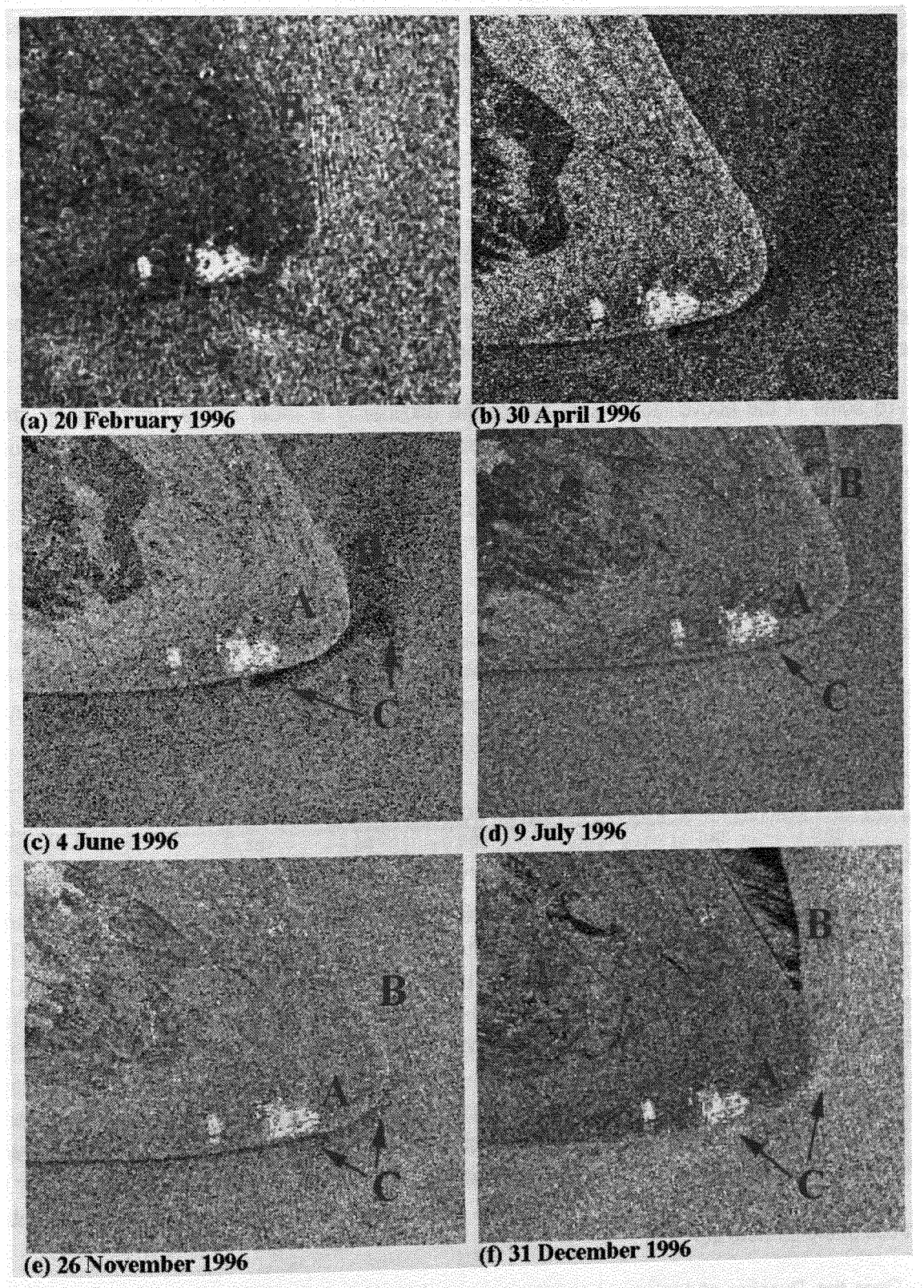

A careful examination of the image in Figure 3.48f shows some bright signature originating near the reactor site. Assuming that the phenomenon is due to the discharged water, then it is surprising that the dark response was observed in the first three images.

The bright signature may have been caused by the ripples and waves on the sea surface which would reflect some of the radar radiation back to the radar antenna. The dark response in the first three images would suggest very calm and smooth surface indicating that discharged water is not causing any turbulence in the water. One would have expected very specular bright response, similar to the one seen from the bulk of the sea. Thus, the difference would have been because of the temperature differences. The temperature of the discharged water could be some 10°C higher than that of the sea water. Even this may vary depending on the time of the year. This difference may be greater in winter than in summer months owing to the seasonal temperature changes in the sea water. The former three images suggest similar state of the sea surface; calm with perhaps small waves. The fact that in Figure 3.48f very little difference can be detected between the water near the coast and that in the sea, except for some bright signature near the reactor site, and that in the main bulk of the sea would suggest that the discharged water is causing some turbulence and its temperature is different from that of the sea water. This would suggest that some reactors are operating. Another interpretation may be that the sea is very rough and is masking, to a large extent, the effect of the warm water near the nuclear site.

To some of the above factors that add to the uncertainty in radar image interpretation are, of course, the tides. From the standard Tables available for predicting tides, it was determined that on 20 February, 3 April and on 4 June the satellite was above the reactor site some two hours before high tide; on 9 July, some five hours after the high tide; on 26 November, just under one hour before the high tide; and on 31 December, about two hours after the low tide. From the June and November images (Figure 3.48c and 4.48e) it can be seen that the dark plume is pronounced when the satellite was above Dungeness close to and just before the high tide (that is, in coming tides). The minimum dark plume was observed on 9 July when the satellite came over the site some five hours after the high tide (that is, out going tides). Thus, the temperature effect may be more pronounced at high tides than in the case of falling tides. However, when the sea is rough, such as was probable on 31 December, the temperature effect may give a different signature.

3.11 A Russian facility observed by optical and radar sensors

Two Landsat TM images were acquired over the Russian plutonium production plant at Kyshtym on 1 August 1987 and on 13 May 1993. Sections of the whole scenes were extracted and a combination of bands 6 (red), 2 (green) and 1 (blue) are shown in Figure 3.49a (1 August 1987) and Figure 3.49b (13 May 1993). The warm water (in red) discharged from nuclear facilities at B and C can be seen at A and D respectively only in Figure 3.49b. In Figure 3.49a the lack of warm water in the reservoir at D indicates that the facility at C was not operational on 1 August 1987. On the other hand the channel that links the large lake and the reservoir also appears red in Figure 3.49(b). This may be because the water used to flow from the large lake but when barrier were erected forming the reservoir, the flow of water stopped. This may have caused silt into the channel giving rise to shallow water which could easily become warm by the sun. Another reason may be because some of the warm water from the large lake may be leaking into the channel although none of it enters the reservoir probably because of the barriers at F.

Over the Russian plutonium production facility, using the ERDAS Image processing software, principal components were determined. PCA was carried out using two Landsat TM images acquired on 1 August 1987 and on 13 May 1993. Summaries of the variance matrix, the component eigenvalues, and the component loadings are given in Tables 3.3 and 3.4. By associating the first three principal components with the primary colours of a graphics display one can often generate a single image which

could account for more than 95 percent (Tables 3.3 and 3.4) of the information in the seven bands of a Landsat scene. The comparison clearly shows the radiometric differences of the two images. A combination of the visible bands 1 (blue), 2 (green) and 3 (red) appears normal to the eyes. These are shown in Figures 3.50a and 3.51a for the two dates. The PCA was carried out on the first image and components 2 (green), 3 (red) and 7 (blue) were chosen and combined (see Figure 3.50b). From the Table 3.3 it can be seen that the component 2 consists of predominantly data from the TM infrared bands 4 and 5 and the component 3 is mainly from the thermal band 6. In order to get maximum data for the latter, component 7 was also used. While most of the data were in component 1, this was not used in order to obtain a better contrast between vegetation and man-made features such as roads and buildings. This is apparent from Figure 3.50b. Note that very little indication of discharged warm water from the facility at C can be detected at D in the reservoir (see Figure 3.51b) while a considerable amount of warm water is being discharged in the lake at A from the facilities at B. This is not surprising since the facility at C is still being built as evidenced by, for example, un-developed land at C and by what appears to be an open channel E linking the facility and the reservoir.

Table 3.3. The Table shows standardised[64] PCA on an image acquired on 01/08/1987

Loading	C1	C2	C3	C4	C5	C6	C7
Ky87_1	0.844594	-0.466049	-0.187959	-0.081719	-0.152827	0.062107	0.015690
Ky87_2	0.897117	-0.332282	-0.209734	-0.106445	0.166295	0.039510	-0.015140
Ky87_3	0.923273	-.0338863	-0.065183	0.082743	-0.006711	-0.146355	0.013398
Ky87_4	0.461376	0.819140	-0.307417	0.133694	0.036524	-0.038259	-0.031057
Ky87_5	0.857738	0.488284	-0.007061	0.127429	0.029719	0.041976	0.083221
Ky87_6	0.824486	0.116375	0.518862	-0.193044	-0.005382	-0.-12472	0.003121
Ky87_7	0.957953	0.116790	0.132765	0.208427	-0.018910	0.040874	-0.074811
%Variance	**70.24**	**19.70**	**6.64**	**2.00**	**0.77**	**0.46**	**0.20**

[64] In the standardised case, the correlation matrix is used for input rather than the usual variance/covariance matrix. For the time series analysis, it is more common to use standardised variables. In this case, all bands have equal weight while un-standardised variables, those bands with greater variance, usually the infra-red bands, will have a greater weight.

Table 3.4. The Table shows standardised PCA on an image acquired on 13/05/1993.

Loading	C1	C2	C3	C4	C5	C6	C7
Ky93_1	0.916133	-0.361631	0.073808	0.093284	-0.123710	-0.021534	0.002543
Ky93_2	0.940677	-0.318215	0.015901	0.036938	0.069783	0.084323	0.016191
Ky93_3	0.969538	-0.206967	0.022989	-0.025654	0.095640	-0.080806	-0.016961
Ky93_4	0.920084	0.066315	-0.379402	-0.059936	-0.028592	0.011789	-0.023577
Ky93_5	0.963084	0.208581	0.019969	-.0156073	-0.014750	-0.016942	0.060875
Ky93_6	0.875780	0.404471	0.011302	0.262549	0.017724	-0.004698	0.004191
Ky93_7	0.935069	0.230120	0.230023	-0.128132	-0.021437	0.030304	-0.044619
%Variance	**86.85**	**7.70**	**2.91**	**1.77**	**0.44**	**0.22**	**0.10**

As these two Landsat images were acquired at different times of the year, to get visually similar images over the site, principal components 1 (green), 4 (red) and 5 (blue) were chosen for the analysis. The composite image is shown in Figure 3.51b. Three striking differences are the positive indication of warm water being discharged into the reservoir at **D**, the site at **C** appears to be developed since there are regular roads and buildings, and the above mentioned channel at **E** linking the facility **C** and the reservoir is covered up suggesting its completion. Moreover, while physical changes such as roads and buildings are easily recognisable from the normal bands 1, 2 and 3 combination, different types of vegetation can not be easily seen in such an image. For example, old roads disappearing at **1** and the construction of a new one at **2** are easily detected from Figures 3.50a and 3.51a. Also, from Figures 3.50b and 3.51b, it can be seen that the PCA helps to differentiate between different types of vegetation and land use. It should be mentioned that there are other small lakes in this area which show red signatures (e.g. a lake below **B** in Figure 3.49b). This may be because the water may be shallow so that the water could be warmed up by the Sun. Also, as mentioned above, some of the body of water in this area has developed considerable amount of silt which may give rise to such strong red signatures.

Figure 3.49. This shows a combination of bands 6 (red), 2 (green) and 1 (blue) of the US Landsat TM images acquired on 1 August 1987 (a) and on 13 May 1993 (b). At A and D in (b) the strong response in red colour from the thermal band indicates the warm water discharged from the main reactor complex at B and a new complex at C respectively. On the other hand in (a) warm water is indicated at A only. Scale: 1:48,000

Source: EOSAT/Landsat.

(a)

(b)

Figure 3.50. An extract from the full scene of a Landsat TM image acquired on 1 August 1987 over the Russian nuclear facility at Kyshtym. (a) is a combination of bands 1 (blue), 2 (green) and 3 (red) while (b) is a combination of principal components 7 (blue), 2 (green) and 3 (red).

Source: EOSAT/Landsat

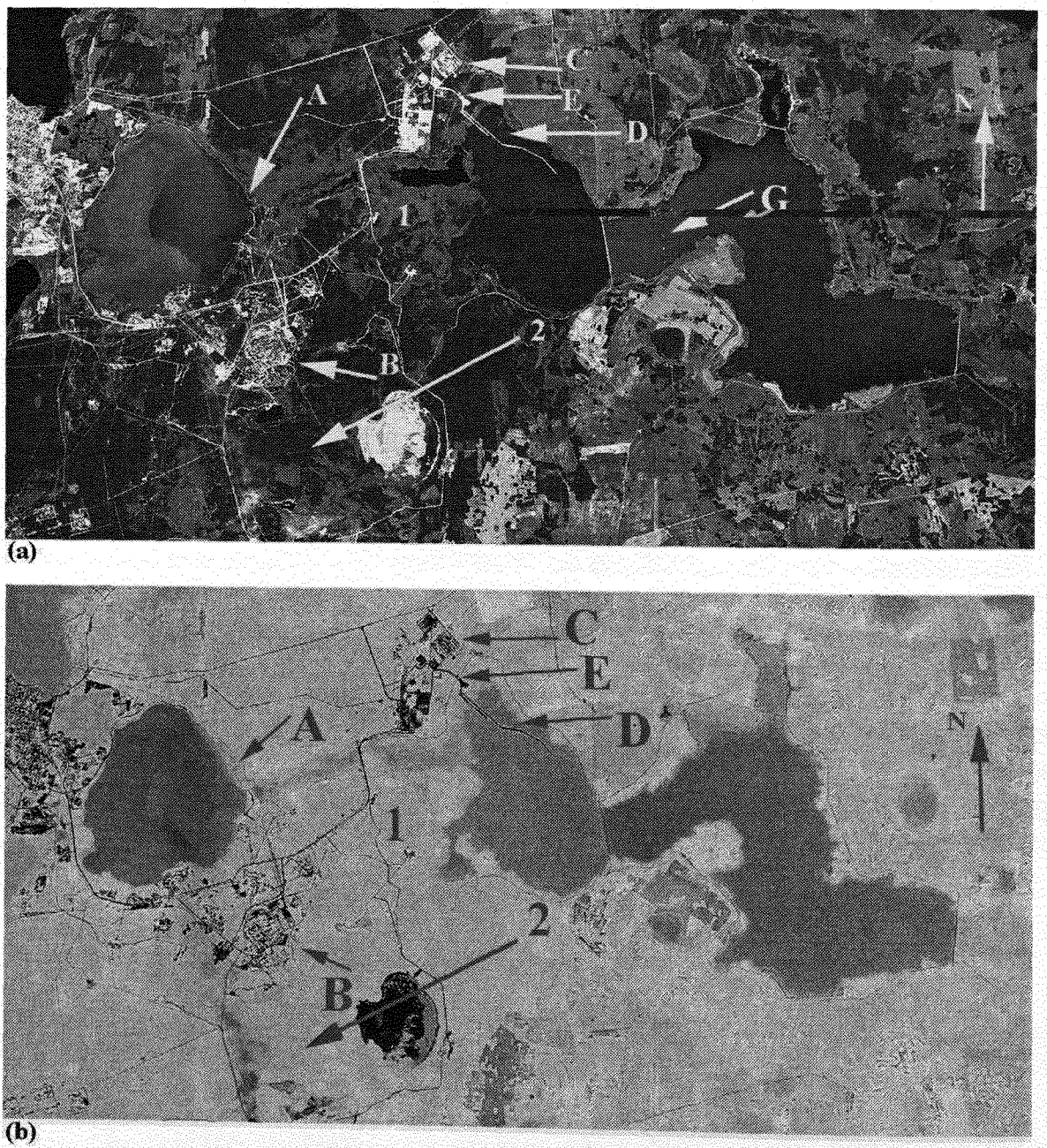

A SAR image over the same area was acquired by the European ERS-1 radar satellite on 7 May 1993 only six days before the acquisition of the second of the above two Landsat scene. An extract from the whole scene is shown in Figure 3.52. The image was co-registered and corrected for size against the Landsat image of Figure 3.48 using ERDAS Imagine 8.2[65] image processing software. The SAR image was then combined with bands 2 (green) and 6 (blue) of the Landsat TM scene. Extracts of the lake **A** and the reservoir **B** were then made and enhanced separately using the Adobe Photoshop

[65] ERDAS Imagine, version 8.2 manufactured by ERDAS Inc., Atlanta, Georgia, USA.

image processor. These are shown in Figure 3.53a and b. It can be seen that the bright signatures in red of the SAR coincide with those of the thermal band in blue.

Figure 3.51. An extract from the full scene of a Landsat TM image acquired on 13 May 1993 over the Russian nuclear facility at Kyshtym. (a) is a combination of bands 1 (blue), 2 (green) and 3 (red) while (b) is a combination of principal components 5 (blue), 1 (green) and 4 (red).

Source: EOSAT/Landsat

(a)

(b)

While these examples are a positive indication of the use of a SAR for detecting warm water, more work is needed.

It can be seen from the above analysis that images acquired from a satellite carrying a SAR sensor could be useful in safeguards applications. Indications are that the discharge of warm water from nuclear facilities into the sea or a lake could be detected by a SAR. At present this is not possible with

the optical thermal sensor if the discharge takes place into a river less than 120m wide. The only thermal sensor in orbit is that carried on board the Landsat 5 satellite with a resolution of 120m. Moreover, a SAR can also detect power lines which is a useful indicator of the nature of a reactor facility.

Figure 3.52. An extract from a full SAR scene acquired by the European ERS-1 satellite on 7 May 1993 shows some bright signatures at A and D, possibly due to the warm water discharged from the nuclear facilities at B and C. Scale: 1:48,000

Source: ESA

Figure 3.53. This shows the lake and the reservoir only from Figures 3.49 and 3.52. Landsat thermal band 6 (blue) and band 2 (green) were combined with the SAR (red). The overlap of the thermal band (blue) and the SAR (red) can be seen clearly.

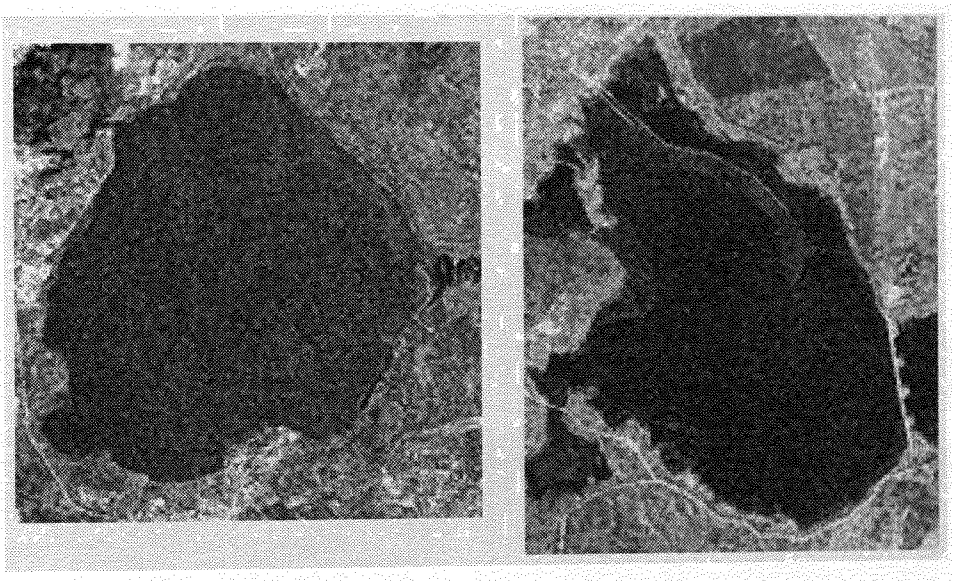

(a) (b)

3.12 Gorleben, the German back end of the fuel cycle facilities

An interim nuclear spent fuel storage plant was built near Gorleben (53° 3'N, 11° 21'E) between 1981 and 1983 and became operational in 1995. During the same period, an interim facility for storage of low-level radioactive waste was also built in the same complex and became operational in 1984. By about 1996, buildings for a pilot conditioning facility were completed (Figure 3.54). This facility is expected to go into operation in 1999. In the vicinity, an exploratory mining operation is being conducted (Figure 3.55) to determine the suitability of the salt dome for a final repository of high-level radioactive waste. This activity will continue until the year 2003. The excavated material is collected in the same area.

Three Landsat TM images, acquired on 24 August 1984 (Figure 3.56a), 31 August 1989 (Figure 3.56b) and 21 August 1997 (Figure 3.56c) over the Gorleben sites, were examined for detecting changes in the sites. A high-resolution image acquired by the Russia KVR-1000 sensor (Figure 3.56d) was also used for the analysis. However, the date of acquisition of the image was not known.[66]

[66] Russian KVR-1000 images taken over Germany are now available on CD-ROMs which contain images with best resolution of about 5m.

Figure 3.54. Plan of the interim storage and pilot conditioning facilities at Gorleben in Germany: (1) Storage hall for spent fuel transport and storage casks; (2) storage hall for waste drums; (3) rain water basin; (4) guardhouse; (5) administrative and social building; (6) workshop; (7) garage; (8) operations building; (9) fence; (10) pilot conditioning facility; (11) electricity supply; (12) utility building; (13) rain water basin.

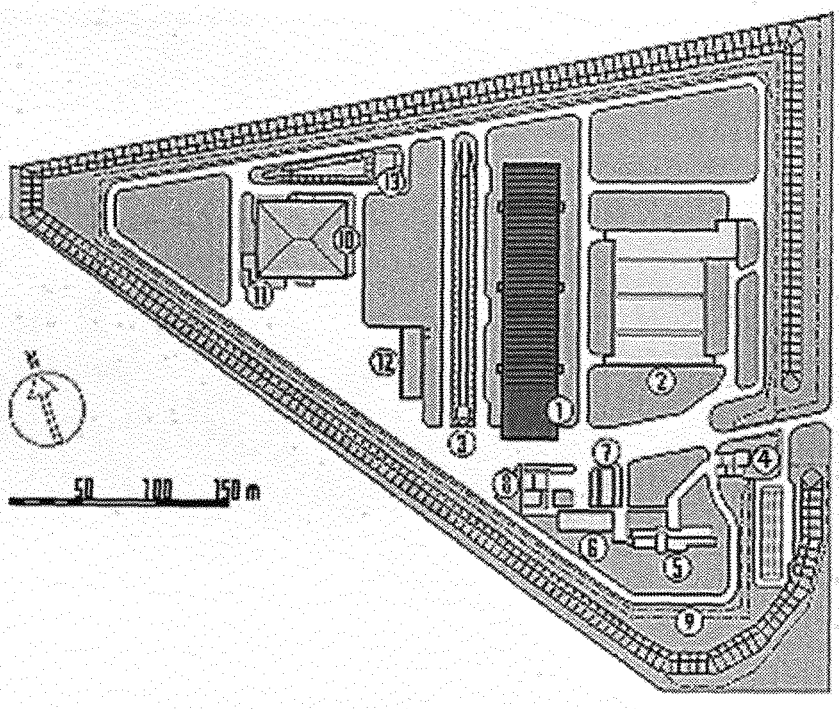

Figure 3.55. Gorleben exploratory mine: Plan of surface facilities: (1) Guardhouse 1; (2) WC's changing rooms, central heating station; (3) office and social building; (4) shaft 1 of mine; (5) guardhouse 2; (6) shaft 2 of mine; (7) oil store; (8) transformer switch station; (9) explosive store; (10) dog kennels; (11) material/equipment store; (12) fuel storage; (13) lodging sanitary container; (14) water pumping station; (15) electric transformer station; (16) splash water pumping station; (17) weather station.

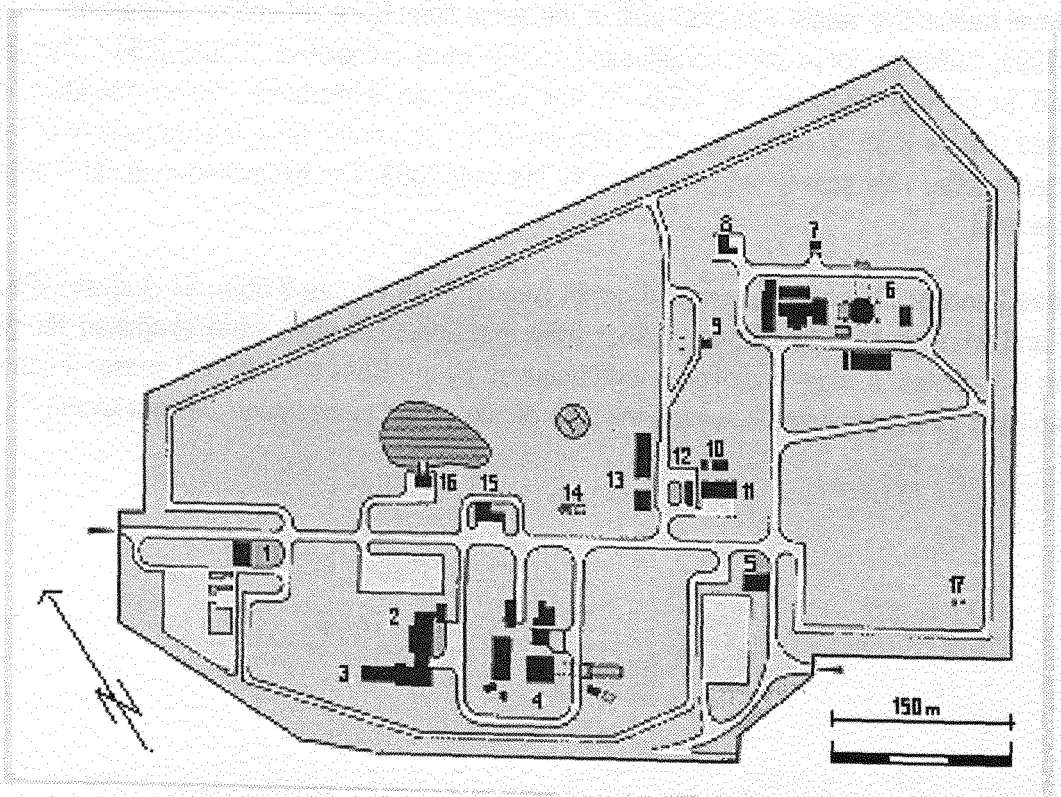

Figure 3.56. Extracts from the Landsat TM images over Gorleben, shown as combinations of the principal components 1 (red), 2 (green) and 3 (blue) (a-c) and a high-resolution image acquired by the Russian KVR-1000 sensor . The dates are indicated.

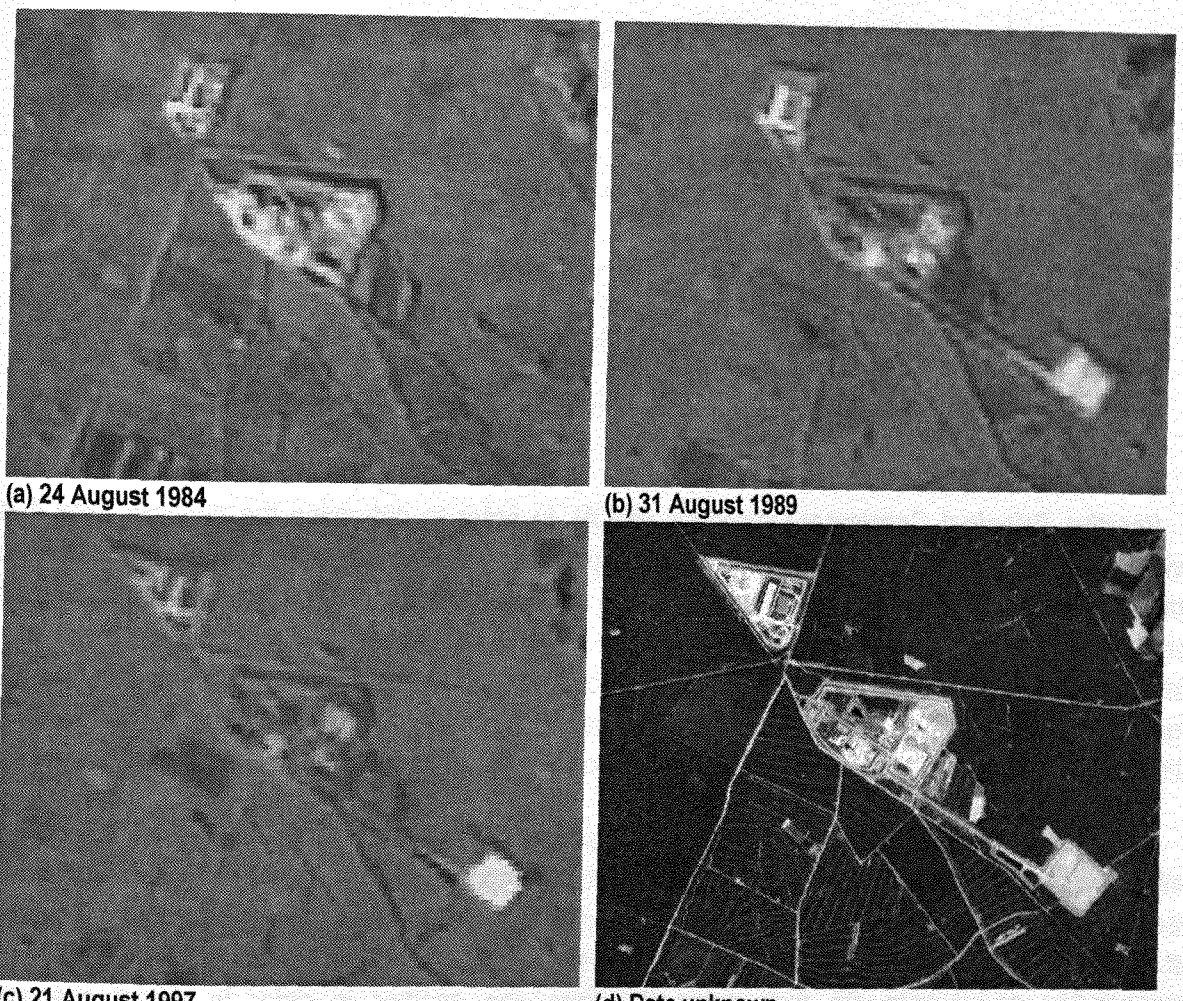

(a) 24 August 1984

(b) 31 August 1989

(c) 21 August 1997

(d) Date unknown

In this section, three methods based upon linear transformations of Landsat TM data have been used to detect changes in the Gorleben sites. They will be briefly described here. (For information on the change detection pre-processing see Appendix III, the mathematical description of the following techniques is given in Appendix IV).

Principal Component Analysis (PCA). The PCA is one technique to determine changes in a site (see the earlier sections on Dungeness and Kyshtym). In this section, principal components (PC) were generated using one band of the two images (bi-temporal):

We consider a bi-temporal feature-space for a single spectral band with the pixel $X_i = [X_i(T_1), X_i(T_2)]$ (Figure 3.57). A principal component establishes the first principal axis along the direction of maximum data variance. Temporally correlated pixels (no-change pixels) will lie along this axis, while uncorrelated pixels (change pixels) will tend to lie above or below it. Thus the projection of pixel intensity orthogonal to the first principal axis – i.e. the second principal components $Y_i(T_2)$ – are a measure of change. Mathematically, the principal components are determined by the eigenvectors of the data covariance matrix and are obtained by a simple diagonalization.

Figure 3.57. Principal component analysis (PCA)

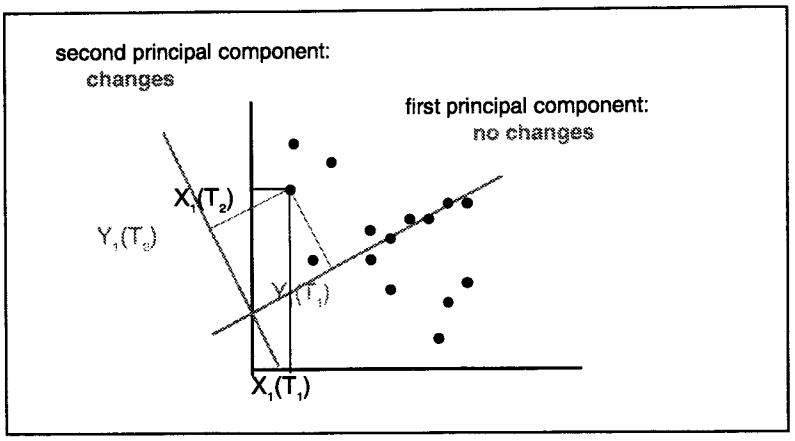

Iterative Principal Component Analysis (IPCA). In order to determine the principle axes it is advisable to use only those pixels which do not represent changes. Wiemker et al.[67] suggested an iterative algorithm in which the pixels determining the covariance matrix are weighted according to their probability of being no-change pixels. In the present study, a somewhat simpler procedure is applied: After the initial determination of the covariance matrix, those pixels with second principal components larger than three standard deviations are excluded from the sample. Then the covariance matrix is re-estimated and again diagonalized. This is repeated until the principal components no longer change.

Multivariate Alteration Detection (MAD). Nielsen and Conradsen[68] recently suggested a modified method which essentially makes use of all multispectral components simultaneously. Their algorithm is based on canonical correlation analysis. Multispectral data taken at two times are transformed so that the first transformed components are maximally and the last components minimally correlated. The corresponding components are then subtracted from one another in order to detect changes. Mathematically the method involves the solution of a generalised eigenvalue problem and has the advantage of being invariant to linear scaling. The latter property makes it insensitive to differences in atmospheric conditions at the times of data collection.

A technique known as the IHS Intensity, Hue, Saturation (IHS)-transformation with a high resolution image helps to visualise the change. Change detection in nuclear sites requires both the spectral resolution and a spatial resolution of a few metres. The currently available images (US Landsat TM multi-spectral and the Russian high-resolution), offer the possibility of merging such data.

RGB (red, green, blue)-IHS transformation was carried out using the three bands of the Landsat TM analysis (three second principal components or three MAD components, for example). The intensity component was replaced by the high resolution KVR-1000 image. Finally a back-transformation of this IHS into the RGB colour system was carried out.

---

[67] Wiemker, R., Speck, A., Kulbach, D., Spitzer, H., and Johann B., "Unsupervised Robust Change Detection on Multispectral Imagery Using Spectral and Spatial Features", **Proceedings of the Third International Airborne Remote Sensing Conference and Exhibition**, Copenhagen, July 1997, vol. I, p. 640-647.

[68] A. Nielsen and K. Conradsen: "Multivariate Alteration Detection (MAD) in Multispectral, Bi-temporal Image Data: A New Approach to Change Detection Studies", **IMM Technical Report No. 1997-11**, Technical University of Denmark, 1997.

All changes were indicated in colours. Only those change pixels exceeding a threshold of a fixed number of standard deviations are shown.

The results of the change detection are represented in Figure 3.58 and Figure 3.59. IPCA and MAD-Transformation show comparable results with regard to the following changes:

1. Changes resulting from construction works on the interim storage area (in connection with the construction of the pilot conditioning facility).
2. Changes resulting from the exploratory mine.
3. Formation of the mining debris heap of removed overburden between 1984 and 1989.
4. Construction of the pilot conditioning facility

Figure 3.58. Bi-temporal change detection for the Landsat TM extracts over Gorleben acquired on 24 August 1989 and 31 August 1989, fused with a high resolution KVR-1000 image. a) PCA: Shown is the second principal component of the channels 5 (red), 4 (green) and 3 (blue) exceeding three standard deviations. b) IPCA: Shown is the second iterated principal component of the channels 5 (red), 4 (green) and 3 (blue) exceeding three standard deviations. c) MAD: Combinations of the MAD Components 6 (red), 5 (green) and 4 (blue) exceeding five standard deviations.

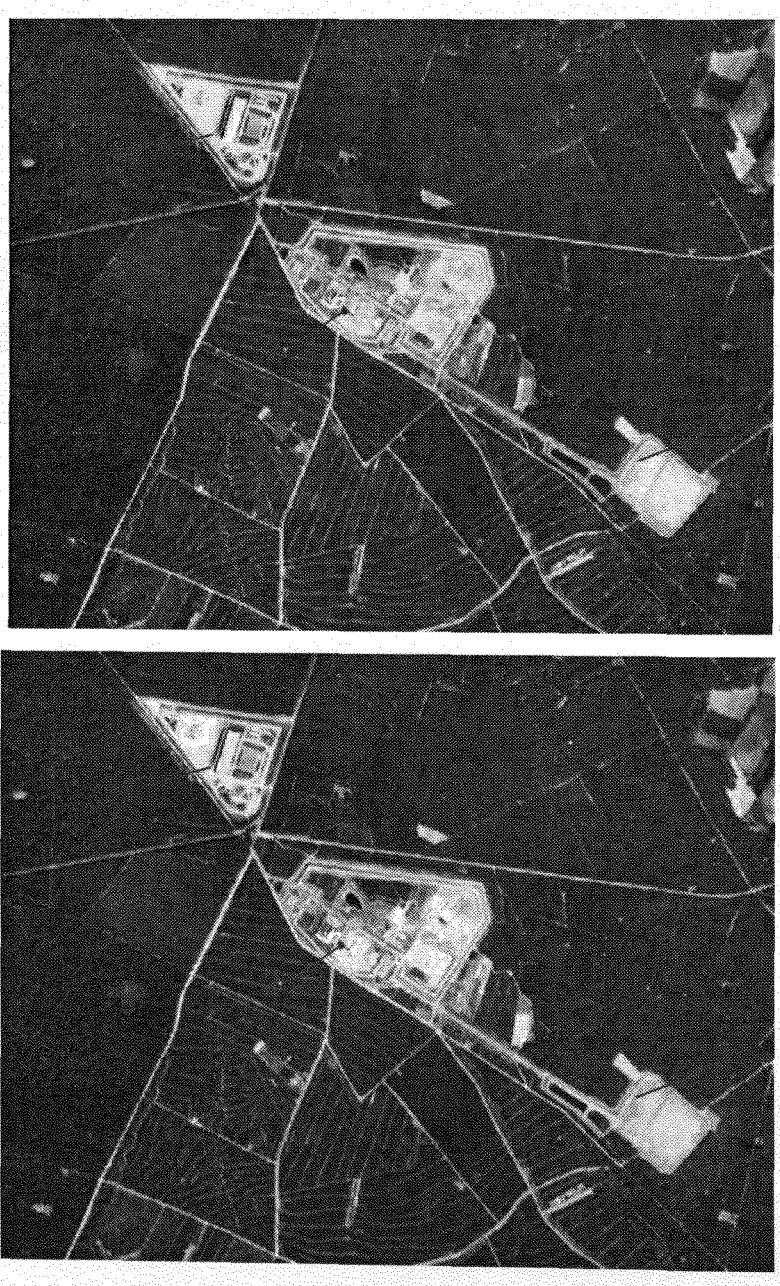

(a)

(b)

Figure 3.58. (continued)

(c)

Figure 3.59. Bi-temporal change detection for the Landsat TM extracts over Gorleben acquired on August 1989 and 21 August 1997, fused with a high resolution KVR-1000 image: Combinations of the MAD Components 6 (red), 5 (green) and 4 (blue) exceeding five standard deviations.

With regard to the IAEA's safeguards procedures, it would help an inspection team to know prior to the inspections where, if any, changes in a site have taken place. The inspected State might have informed the Agency of such changes. On the other hand, if the Agency is not informed, it can request the State for explanations for the changes and, if necessary, carry out on-site inspections.

4 CONCLUSIONS

In this study, some preliminary results are presented in which different sites were examined using commercially available satellite images. The sensors that recorded the multispectral data were sensitive to visible, near and far infrared (IR) and long-wavelength IR (thermal) and the panchromatic in the visible range of the electromagnetic spectrum. Several radar images were also examined to detect effects of warm water discharged in a lake, a reservoir and into the sea.

For an undeclared nuclear facility examined the following can be said:

a) Features such as passive defences like perimeter fences can be identified.

b) Active defences like military airfields and surface-to-air-missile (SAM) sites can be observed.

c) It is also possible to detect ammunition storage areas.

d) Observations of facilities in the thermal IR region, when relatively large areas are involved, can be useful in determining the operational status of a facility.

e) Undeclared sites tend to be in remote regions.

f) Facilities are usually located near rivers, lakes or reservoirs.

g) Images acquired over a period of time could be used to assess the development and operational characteristics of a facility by detecting changes in the images.

h) Power lines associated with reactors producing electricity can be detected in images with good contrast.

With the examined declared sites the following features were observable from space:

a) Depending on the type of a reactor, it may be situated near a source of water supply or it may have large cooling towers associated with it; an example of the latter is a gas cooled reactor.

b) Images acquired over a period of time could be used to assess the development and operational characteristics of a facility by detecting changes in the images.

c) The use of thermal IR images gives an indication of the operational status of a facility.

d) The T-shaped building associated with some centrifuge enrichment facilities such as these at Almelo and Gronau, large buildings required for housing cooling ponds for spent fuel and reprocessing plants can be detected and recognised (however, all centrifuge facilities may not necessarily display the T-shaped building feature).

e) Power lines, associated with reactors generating electricity, can be detected when there is good contrast in an image.

In order to determine the operational characteristics, cooling towers associated with reactors were observed using panchromatic and multispectral images. It was found that when the atmospheric

temperature was low, condensation above and within the cooling towers occurred. This was easily detectable. On the other hand, during warmer weather, the absence of vapour condensation required looking into the cooling towers using thermal band of the Landsat satellite to determine the presence or absence of warm air and probably water. However, the usefulness of the thermal sensor on board the US Landsat satellite is limited if the cooling towers, rivers, lakes and reservoirs were smaller than 120 m, the resolution of the sensor.

It should be emphasised that observations from space should not be the only source of information for the IAEA to carry out its safeguards procedures. When it comes to detecting undeclared sites, analysis of information available from open sources, such as newspaper and journal articles, should be used to determine any indication of undeclared activities. A member state could provide the IAEA information on certain undeclared nuclear facilities. Civil remote sensing satellite data can then be used not only to verify the veracity of all such information but also to determine the precise location and the nature of the observed nuclear facilities. There is also scope for deploying the technique to verify the consistency of information declared by States including the site boundaries and facilities adjacent to declared facilities. It could also be utilised in any future use of wide area environmental sampling, for example, to indicate regions of the world where undeclared activities could not be performed above ground.

Using some of the above criteria, identification of certain nuclear plants may be possible. If necessary, this could be followed by a request for on-site inspections. The Agency's inspection request could then be accompanied by data from civil remote sensing satellites that it has acquired and analysed.

Finally, during the training period, the trainees need to keep an open mind and not be prejudiced by the experience they may have had of aerial or high resolution reconnaissance satellite data. Whilst the data from civil remote sensing satellites are not as good, with a certain amount of innovation, they can still yield very useful information. Most important is the fact that such data are commercially available.

In the future, 1m resolution will be available which is sufficient to detect relevant structures of undeclared facilities.

Linear transformations (PCA, IPCA, MAD) were investigated to determine their usefulness in the detection of changes in a scene and as an aid to image interpretation. Following main conclusions were drawn:

1. Several ways of detecting changes on the ground were examined:

   a) Two panchromatic images taken at different times were compared to determine whether any changes had taken place on a site; while differences could be detected by examining the images by eye, it was also found that a study of the reflectance properties of a section of the site could reveal whether any changes have occurred.

   b) In a multi-spectral image, the principal component analysis indicated that the technique is very useful for studying changes in the spectral characteristics of an image rather than the examination of physical shapes of objects on the ground. For example, the method is very useful for detecting small changes in temperature or changes in the spectral characteristics of vegetation and other objects on the ground.

c) Linear transformations (principal component analysis, iterative principal component analysis and multivariate alteration detection) are very sensitive change detection techniques, giving indication as to where man-made changes may have taken place.

d) Data fusion using the IHS transformation is a useful technique when a high resolution panchromatic image is combined with a low-resolution multi-spectral image, in order to facilitate interpretation.

2. Radar images acquired over two sites, for which optical images were also available, indicated that radar could be a useful tool for detecting changes in temperature in water. This could give a day and night and all weather capability for monitoring nuclear activities of States, particularly those reactors that may be used to produce plutonium.

3. Satellite imagery can be a very useful aid to inspection planning, in the evaluation of information (e.g. site map, status of closed down/decommissioned facilities or facilities under construction) provided by Member States. Moreover, it could also be useful in the assessment of other information available to the IAEA (e.g. from open sources), and that compiled from national technical means.

4. As part of the Agency's safeguards procedures, if the wide area environmental sampling technique is shown to be technically feasible and cost-effective, then observation satellites could become an additional useful tool, for example, in determining where environmental monitoring measures might be implemented. In the case of Iraq, wide area sampling is carried out without the use of satellites. However, this is a unique case. In other Member States, in order to determine where sampling equipment should be deployed, the use of satellite observations may be a useful way to proceed or it may be the only way to proceed.

The results of this study are encouraging. It was shown that current generation commercially available panchromatic images from satellites can detect and identify undeclared facilities. Nevertheless, more work needs to be done. For example, it is necessary to carry out an extensive examination in which power reactors such as Candu and Magnox types, dedicated plutonium production reactors, research reactors, enrichment and reprocessing facilities should be examined using panchromatic and multispectral images having both medium (5-10m) and high resolutions (1-2m). The use of stereoscopic images should be examined. This is because it is possible to extract more information from such data even at low resolution (such as 10m from SPOT or 6m from the Indian IRS-1C satellites) if stereoscopic images and computer enhancement is used. An improvement by a factor of $\sqrt{2}$ could be obtained in effective resolution. Thus, an image from the Indian IRS-1C satellite, which has a resolution of 5.8m, could have effective stereo image with a resolution of about 4m pixel. Moreover, stereo images facilitate measurements of the dimensions of objects being observed. Through such images, description of targets may become easier. Within the next one to three years, images with resolutions between one and three metres will become available. Such data should also be examined.

Looking into the future, another question, which needs to be addressed in detail, is that of data transmission to the base ground receiving station from various commercial observation satellites. Although there are a number of commercial communications spacecraft in orbit at present, they are probably not able to handle the large data rates generated from observation satellites. It is possible that the operators of such satellites could incorporate improved facilities in their satellites so that they can transmit data from civil remote sensing satellites.

The method for detecting changes on the ground needs to be examined more closely using images taken at different times. It would be beneficial to examine more images over the sites analysed in this preliminary study. An important part of the study would be the use of radar sensors. As the interpretation of radar data is difficult, a considerable amount of work is needed in this area. Also with the imminent availability of higher resolution data than is currently available, the importance and usefulness of commercial satellite imagery for the IAEA will increase.

Various image processing and interpretation techniques also need to be examined, i.e. mathematical tools requiring software development. Apart from the geometric correction, an accurate atmospheric correction is essential for change detection. In order to minimise errors in the analysis, it is necessary to make use of atmospheric correction algorithms or to use change detection techniques with images taken at the same time of the day and during the same month of the years. Image classification is another procedure for change detection. Post-classification comparison analysis of two independently produced classified images with the view to detecting changes in the pixel classes between two dates minimises or bypasses the problems of geometric and radiometric differences between two dates. In multi-temporal classification, a combined data set of two or more dates can be analysed in supervised or unsupervised mode to identify changes. Classification algorithms for both applications are for example Fuzzy Clustering, Maximum Likelihood, Neural Networks, as well as combinations of them. Finally, details about the spectral signatures of the sites being examined, for example, radiometric measurements on different building materials, would simplify the image interpretation. The commercial availability of such tools is very limited. Therefore, it is necessary to develop the appropriate software.

From the safeguards point of view it is important to have a spectrum of tools available for image interpretation particularly when non-compliance issues come up. The Agency needs to be absolutely certain that a non-compliance has occurred.

The IAEA has perhaps five options to choose from:

- not to adopt the use of civil satellite imagery;
- to rely on the member states to acquire information from space and inform the Agency of any irregularities;
- to create or utilise regional verification agencies similar to the Western European Union Satellite Centre (WSC);
- to wait until an international verification agency is organised under the United Nations;
- to acquire commercially available satellite images and undertake analysis in-house. (This could be triggered by other information, for example, as supplied by Member States or from information analysis.)

The option of not using satellite imageries would ignore the potential benefits of the utility of such information. Reliance on information supplied by Member States has not worked satisfactorily so far because of political problems and perceived vested national interests. Evidence provided to the IAEA on nuclear activities in DPRK acquired by observation satellites was dismissed by the DPRK as being fabricated intelligence information and exacerbated the difficulties being encountered by the IAEA in attempting to confirm the extent of DPRK's compliance with its NPT obligations. Additionally,

dependence upon the provision of information from Member States can give rise to timeliness problems: for example, information on Iraq was made available to the IAEA too late. It is thus not politically sensible for the IAEA to be dependent entirely upon others to provide such information.

The IAEA could request information from or contract the work out to the existing regional agencies, such as the WSC. There are other international treaties elsewhere which might provide the basis for possible satellite verification agencies. For example, in the South Pacific region the 1985 Treaty of Rarotonga is in force. Both China and Russia have already signed the Protocols and France, the UK and the USA have announced their intentions to do the same. The IAEA is responsible for monitoring this Treaty under safeguards agreements with the Member States and a regional satellite capability might prove politically and technically valuable. Other important regions are Africa, the Middle East, the Indian Sub-continent and the Latin Americas. This option, however, is a medium term option: the necessary infrastructure does not exist and would take some time to put in place. The need to enhance IAEA safeguards exists now and it would be inappropriate not to utilise the potential offered by satellite imagery sooner rather than later.

Similarly the fourth option of waiting for the creation of an international verification agency under the auspices of the United Nations is very laudable but is unlikely to be realised for some considerable time. Ultimately the adoption of such an option might be the most appropriate long term aim. Such a new Agency might also satisfy the needs of individual states as well as those of the IAEA.

For the immediate future this then leaves the fifth and final option - to acquire commercially available satellite images and undertake analysis in-house. This study has confirmed that:

- there is significant potential in the application of the use of civil satellite imagery for safeguards;
- this can be achieved at relatively modest cost (see Appendix V);
- the transfer of the necessary technology into the IAEA does not present insuperable difficulties.

The technology is also changing rapidly particularly with respect to the quality of commercially available data which will significantly enhance the value of deploying the technique.

APPENDIX

I AVAILABILITY AND CAPABILITIES OF CIVIL/COMMERCIAL REMOTE SENSING SATELLITES

II.1 Current civil remote sensing satellites and their capabilities

At present seven countries – Canada, the PRC, France, India, Japan, Russia and the United States - launch and operate civil remote sensing satellites (see Table I.1). The European Space Agency (ESA, a 15-nation consortium)[69] joined these when the ERS-1 satellite was launched on 16 July 1991. Of these, only France and the USA have been actively distributing their satellite data on a commercial basis. These have now been joined by Canada, India, Japan and the Russian Federation.

Table I.1. Current civil remote sensing satellites.

State	Satellite	Launch date	Resolution (m pixels)	Revisit cycle	Channels
Canada	Radarsat		6-25		
ESA	ERS-1	16/07/1991	25-30	3 days	1
	ERS-2	02/05/1994	25-30	3 days	1
France	SPOT-1	22/02/1986	10-20	2.5 days	4
	SPOT-2	22/01/1990	10-20	2.5 days	4
	SPOT-3	26/09/1993	10-20	2.5 days	4
India	IRS-1A	17/03/1988	36-72	22 days	4
	IRS-1B	29/08/1991	36-72	22 days	4
	IRS-P2	15/10/1994	33-37	24 days	4
	IRS-1C	28/12/1995	5.8-69	5 days	5
Japan	MOS-1	19/02/1987	50	17 days	4
	MOS-1	07/02/1990	50	17 days	4
	JERS-1	11/02/1992	18-24	44 days	1
USA	Landsat-4	16/07/1982	30-120	16 days	7
	Landsat-5	01/03/1984	30-120	16 days	7
Russia	KFA-1000	Early 1980s	6 m	14 days	2
	Almaz-1	31/03/1990	15-30	1-3 days	1 radio-meter
			10-30 km		

Under a commercial agreement, the data from the Indian remote sensing satellite (IRS) are received and marketed globally by the US EOSAT Co.[70] Argentina, Brazil (in collaboration with the

[69]Membership consists of Austria, Belgium, Denmark, France, Germany, Ireland, Italy, the Netherlands, Norway, Spain, Sweden, Switzerland, the United Kingdom. Finland became an Associate Member in January 1981 and ties were forged with Canada by virtue of an agreement signed in December 1981 and renewed in May 1989.

[70]**Annual Report, 1994-95,** Government of India, Department of Space.

PRC), Canada and Sweden have developed plans for such spacecraft. While Canada under its Paxsat[71] has carried out studies on satellite requirements for verification of arms control agreements and crisis monitoring and it is very active in the field, Sweden seems to have lost interest in its Tellus project[72]. Israel launched two satellites on 19 September 1988 and 3 April 1990. The former may have been a first experimental surveillance spacecraft. The latter may have been an experimental satellite with two-way communications capability. It re-entered the earth's atmosphere on 7 September 1990.

I.2 Satellite capabilities and orbits

A satellite orbit is usually elliptical with the centre of the earth at one of the foci of the ellipse. There are six basic parameters, called the orbital elements, which completely describe the size, shape and orientation of an orbit of a satellite in space. Of these Ω, the right Ascension of the ascending node and ω, argument of perigee are relevant for the present discussion. The position of the orbital plane in space is usually given in a terrestrial sidereal rectangular co-ordinate system, the axes of which are shown in Figure I.1. The origin, O, of the co-ordinate system is the centre of the earth; the z-axis is oriented towards the North Pole and the earth's equatorial plane is in the xy-plane. The x-axis is oriented towards the Vernal equinox or the first point of Aries.[73] The point of intersection of the satellite ground track[74] with the equator is known as the ascending node. In Figure I.1, it is marked N. The angle Ω between the x-axis and line ON defines the right Ascension of the ascending node. During the lifetime of a satellite Ω does not remain fixed. This is because the orbital plane turns round the earth's axis while keeping the orbital inclination[75] constant. The change in Ω is known as precession. This occurs because the earth is not spherical so that its centre of gravity is not at the same point as its centre of mass. Moreover, the mass is not uniformly distributed. For low altitude orbits with small orbital inclinations, i, the rate of change of Ω can be as much as 9° per day. However, for an orbital inclination of 90°, this is zero. Because of this, it is possible to compare, for a particular day, the orbital planes of various satellites. All the satellites considered here are in circular orbits with inclinations of about 90°. Such an orbit is called a polar orbit (see Figure I.2). For observation satellites the change in Ω is used so that they pass over a region of interest on the earth at the same time of the day throughout the active lifetime of the satellite. Therefore, the reconnaissance photography always refers to the same local time so that changes in activity in the region can be compared from day to day. This is achieved by placing a satellite in a Sun-synchronous orbit in which the satellite is orbited with its orbital inclination of almost 90°. The plane of the satellite orbit contains both the earth and the Sun. In this type of orbit the satellite crosses, for example, the equator, at just about local noon on the sunlit side of the earth and local midnight on the dark side. The earth rotates under the satellite orbit, which is fixed in space, at a rate of 15° per hour, so that the equatorial and temperate zones of the earth can be photographed with the Sun always high in the sky. The orientation of the ellipse within the orbital plane of a satellite is given by ω, the second of the two orbital elements considered. It is the angle between the line **ON** (see Figure I.1) in the equatorial plane and the line **OP**, where **P** is the perigee. The line **OP** always lies

[71] **PAXSAT Concept: The application of space-based remote sensing for arms control verification**, Verification Brochure no. 2, 1987, (Published by the Department of External Affairs, Canada).

[72] **"Project Tellus - Technical study of a verification satellite"**, September 1988.

[73] The orbital plane of the earth is called the plane of the ecliptic. The angle between the earth's equatorial plane and the ecliptic plane is 23° 7'. The line of intersection of these two planes defines an important direction in space, known as the point of Aries. At any particular time this direction is exactly known and all celestial directions can conveniently be referred to it.

[74] This is the projected path traced out by a satellite over the surface of the earth.

[75] This is the angle between the orbital plane of the satellite and the equatorial plane of the earth.

along the major axis of the ellipse. The oblateness of the earth also affects ω, which for all except one value of orbital inclination is not constant. This means that the major axis of the orbit rotates in the orbital plane in the direction of motion of the satellite. The rate of change of ω is zero when the orbital inclination is 63.4°. Thus, a satellite launched at this orbital inclination, its perigee will remain stable along any chosen latitude. For other values of orbital inclination, ω could vary up to 5° per day.

Figure I.1. Geometry of a satellite orbit.

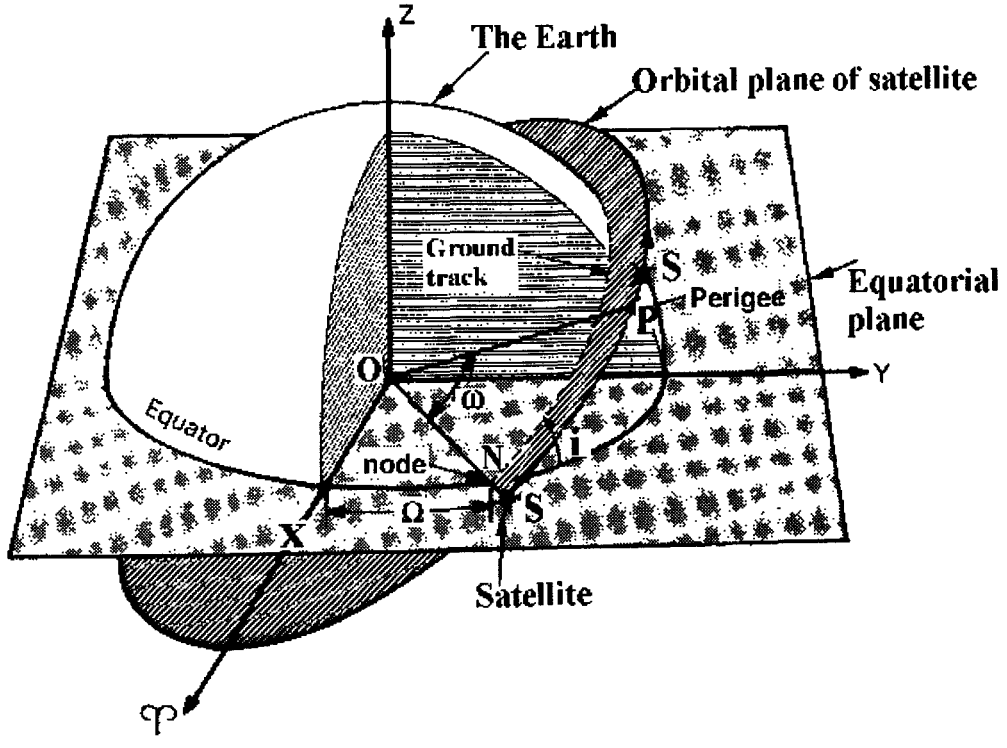

Figure I.2. Circular sun-synchronous orbit of an observation satellite with an orbital inclination of between 97° and 101°

For some of the satellites listed in Table I.1, the relative positions of their orbital planes are indicated in Figure I.3. It can be seen SPOT-1, -2, MOS-2, and ERS-1 are all in the same orbital plane. From this plane, the orbital plane separations of IRS-1B, MOS-1, Landsats 4 and -5, and IRS-1A are 2°, 5°, 15°, and 28° respectively. The Landsat-4 and -5 are in the same plane. The numbers in brackets in Figure I.3 are the perigee positions of all the satellites relative to the equator. The similarity of parameters for the two Landsat indicates that Landsat-5 was a replacement for Landsat-4. On the other hand the two IRS satellites are probably being used in order to obtain wider coverage. Their orbital planes are separated by 25.75°. The period of these satellites is 103.1 min so that, for example, during this time a point observed by IRS-1B has moved under the orbit of IRS 1A since the earth would have rotated by 25.78°. However, because of its different perigee position, the satellite will not observe the same object.

Consider the constellation of all the nine satellites. As these are not launched to operate in collaboration with each other, their orbits are such that observations of the earth can not be made in any logical fashion. Nevertheless, an examination of the orbital parameters of these spacecraft indicates that they are not all in one orbital plane. They are also widely dispersed relatively to each other in their orbital planes. This means that a more frequent and wider coverage is still possible. While SPOT-2, -1, MOS-2 and ERS-1 are in the same orbital plane, their perigee positions, relatively to that of SPOT-2, are at 33.1°, 30.1°, and 44.8° respectively. It is assumed here that the relative value of ω for all the satellites remains constant. This means that SPOT-1 could observe the same target in just over 9 minutes of the SPOT-2 leaving it. During this time the earth has rotated by just over two degrees. The ERS-1 would be over the target in 12.5 minutes during which time the earth would have rotated by about three degrees. This would still enable the satellites to observe the target with the radar sensor. With the Landsats and the IRS-1A being in different orbital planes, the target next comes under the orbits of these satellites so that the revisit time could be much less than those indicated in Table I.1 if data from different satellites are used. Not only this but if in future the launches of such satellites are co-

ordinated in such a way that their orbital planes are spread out evenly, the revisit time can be improved even further without any additional satellites. Moreover, with some ten satellites evenly spread out, there would not be any need for additional satellites.

Figure I.3. Positions of the orbital planes of some of the remote sensing space craft relative to SPOT-2 observed on 23 August 1993. Numbers in brackets are perigee positions of satellites measured from the equator.

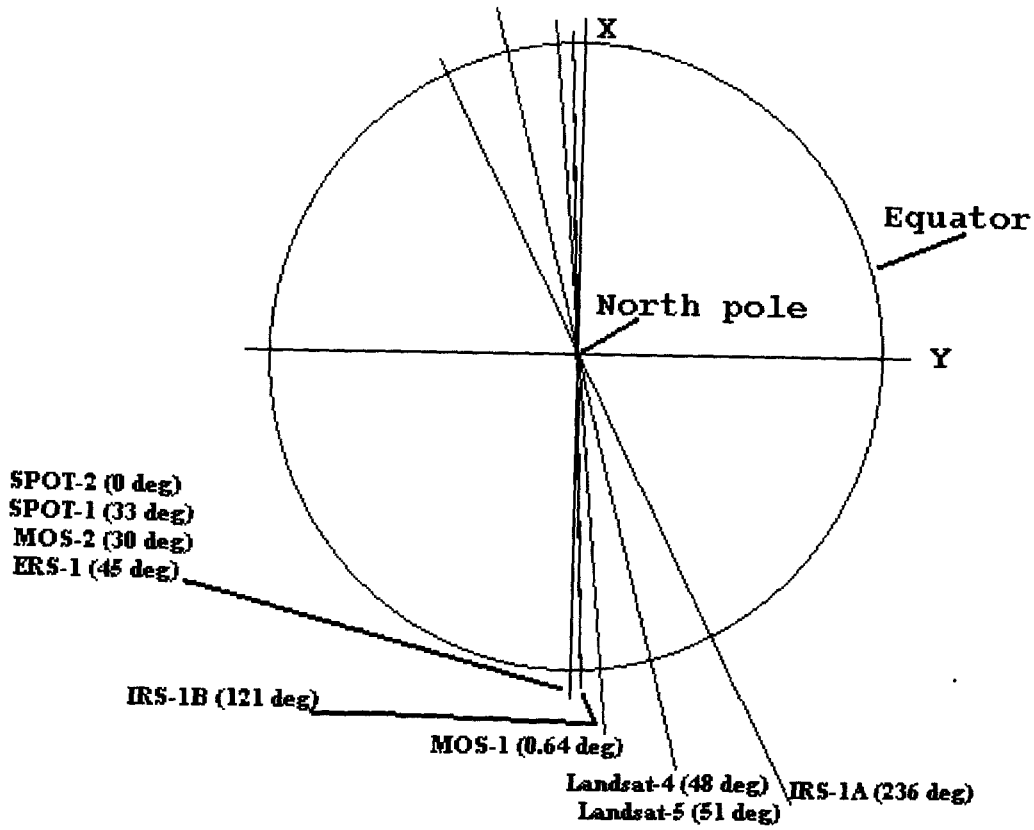

Normally information gathered from space is either recorded on an on board tape recorder to be played back when the satellite is over a ground receiving station or it can transmit the data via communication satellites to the main ground station. The latter depends on whether a communications spacecraft is capable of handling the data rates resulting from observation satellites. For example, the US Landsat-5 transmits the TM data at a rate of 83 MB/s. While the French SPOT satellite has a tape recorder on board, its data transmission rate is 50 MB/s and that of the European ERS-1 is 100 MB/s. The commercial communications satellites are probably not capable of handling such large data rates at present.

Using the ratio between the photographic resolution[76] and pixel size of about two, resolutions of various commercially available data are indicated in Figure I.4. The resolution in the Figure is in photographic resolution.

[76]The concept of resolution is a complex one. The spatial resolving power or resolution of an imaging system is the ability of the sensor to record small details in the scene. The quantification of the smallest detail or size of object that can be seen in an image is, however, a complicated issue and depends both upon the spatial resolution of the system and the

Figure I.4. Comparison of resolutions from different sensors using various space platforms. All the figures are given in photographic resolution so as to facilitate the comparison.

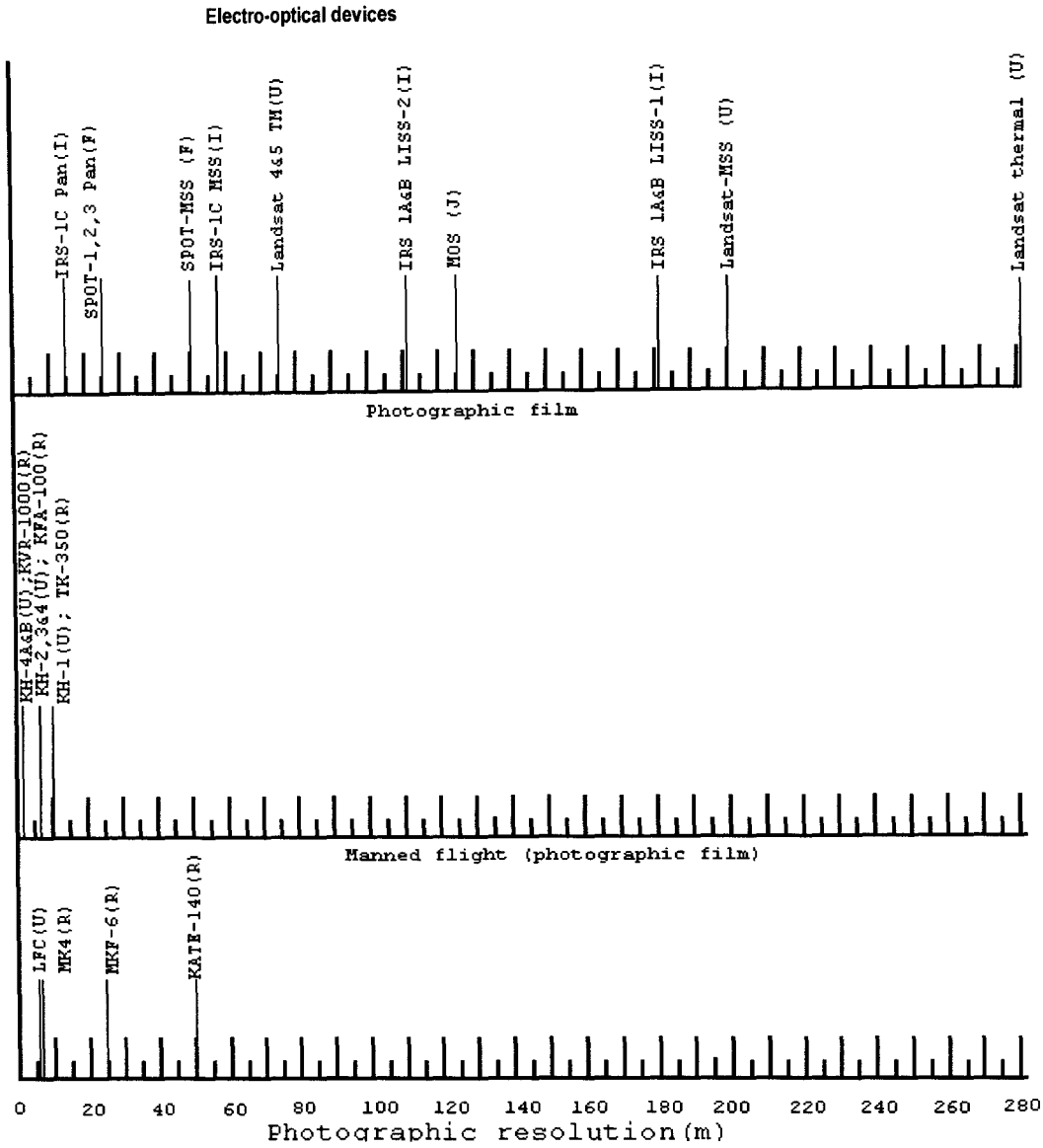

Key

F = France; I = India; IRS = Indian Remote sensing Satellite; J = Japan; LCF = Large Format Camera; LISS = Linear Imaging Self Scanning Sensor; MOS = Marine Observation Satellite; MSS= Multi-Spectral Scanner; Pan = Panchromatic; R = Russia; SPOT = System Pour l'Observation de la Terre; TM = Thematic Mapper; U = USA.

characteristics of the scene being observed. These include lighting conditions, configuration, size and shape of the objects being observed and atmospheric effects on the light travelling to and from the object being observed. The resolving power of the sensor may be defined as the minimum distance between two identical small objects when they can still be distinguished as two separate objects. While such a definition holds true for a photographic film camera system, for scanning devices a new concept, the instantaneous field of view (IFOV), has to be considered. The IFOV is defined as the size of the spot on the ground "seen" by one particular point in the image or seen by a scanning sensor at the instant of observation. A scanner is made of a series of small sensors each of which is called a pixel or picture element. This represents the point in the image. In this report resolution is referred to as a pixel size or the photographic resolution (or ground resolution) which depends on the contrast ratio. For a contrast ratio of 2:1, the resolution is about 2 to 2.4 times the IFOV. In this report it is taken to be two.

APPENDIX

II INTERPRETATION OF SATELLITE INFORMATION

II.1 Type of space-based data

Sensors on board satellites record images of the earth's surface by measuring reflected solar or emitted energy or that scattered from a radar. Two types of imageries are commercially available. (i) From French, Indian and Russian satellites, high spatial resolution data (6m, 10m or about 1m pixel equivalent respectively) are acquired. These are panchromatic images and they record total reflected energy across a very broad waveband of the electromagnetic spectrum (EMS) throughout the visible and infrared range(0.51-0.73 μm). (ii) Lower spatial resolution data (20-50 m pixels) are available from French, Indian, Japanese, Russian and US satellites. These are multispectral images which record reflected and emitted energy simultaneously in a number of narrower wavebands of the EMS [0.45-0.52 μm (blue), 0.52-0.6 μm (green), 0.6-0.7 μm (red), 0.76-0.9 μm (near infrared -IR), 1.55-1.75 μm and 2.08-2.35 μm (far IR), and 10.40-12.50 μm (thermal)]. While limitations of optical sensors are recognised, the use of radar data would extend the range of useful information available. Satellite data can be purchased as photographic prints, on computer compatible tapes (CCTs) or on CD-ROM. Clearly the first is the least flexible because image enhancement can be limited on a photographic image. However, this is the least expensive. All satellite data suppliers provide the data on CCTs or on CD-ROMs. Majority of the images used in this study were acquired on CCTs (see Table II.1). Most currently available tape drives are designed to read CCTs recorded at 1,600 bits per inch (bpi) or 6,250 bpi. Generally the data volume for each band in a multispectral image or that for a panchromatic image can be between 27 and 100 MBytes.

All the field definitions generally follow American National Standards Institute (ANSI) and International Organisation for Standardisation (ISO) standards. The file data on the whole are written in American Standard Code for Information Interchange (ASCII) which uses 7 bits per character plus an additional bit reserved as either an extension of the character set or as a parity bit. The difference between different products may be found in the image structure. There are two types of formats for this: the Band-Interleaved-by-Line (BIL) and the Band-SeQuential (BSQ). With the BIL option, there is only one imagery file for all the spectral bands. In this case each image line corresponds to several records depending on the number of spectral bands. For example, for SPOT each multispectral image line corresponds to three records, the first for spectral band XS1, the second for spectral band XS2, and the third for spectral band XS3. In the BSQ structure, each spectral band constitutes a separate logical volume[77]. For example, in the case of the US Landsat multispectral data, there are seven logical volumes, each one comprising several files and in particular an auxiliary data file and an imagery file. Thus, spectral band 1 data are contained in the imagery file of the first logical volume, the spectral band 2 data in the imagery file of the second logical volume, and spectral band 3 image data in the third logical volume and so on. On the other hand the French SPOT images can be obtained in either BIL or BSQ structure. Image data from Indian IRS satellites contain actual video data in BIL format.

[77]A logical volume is a logical collection of one or more files recorded consecutively. A logical volume contains one or more bands for a scene.

Table II.1. Spectral sensitivities of some of the civil satellites. (MESSR=Multispectral Electronic Self-Scanning Radiometer; VTIR=Visible and Thermal IR Radiometer; MSR=Microwave Scanning Radiometer).

Satellite	Spectral range (μm)	Resolution (m pixel)	Colour/band
USA	0.45-0.52	30	Visible blue/1
Landsat-4 & -5	0.52-0.60		Visible green/2
	0.63-0.69		Visible red/3
	0.76-0.90		Near infra-red/4
	1.55-1.75		Mid infra-red/5
	2.08-2.35		Far infra-red/7
	10.40-12.50	120	Thermal infra-red/6
France	0.50-0.59	20	Green/1
SPOT-1, -2 & -3	0.61-0.68		Red/2
	0.79-0.89		Near-iInfra-red/3
	0.51-0.73	10	Panchromatic
India	0.45-0.52	73	Visible blue/1
IRS-1, -2 and -	0.52-0.59		Visible green/2
1P	0.62-0.68		Visible red/3
	0.77-0.86		Near infra-red
	0.45-0.52	36	Blue/1
	0.52-0.59		Yellow/2
	0.62-0.68		Red/3
	0.77-0.86		Near infra-red
IRS-1C	0.62-0.68	188	Visible
	0.77-0.86		Near infra-red
	0.52-0.59	23.5	Visible
	0.62-0.68		Visible
	0.77-0.86		Near infra-red
	0.50-0.75	5.8	Visible panchromatic
Japan **MOS-1**	MESSR		
	0.51-0.59	50	Visible
	0.61-0.69		Visible
	0.72-0.80		Near infra-red
	0.80-1.10		Near infra-red
	VTIR		
	0.50-0.70	0.90km	Visible
	6.0-7.0	27km	Water vapour band
	10.5-11.5		Thermal infra-red
	11.5-12.5		Thermal infra-red
	MSR		
	23.8 GHz	32km	Microwave radiometer
	31.4 GHz		

Generally the images can be pre-processed by the suppliers to a required level. For example, the basic level consists of normalisation of the CCD detector response in each spectral band but no geometric corrections are performed. The next level may have radiometric corrections as well as geometric corrections. These are distortions introduced by, for example, the earth's rotation and panoramic effect. In this case the absolute location accuracy could be about 800m. The next level in which, for example, geometric and location accuracy have been enhanced; the location accuracy could be of the order of 30m. As the degree of corrections applied increases, the cost of the data also increases.

For this study, optical and radar sensors have been used for observations of various nuclear facilities. Most of the data were acquired on CCTs with the basic radiometric and geometric corrections provided by the data suppliers.

II.2 Some basics of image processing and interpretation

Different materials on the earth's surface may appear similar in panchromatic images as they reflect the same total amount of solar energy. However, in certain bands of a multispectral image such surface materials will reflect different amounts of energy and therefore appear different. Thus, multispectral images may contain a greater amount of information for discriminating different surface materials but the trade-off between spectral and spatial resolution means that panchromatic images may contain a greater amount of spatial detail for identifying surface features. Often the greatest amount of information can be derived by using both panchromatic and multispectral images of the same area, in a combined analysis.

Generally optical and radar sensors are deployed on separate observation satellites. Examples of the former are the French SPOT and the US Landsat satellites, and those of the latter are the European ERS-1, Canadian Radarsat and the Japanese JERS-1 spacecraft. Whilst the SPOT satellites carry panchromatic as well as multispectral optical sensors, only the latter is deployed on board the current US Landsat satellites. However, the range of wavelengths over which the sensor is sensitive is much greater for the Landsat satellites. Spectral sensitivities of some of the civil satellites are shown in Table II.1.

In electro-optical systems, signals are transmitted directly to a ground station for processing if the satellite is in line of site, relayed via satellites or they can be recorded on a tape recorder for transmission at a later time. The signals are then converted into digital numbers representing images and processed for interpretation.

Image processing . Since the scene is recorded on board the satellite in digital form, it is transmitted to ground station where computers reconstruct the image. During the reconstruction of the image the computer decodes the binary data and allocates the appropriate tone to each pixel[78]. The image can then be displayed on a monitor screen or as a photographic print. However, at this stage the image is in a basic raw form which needs to be corrected for a number of factors. This is termed pre-processing. Initially the data, as acquired from the satellite, have to be corrected for the earth's

[78]A scanning device on board a satellite consists of a series of very small light sensors. Thus, when a resolution of a sensor is quoted as 30 m, it means each small sensor of the scanner records an area, or a pixel, 30 m x 30 m on the earth's surface. On the other hand for a photographic camera, the resolving power or resolution may be simply defined as the minimum distance between two identical small objects when they can still be distinguished as two separate objects.

curvature, its rotation and for the errors introduced due to the attitude of the satellite and due to atmospheric distortions. Further corrections, such as the geometric distortions resulting in uncertainties of a few kilometres in relative positions of objects in the scene become necessary, particularly when change detection is considered. This is either corrected by identifying a number of landmarks such as airport landing-strips and highway intersections on the image and on a map and then calculating a least-square fit or by defining ground control points on the image and on a already geocoded image of the same area. The results are then used to correct the whole image. This is called the geometric correction.

Image processing involves, for example, contrast stretching. Sensors on board remote sensing satellites are designed with sensitivity over a very wide range of spectral intensity and wavelength of radiation. Thus, a sensor could be used, for example, to monitor very reflective surface of ice and relatively dark surface of forests and vegetation. However, in practice, generally such a wide range of variation does not occur in a scene so that the image often appears murky and even-toned. This is overcome by spreading the recorded reflectance values across the whole of the tonal range available. In this way the distinction between tones becomes much more pronounced. Thus, during the computer processing, the minimum and maximum reflectance values of the pixels present in the image are assigned 0 and 255 respectively and the individual values are stretched out maintaining the shape of the reflectance distribution curve. Thus, the tonal gaps between the values are widened. The result is a much more contrasting image. The process is called contrast stretching. In an electro-optical device, because the signal to noise ratio is much higher than that obtained on a photographic film (due to grain), it is possible to stretch the contrast. This would enable more information to be extracted from images from electro-optical devices.

The gradations between 256 different tones are not distinguished by eye. One way of overcoming this is to assign different colours to different tones or a group of tones. Thus, during computer processing, in a particular spectral band, a series of slices across the image are taken and assigned in an arbitrary way a colour to the particular group of digital numbers representing a particular feature. The process is applied to the whole of the image. In this way a rough classification is also obtained. The process is called density slicing.

Apart from the above techniques to improve the ability to extract information and to interpret a digital image, edge enhancement is also used. This is the sharpening of edges to highlight objects of interest.

Image interpretation. For monitoring the operational characteristics of nuclear facilities, Landsat type data are more useful because of the thermal band. A characteristic of an operating nuclear reactor, for example, is the discharge of warm water used to carry away heat from the reactor core. The water eventually is either discharged into a river, or a lake or into the sea. Detection of warm water would indicate, for example, that the plant is operational.

Atmospheric scattering is more pronounced in the visible bands and increases as the wavelengths decrease. This corresponds to Landsat thematic mapper (TM) bands one, two and three. Thus, often bands three, four and five are used in order to minimise the atmospheric effects. Most vegetation is strongly reflective in the near IR (TM band four). In false colour IR photography, healthy forests and fields, for example, appear bright red. Fallow fields appear in grey or blue-grey hues. Coniferous forests appear dark red - sometimes almost black because of their overall low reflectance. Bands five and seven normally measure reflected energy which identify the absorption of water. As plant and soil

moisture increase, the amount of energy reflected in these bands decreases. Generally, the wetter the object, the darker it will appear in these bands. Thus, for example, rivers and lakes appear dark in band five. The TM sensor collects most thermal information using band six which detects emitted energy. However, the spatial resolution is poor compared to the other bands (120m pixel size).

It should be remembered that red light travels some 5-10m through clear water. From space, therefore, objects only 5-10m below the surface of the water could be seen in the Landsat TM images in band three and possibly band four. This is important in the context of this study. When determining the operational characteristics of a reactor, the temperature of a body of water used for cooling is used. If water is shallow, high reflectance may be registered in the thermal band because of the heating of the small volume of water by the sun. This may lead to misinterpretation of the data. While intense heat sources emit energy at shorter wavelengths making it possible to see the emitted energy in TM bands five and seven, it may not be useful for the detection of nuclear facilities in their normal operational mode.

Thus, combination of visible bands one, two and three creates an image which appears normal to the eyes when the three bands are assigned blue, green and red guns on a colour monitor respectively. Radiation in bands four, five and seven and the thermal band six are invisible to human eyes. Data from these bands can be displayed individually as monochromatic images or they can be presented in one or more of the blue, green and red colours as a composite to become visible.

Interpretation is a process of extracting information from images. The amount of information that can be obtained from a particular image and the accuracy with which it is interpreted depends, to some extent, on the knowledge of the objects and their reflectance characteristics, the area in the scene and the experience that an interpreter has. The ability to recognise objects depends on such factors as the spectral and spatial resolutions, and contrast in the image. Thus, interpretation essentially involves measuring objects in the scene, identifying them and using this and some "collateral information" to answer some specific questions. The latter could, for example, be material from open literature, field work and photo interpretation keys.

Apart from interpretation of images by humans, computer-aided interpretation is becoming very important. This is particularly so in treaty verification now because some of the recent treaties (for example, the Intermediate-range Nuclear Forces - INF) require detailed descriptions of weapon facilities and their line drawings. The latter could be digitised enabling the computer to locate automatically and identify a particular facility in a scene. This is called pattern recognition. While such techniques can be used for relatively simple patterns described in the INF treaty, automatic pattern recognition is complex and perhaps the capability is not widely spread in the civil field. This and other factors used in automatic interpretation techniques are summarised in Table II.2. Interpretation in this report is interactive and no automatic computer analyses were carried out.

Table II.2. Summary of techniques used in computer-based interpretation.[79]

Interpretation elements	Spectral	Spatial	Stereo	Techniques
Tone	√	–	–	Density slicing
Colour	√	–	–	Multispectral classification
Texture	√	√	–	Texture classification
Pattern	√	√	√	Spatial transforms and classification
Size	–	√	√	Segmentation algorithms and size feature classification
Shape	–	√	√	Syntactic classification
Site	–	√	–	A Priori, Modified
Association	–	√	–	Contextual classification

It can be seen from Table II.2 that spatial resolution is a very important factor in image interpretation process. Spectral sensitivity, when changes in the scene occur and stereoscopic images could also add considerably to the task of interpretation. Examples of these are the detection of the use of camouflage, changes in vegetation from nuclear radiation or the use and testing of biological weapons[80] and chemicals from chemical weapons tests, possible detection of underground tests of explosives, particularly nuclear,[81] and new constructions such as roads and mining activities. The image interpretation task is carried out at essentially five levels: detection which is the discovery of the existence of an object without recognising it; recognition is the ability to determine the identity of a feature or object in a scene; identification is the ability to place the identity of a feature or object in a scene as a precise type; description requires such items as size, configuration, components construction and count of equipment; and analysis in which precise description of a feature or an object or component in the scene is given. The resolutions of sensors required for these tasks will vary. Most of the time, resolution between 1m and 30m (pixel size) would be adequate for most verification purposes.

II.3 Some signatures for recognition of undeclared facilities

Some signatures associated with various components of the nuclear fuel cycle which might be recognised in images acquired from civil remote sensing satellites are summarised in this section. It is expected that a civil nuclear facility could be recognised because of light passive protection and lack of active security arrangements such as anti-aircraft and missile defence systems that usually surround a military complex. Also using multispectral images, particularly in the thermal IR region of the spectral bands, it is expected that the purpose of a nuclear reactor, for example, could be determined by monitoring excess heat generated. For plutonium production, most common reactor types would have

[79] Ondrejka, R.J., in Arms Control Verification, (edt) Tsipis, K., Hafemeister, D.W., and Janeway, P., (Pergamon/Brassey's, New York, 1986), p.96.

[80] Goldman, M., Ustin, S., and Warman, E.A., "Radiation exposure near Chernobyl based on analysis of satellite images", **U.S. Department of Energy Report no. UCD-472-510**, December 1987; and Linthicum, K.J.L., Baily, C.L., Davies, F.G., and Tucker, C.J., "Detection of Rift Valley fever viral activity in Kenya by satellite remote sensing imagery", **Science**, vol. 235, 27 March 1987, pp.1656-1659.

[81] Jasani, B., "Verification of a comprehensive test ban treaty from space - A preliminary study", **Published by the United Nations Institute for Disarmament Research, Geneva, 1994.**

to be shut down frequently in order to remove the fuel so as to avoid the build up of undesirable isotopes of plutonium. When being used solely for power production, for economic reasons, power plants are allowed to operate for longer periods of time and shut down only for more infrequent refuelling and servicing. Exceptions to this are the Candu and the Magnox reactors for which on load refuelling is possible. But here again, when refueling or changing fuel pins, the reactor power output lowered resulting in possible less thermal output. On the other hand if such facilities are under the IAEA safeguards, then on site cameras would detect any movements of the fuel from the reactors.

A plutonium production facility capable of producing 1,000kg of plutonium a year would generate waste heat at an average rate of about three megawatts.[82] The hot water from a production reactor is usually discharged into a river, a lake, a cooling pond or through cooling towers. In the case of a lake or a pond, unless the water is efficiently mixed, it would be difficult to hide the rise in temperature of water from satellite-based thermal sensors.

Thus the task for observation satellites in monitoring declared and undeclared facilities would be to:

a) monitor dismantling or shut-down of plutonium production plants using thermal IR sensor and possibly radar;

b) monitor start-up dates and mode of operation (e.g. operational cycle) of known operational production and certain power reactors;

c) monitor operational characteristics of research reactors and their possible upgrading;

d) detect undeclared facilities and monitor the items listed in (a)-(c); and

e) monitor other fuel cycle facilities such as mining and milling and spent fuel storage areas.

[82]von Hipple, F., and Levi, B.G., "Controlling nuclear weapons at the source: Verification of a cutoff in the production of plutonium and highly enriched uranium for nuclear weapons", Arms control verification - The technologies that make it possible, (edt) Tsipis, K., Hafemeister, D.W., and Janeway, P., (Pergamon-Brassey's, Washington, 1986) p. 377.

APPENDIX

III Change detection pre-processing

III.1Change detection

Change detection is a process in which differences in the status of an object or a phenomenon are identified by observing them at different times.[83] This essentially assumes that changes in buildings and associated infrastructure will result in changes in grey level values of the relevant pixels. However, changes have to be larger than those due to changes in the radiance caused by natural factors such as differences in atmospheric conditions or in the sun angle or differences in soil moisture. Some of these effects can be reduced. For example, satellite data should be acquired at the same time of the year in order to avoid the problems of different sun angles and status of the vegetation. Correction due to different atmospheric conditions depends on the knowledge of both the radiometric values of objects/areas of interest and the meteorological conditions. Other factors that may indicate that there are changes in an image are, for example, insufficient co-registration of two images and different illumination due to different elevation of the sun.

III.2Spatial registration

Analysis of multi-temporal data requires accurate spatial registration of the images. The software, GCPWorks (EASI PACE), used in the present study for this co-registration, offers different mathematical models (polynomial transformations first to fifth order, thin plate spline) or mosaicking and re-sampling methods (nearest neighbour, bilinear interpolation and cubic convolution). The registration of the two geocoded Landsat TM Images as well as the registration of the high resolution KVR-1000 image were carried out using the first order nearest neighbour algorithm; the registration of one geocoded and one non-geocoded Landsat TM image was done by a third order cubic convolution.

III.3Radiometric correction

In addition, radiometric correction needs to be applied before proceeding with the detection of changes in a scene. The radiance signature for a given object varies with changes in radiometric conditions, particularly those due to atmospheric conditions and the sun azimuth and elevation angles that are generally provided in the header of satellite images. These effects can be corrected using either the EASI PACE module Atmospheric Correction, Lowtran-7 or S6 code that can be downloaded from the Internet. Also self-written programme software packages could be used.

---

[83] ***Ibid***. Kokoski, p. 109.

[83] Singh, Ashbindu (1989): "Digital change detection techniques using remotely-sensed data", **International Journal of Remote Sensing**, vol. 10, no. 6, pp.989-1003.

APPENDIX

IV Mathematical description of principal component analysis and multivariate alteration detection

IV.1 Principal component analysis

Representing multispectral pixel intensities measured at two different times by random vectors $X(T_1)$ and $X(T_2)$:

$$X(T_1)=\begin{pmatrix} X_1(T_1) \\ \vdots \\ X_N(T_1) \end{pmatrix} \qquad X(T_2)=\begin{pmatrix} X_1(T_2) \\ \vdots \\ X_N(T_2) \end{pmatrix}$$

we consider a bi-temporal feature space for the ith component

$$X_i = [X_i(T_1), X_i(T_2)], \quad i = 1...N.$$

For each spectral band we seek linear combinations

$$Y = a^T X = a_1 X_i(T_1) + a_2 X_i(T_2)$$

such that the transformed vector has maximum variance:

$$var(Y) = var(a^T X) \rightarrow \text{maximum.}$$

This establishes the first principal axis, along which the temporally correlated pixels (no-change pixels) will lie. Hence the projection of pixel intensity orthogonal to the first principle axis – i.e. the second principal component – is a measure of change. The principal axes may be determined by diagonalizing the sample covariance matrix for the bi-temporal image. The eigenvectors then give the principal axis directions, while the corresponding eigenvalues are the variances of the data along these directions. Thus a threshold in units of standard deviations along the second principal axis (change axis) is determined by the square root of the smaller of the two eigenvalues of the covariance matrix.

IV.2 Multivariate Alteration Detection (MAD)

If we represent multispectral pixel intensities measured at two different times by random vectors X and Y:

$$X = \begin{pmatrix} X_1 \\ \vdots \\ X_N \end{pmatrix} \qquad Y = \begin{pmatrix} Y_1 \\ \vdots \\ Y_N \end{pmatrix}$$

N being the number of spectral components, then we seek linear combinations

$$u = a^T X = a_1 X_1 + \ldots + a_N X_N$$
$$v = b^T Y = b_1 Y_1 + \ldots + b_N Y_N$$

such that the different of the transformed vectors has maximum variance:

$$var(u - v) = var(a^T X - b^T Y) \rightarrow \text{maximum},$$

subject to the constraints

$$var(u) = var(v) = 1.$$

Under these constraints we have

$$var(u - v) = var(u) + var(v) - 2\,cov(u,v) = 2(1 - corr(u,v)).$$

Therefore we seek vectors a and b which minimise the positive correlation corr(u,v).

Determination of the linear combinations is done by canonical correlation analysis which is described e.g. in Anderson [84].

The multivariate alteration detection is defined as

$$\begin{bmatrix} X \\ Y \end{bmatrix} \rightarrow \begin{bmatrix} a_p^T - b_p^T \\ \vdots \\ a_1^T - b_1^T \end{bmatrix}$$

where a_i and b_i are the defining coefficients from a standard canonical correlation analysis. X and Y are vectors with mean zero.

[84] T.W. Anderson: An Introduction to Multivariate Statistical Analysis, 2nd edition, New York. Wiley, 1984, pp. 480-520.

APPENDIX

V EQUIPMENT AND TRAINING REQUIREMENTS

V.1 Equipment

It is often argued that the equipment[85] and the operational costs of an image interpretation centre would be too high for an Agency such as the IAEA. However, the cost of equipment for the WEU Satellite Centre (WSC) indicate that it may not be so high. This centre was established by the WEU Member States in 1991 at Torrejón near Madrid, Spain. It was declared operational in 1995.[86] The main tasks for the WSC are:

- verification of arms control agreements;
- monitoring crises affecting European security;
- monitoring risks to the environment.

In this chapter, the equipment and the manpower requirements are considered very briefly should the IAEA decide to use data obtained from space. Should such a decision be taken, then it would be necessary to establish equipment essential to perform the following tasks:

- Data reception
- Data storage
- Data retrieval
- Data processing
- Data output
- Data management

Data reception

As mentioned in appendix II space-based information comes, for example, in the form of photographic prints, positive or negative transparency, CCT or CD-ROM. These must be logged by the system and stored in such a way that the information is retrieved with ease. The data needed for such a centre are not always satellite images in digital form, but could also be, for example, treaty documents, maps, and general information on a country's nuclear programme and even its attitude towards all aspects of the uses of nuclear energy.

---

[85]The information for this section is based on the data provided by Cray Systems, who were the prime contractor equipping the Western European Union Satellite Centre in Madrid, Spain.

[86]**Letter from the Assembly,** No. 22, September 1995, (Information Letter from the Assembly of Western European Union), p.2.

A typical system for receiving the data could be tape readers and scanners. The former would read satellite imagery data for processing and interpretation while the latter would read documents such as maps and even photographic imageries. It should be remembered that the satellite data provided by various suppliers are never in standard format. The data reception would convert the information into the form that the image processing system can handle. A very important function of the data reception section is quality control. Its function is to check that any data received by the centre are accurate and of high quality.

Data storage

All data stored at the Agency Library must be recorded in such a way that a user can search using many different criteria (cataloguing). It should be also be stored in such a way that its retrieval is easy. The data can be stored, for example, on Winchester hard disk, tapes, re-writeable optical disk and CD-ROM. The latter is preferred because of its longevity, but for speed of writing and the speed of access, the Winchester hard disk has considerable advantage.

Data retrieval

In order to retrieve data, a common technique is to use the Browse facility provided by manufacturers of equipment. This usually consists of sub-sampled version of the map and image data stored in the Library. Because they are small in size, a few kB, they can give a near real-time view of the data.

Data processing

Once a set of data is selected, the appropriate tools are required to process and analyse the data. There are many image processing packages available (for example, ERDAS, ERMAPPER, and PCI) the choice of which will depend on the needs and particular requirements of the data centre. The requirements are:

- ability to read many different data sets
- ability to make measurements
- variety and fidelity of data filters
- "mosaicing" capability
- ability to superimpose data sets from different sources
- links to vector geographic information systems (GIS)
- support for a wide range of printing and plotting equipment.

Apart from the ability to process image (raster) data, the need to interpret vector data is becoming increasingly important. Many maps are now provided in a vector GIS form which allows attribute information (such as width of road, height above sea-level, and surface type) to be associated with a line. The ability to overlay this map information on top of the raster data is vital and the ability to then edit the vector data whilst it is superimposed is extremely useful.

Data output

As the Agency deals with a wide variety of data, it needs a corresponding wide range of data output devices. Some are specific for particular data-types (for example, pen-plotter for maps) but others can be used for all data-types so that the most suitable one can be chosen. A typical set of data output devices could include:

- Dye-sublimation printers
- Thermal-wax printers
- Pen plotters
- Ink-jet plotters
- Electrostatic plotters
- Screen copiers
- A fully-functioning photographic laboratory

Data and network management

The size and sophistication of the data centre should be in relation to the amount of work it is expected to perform. The computer system chosen must be able to grow with the data centre's requirements. This leads to a computer architecture in which the data are held centrally and the users have powerful desk-top workstations. The links between the server and workstations are provided by a local area network (LAN). A popular computer operating system must be chosen. UNIX is the current market-leader and is supported by a number of very powerful workstations (SUN, Digital, Hewlett-Packard, IBM etc.) and has a large amount of suitable application software.

System configuration

A very basic system is considered in order to get some idea of the type of equipment that might be needed and also to enable one to calculate the cost involved.

Hardware:

- One data-reception and data-retrieval workstation (UNIX mid-range workstation with 64 MB RAM, 1 GB disk graphic card, CCT and CD-ROM readers)
- One data processing workstation (UNIX high-range workstation with 64 MB RAM, 1 GB disk, 32-bit graphic card)
- One data server (UNIX high-range workstation with 64 Mb RAM, 20 GB disk)
- One AO digitiser
- One A4 dye-sublimation printer
- One AO plotter

- One A4 monochrome laser printer
- Ethernet network

Off-the-shelf software:

- Image processing software
- Vector GIS
- Word-processor - for document generation
- Relational database - as the library database

A more sophisticated system would upgrade such components as the data storage system from a workstation to a proper data server with possibly optical disk juke-box. Other items that can be added, for example, are more image processing workstations.

Costs

The overall cost of the equipment is likely to be of the order of £400,000. Details of these are shown in Table III.1. There would be additional costs for, for example, project management, installation and setting to work, training for the use of the equipment piece by piece and the system as a whole, site installation design and testing (factory acceptance, site acceptance). This could well double the cost of the equipment.

V.2 Training requirements

Training requirements will depend on image interpretation tasks, the kind of imagery used and on the image processing, image analysis, data extraction and information handling equipment and software packages available. The first requirement would be the understanding of image structures of different sources of digital images. The next is the understanding of the image processing and information handling, such as merging of different images and data sets and computer assisted geographic information systems (GIS). The knowledge of various image enhancement techniques, interactive as well as automated, would also be required.

It would also be essential to learn about the objects to be interpreted in an image. For this it would be necessary to know their shapes and dimensions. The knowledge of the spectral properties of materials expressed as reflectance of surfaces in the visible as well as in the IR range of the spectrum is also needed. For thermal IR radiation, the relationship with temperature, thermal inertia and heat emissivity needs to be studied.

For SAR, knowledge of surface properties such as the dielectric properties and the effects of look angle and scan direction with respect to the orientation of objects would be required so as to be able to interpret radar images. The knowledge of the ability of objects to reflect different wavelengths of radiation is also of considerable importance. An appreciation of stereo images and their advantages and limitations need to be studied.

The understanding of natural features on the earth's surface, such as soil patterns and vegetation, and man-made features, such as land use, technical infrastructure for transport and communications, housing and mining, would also help in image interpretation task. Among the man-made activities, it is important to be able to distinguish between civilian and military activities.

Access to very high resolution satellite imagery data has been confined to only the USA and Russia and to some extent the People's Republic of China (PRC). The first two states share, to a limited extent, such data with their allies. However, this changed somewhat when France launched its military reconnaissance satellite (Helios-1) in 1995. It has agreed to share some of the data with the WSC. During its experimental phase of three years, the WSC trained its staff using civil satellite imagery. Whilst the quality of data from Helios-1 is probably not as good as those from, for example, the US reconnaissance satellites, it is considerably better than civil remote sensing data. Therefore, the WSC should be able to implement its task more effectively. Nevertheless, the training that the WSC photo-interpreters received from the use of civil data is likely to be of considerable value. For the foreseeable future, very high resolution data is not going to be available to many. It is generally assumed that verification and crisis monitoring cannot be carried out using civil satellites because "you cannot see much". Such a conclusion in drawn by people who have either used aerial observation data only or they have access to images from military reconnaissance satellites and, therefore, they tend to discard the value of commercial satellite data.

Table V.1. Cost of various basic equipment continued on page 119

Equipment	Quantity	Unit price (£ x 1,000)	Price £ x 1,000)
Data reception			
Scanner	1	40	40
CD-ROM	1	1	1
EXABYTE	1	2	2
CCT	1	6	6
Workstation including:	1	16	16
Graphic board	1	4	4
Disk (2 GB)	1	1	1
Database software	1	1	1
Ingestion software	1	10	10
Data storage			
Server including	1	20	20
Disk (2 GB)	10	1	10
CD-ROM	1	1	1
EXABYTE	1	1	1
Database software	10	1	10
Retrieval			
Workstation including:	1	16	16
Graphic board	1	4	4
Disk (2 GB)	1	1	1
Database software	1	1	1

Table V.1 continued. Cost of various basic equipment.[87]

Equipment	Quantity	Unit price (£ x 1,000)	Price £ x 1,000)
Processing devices			
Workstation including:	2	20	40
Second monitor	2	3	6
Graphic board	4	4	16
Disk (2 GB)	4	1	4
A0 Digitiser	2	3	6
IP software	2	40	80
GIS software	2	40	80
Database software	2	1	2
Word-processing software	2	3	6
Output devices			
A4 colour printer (high resolution)	1	6	6
A4 monochrome printer	1	2	2
A0 Plotter	1	6	6
Network			
Ethernet	1	5	5
Total			**404**

It is very important to realise that when using civil satellite data, it is essential to have considerable knowledge of the type of objects and activities being investigated in the image. Therefore, the first task for a trainer is to make the trainee aware of the availability of information in either the public domain or within organisations such as the IAEA. With such knowledge and knowing the shapes and sizes of the objects being investigated in an image, it is possible to extract considerable amount of information from

[87]The prices do not include the cost of custom software, installation and delivery charges.

even the crude images obtained from civil remote sensing satellites. For example, while it is not possible to detect a helicopter by a civil satellite carrying an optical sensor, it is perfectly possible for it to detect and identify a helicopter base. Using, for example, data acquired from a radar satellite over the same area, it is possible to identify very strong signatures over each helicopter pad when a vehicle is present thus indicating the presence of a helicopter. Also if the operational characteristics of a nuclear facility is to be determined, it is necessary to use a multispectral image rather than just high resolution panchromatic data. For example, an image in the thermal band of a Landsat satellite could give information on whether a reactor is operating by determining the temperature of water in a lake, river, or a reservoir into which the cooling water may be discharging. Thus, it is not necessary only to look at the activities going on around a facility with a very high resolution image. It should be recognised, therefore, that data from several types of sensors may be used to get a complete picture of what is happening on the ground.

In the case of inspectors who are used to looking at facilities on the ground, it is important that they can relate the shapes and sizes of various types of facilities observed in a satellite image. For this, it is important that the interpreters are able to combine data to obtain stereoscopic images. Not only this but they should be able to combine images from different satellite sensors to extract both spectral and spatial information.

Thus, perhaps the most important task for a trainer is to be able to change the mindset of interpreters who may be used to looking at very high resolution data. Furthermore, an interpreter needs to have extensive knowledge of arms control agreements and the types of activities to be monitored. Lastly, an interpreter needs to be more innovative when using civil satellite data.

Appendix

VI ACRONYMS

AGR	Advanced Gas-cooled Reactor
Am	Americium
ANSI	American National Standard Institute
ASCII	American Standard Code for Information Interchange
BIL	Band-Interleaved-by-Line
BNFL	British Nuclear Fuel plc
BSQ	Band-SeQential
CCT	Computer Compatible Tape
CD-ROM	Compact Disk-Read-Only Memory
CNES	Centre National d'Études Spatiales
CD	Conference on Disarmament
dpi	Dots Per Inch
DPRK	Democratic People's Republic of Korea
EMS	Electro-Magnetic Spectrum
EOSAT	Earth Observation Satellite Company
ERS	European Remote Sensing
GB	Giga Byte
GHz	Giga Hertz
GIS	Geographic Information System
IAEA	International Atomic Energy Agency
IFOV	Instantaneous Field of View
INF	Intermediate-range Nuclear Forces
INFCIRC	Information Circular
IPCA	Iterative Principal Component Analysis
IR	Infra-Red
IRS	Indian Remote Sensing satellite
ISO	International Organisation for Standardisation
JERS	Japanese Earth Remote Sensing satellite
kB	Kilo Byte
LAN	Local Area Network
MAD	Multivariate Alteration Detection
MB	Mega Byte
MESSR	Multi-spectral Electronic Self-Scanning Radiometer
MHz	Mega-Hertz
MOS	Marine Observation Satellite
MOX	Mixed Oxide
MSR	Microwave Scanning Radiometer
MWe	Mega Watt Electricity
MWth	Mega Watt Thermal
MW	Mega Watt
NNWS	Non-Nuclear-Weapon-State

NPT	Non-Proliferation of nuclear weapons Treaty
NWS	Nuclear-Weapon-State
PC	Principal Component
PCA	Principal Component Analysis
PRC	People's Republic of China
Pu	Plutonium
RAM	Random-Access Memory
SAGSI	Standing Advisory Group on Safeguards Implementation
SALT	Strategic Arms Limitation Talks
SAR	Synthetic Aperture Radar
SPOT	Système Probatoire d'Observation de la Terre
START	Strategic Arms Reduction Talks
SW	Separative Work
THORP	Thermal Oxide Reprocessing Plant
TM	Thematic Mapper
VRAM	Variable Random-Access Memory
VTIR	Visible and Thermal IR Radiometer
WEU	Western European Union
WEUSC	WEU Satellite Centre
XS	Multi-Spectral

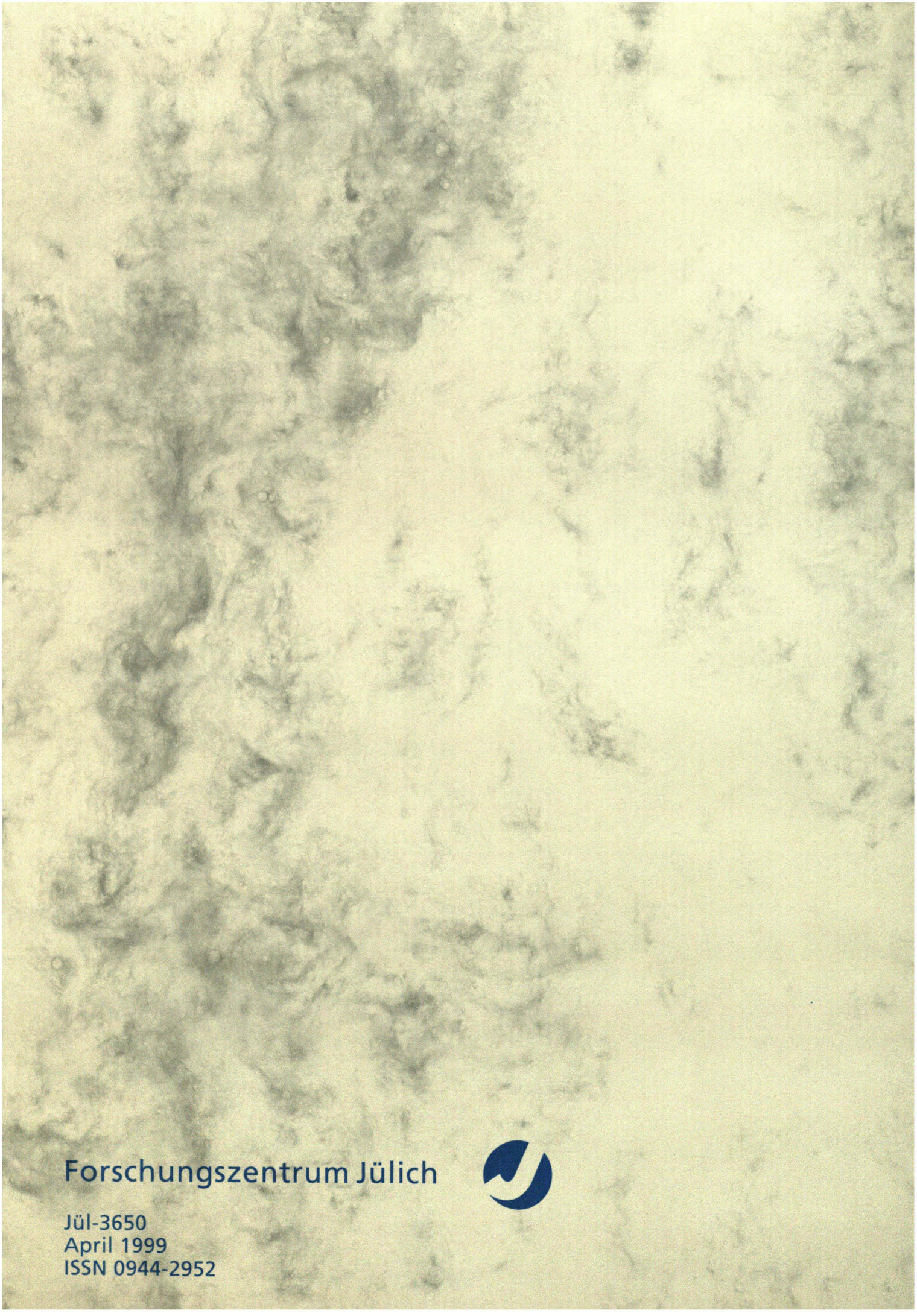

Forschungszentrum Jülich

Jül-3650
April 1999
ISSN 0944-2952